PHYSICAL REVIEW D VOLUME 24, NUMBER 5 1 SEPTEMBER 1981

General theory of weak processes involving neutrinos. I. Leptonic pseudoscalar-meson decays, with associated tests for, and bounds on, neutrino masses and lepton mixing

Robert E. Shrock
Institute for Theoretical Physics, State University of New York at Stony Brook, Stony Brook, New York 11794
(Received 30 September 1980)

In this paper and the others in the series we present a generalized theory of weak leptonic and semileptonic decays which consistently incorporates the possibility of nonzero neutrino masses and associated lepton mixing. In the present work we give an analysis of the leptonic decays of charged pseudoscalar mesons within the generalized theory. The charged-lepton spectrum from such a decay is shown to consist not just of a single line, but instead a discrete set of lines. We state the precise meaning of neutrino-mass limits. The analysis leads to a new and very sensitive test for neutrino masses and mixing and to a corresponding proposal for new experiments on π_{l2} and K_{l2} decays. This test involves a measurement of the charged-lepton momentum or energy spectrum and is capable of yielding the mass and weak coupling coefficient, individually, for each neutrino that can occur in such a decay. The test is applied to existing data to derive correlated bounds on these quantities. The use of this test as a low-energy probe of the number of lepton generations is proposed. We also discuss an extended spectral test involving measurement of the charged-lepton polarization. Next, we give an analysis of the constraints arising from the ratios $B(M^+\to e^+\nu_e)\,/\,B(M^+\to\mu^+\nu_\mu)$, where $M=\pi$ or K, which takes proper account of the experimental cuts that are used to define e^+"ν_e" and μ^+"ν_μ" events. Finally, the general theory of the leptonic decays of heavy 0^- mesons is presented, together with tests for neutrino masses and mixing which make use of the momentum spectra, integrated e/μ yields, and possible decays of sufficiently heavy neutrinos.

I. INTRODUCTION

In this paper and the others in the series we shall present a generalized theory of weak leptonic and semileptonic decays which consistently incorporates the possibility of nonzero neutrino masses and associated lepton mixing. The observation underlying this generalized theory, and the meaning of neutrino-mass limits, were discussed briefly before.[1] In Ref. 1 a new class of tests for such masses and mixing which follows from the basic observation was proposed and applied to existing data.

In the conventional theory of weak interactions, it was generally assumed that neutrinos were massless. This assumption was not always used, but when the more general possibility of nonzero neutrino masses was considered in the context of weak decays, it was implicitly assumed that the weak neutrino eigenstates ν_e, ν_μ, and more recently ν_τ, were also mass eigenstates. Thus, one reads in textbooks of nuclear and particle physics, the journal literature, and past editions of the Review of Particle Properties of the "masses" of the electron and muon neutrinos, "$m(\nu_e)$" and "$m(\nu_\mu)$", the effects which they would have if nonzero, and the upper limits on them. A similar comment applies for "$m(\nu_\tau)$". One also reads of a given weak leptonic or semileptonic decay being considered as a *single* decay, e.g., $\pi^+\to\mu^+\nu_\mu$, $\mu\to\nu_\mu e\bar{\nu}_e$, or nuclear β decay $(Z,A)\to(Z,+1,A)+e^-+\bar{\nu}_e$, not only in the case of zero neutrino mass, but also in the case where these masses are allowed to be nonzero. This is true, for example, of all the original papers which set upper limits on "$m(\nu_e)$", "$m(\nu_\mu)$", and "$m(\nu_\tau)$". However, in precisely the case where the above assumption that there existed well-defined entities $m(\nu_{l_a})$, $l_a=e,\mu,\tau$, was made and was nontrivial, viz., the case where these were allowed to be nonzero, this assumption was not in general valid. The reason is very basic: If neutrinos are massive (and nondegenerate[2]), then the weak neutrino eigenstates ν_{l_a}, defined as the states which couple with unit strength to the corresponding charged leptons l_a (where $\{l_a\}=\{l_1\equiv e, l_2\equiv\mu, l_3\equiv\tau,\ldots l_n\}$) are not themselves mass eigenstates, but rather linear combinations of the neutrino mass eigenstates, which will be denoted ν_i, $i=1,\ldots,n$.[3] This fact is particularly transparent in the context of the current gauge theories of weak interactions, where the weak neutrino eigenstates are gauge-group eigenstates, but it could have been realized before their advent.

If the lack of validity of this assumption were just a minor matter of notation, then, it would have little interest. But it is not; it has led to very real consequences in the history of experiments which sought to observe or set upper limits on neutrino masses. For example, nuclear β-decay experiments attempting to detect or place an upper bound on "$m(\nu_e)$" have always assumed that there was only one such limit to be obtained in a given experiment, have chosen the well-measured β decay with the smallest Q value, $^3\mathrm{H}\to{}^3\mathrm{He}+e^-+\nu_e$, to study, and have always searched only for the early falloff in the Kurie

plot near the maximum electron energy which a nonzero ν_e "mass" would allegedly cause. The most recent experiments on the decay reported in 1980 still follow this practice. But, in fact, as was pointed out in Ref. 1, (1) contrary to what is stated in textbooks, this early end-point falloff in the Kurie plot is *not* the most general signature of nonzero masses for one or more of the mass eigenstates ν_i contained in the weak eigenstate ν_e, i.e., even if "$m(\nu_e)$" were nonzero there would *not* necessarily be any early end-point falloff, but rather one or more kinks at lower E_e in the Kurie plot; (2) the Kurie plot from *any* well-measured β decay (obviously also the recoil energy spectrum in a β decay which proceeds via electron capture) can serve as a test for neutrino masses; the Q value does not have to be small; (3) the relative agreement of corrected $\mathcal{F}t$ values for a set of superallowed $0^+ \to 0^+$ Fermi β decays yields a very good correlated limit on neutrino masses and mixing; and (4) in view of item (1), it was perfectly possible that decades of nuclear β-decay experiments which had purported to set upper limits on "$m(\nu_e)$" had, because of their tacit neglect of lepton mixing, missed a positive signal of nonzero neutrino masses as large as several MeV. Accordingly, a rough but general analysis of β-decay data was carried out and the resulting bound on neutrino masses and mixing was given in Ref. 1. Similarly, the same tacit assumption is evident in the experiments which set upper limits on "$m(\nu_\mu)$"; for example, in the $\pi_{\mu 2}$ experiments it was thought that the μ spectrum would consist of a single line [possibly shifted downward slightly because of a nonzero value of "$m(\nu_\mu)$"], and so they never searched for a multitude of additional lines in the μ spectrum and indeed set cuts which, in many cases, would have precluded the detection or analysis of such lines. Consequently, just as in the case of nuclear β decay, because of their implicit assumptions that ν_{i_a} was a mass eigenstate in the massive as well as the massless case, and hence neglect of lepton mixing, it is possible that they missed a positive signal of massive neutrinos. Thus, the differences between the generalized theory of weak leptonic and semileptonic decays and the conventional theory do not just consist of unimportant details, but have had demonstrable effects in the history of weak-interaction experimentation. The correct generalization of the conventional theory of weak decays leads to fundamental changes in the conclusions to be derived from weak-interaction data, including a reformulation of the meaning of neutrino-mass limits (which do not prohibit the occurrence of a neutrino with a mass of ~1 MeV in a nuclear β decay, or the occurrence of a neutrino with a mass of ~100 MeV in the decay $K^+ \to e^+ \nu_e$), and the meaning of the ratio of branching ratios $B(M^+ \to e^+ \nu_e)/B(M^+ \to \mu^+ \nu_\mu)$, where $M = \pi$ or K (which is seen to depend sensitively on the cuts that were imposed in various experiments, which would have entirely excluded decays into sufficiently massive neutrinos). Similarly, one must reinterpret past experimental conclusions concerning radiative decays such as $\pi^+ \to \mu^+ \nu_\mu \gamma$, as well as data on μ (and τ) decay, including the meaning of the spectral parameters ρ, η, ξ, and δ in the presence of neutrino masses and mixing. It is also necessary to reinterpret the meaning of many fundamental weak-interaction constants. Perhaps most important, the generalized theory leads to concrete proposals for new and extremely sensitive, but not overly difficult, experiments to detect possible neutrino masses and mixing. These experiments do not require great energies or new accelerators and could have been performed many years ago if the effects of lepton mixing in a general theory of weak decays had been appreciated. Perhaps the most promising of these experiments rely upon the leptonic decays of charged pseudoscalar mesons and are capable of yielding the masses and weak-mixing-matrix coefficients individually for each neutrino which is allowed by phase space to occur in these decays. Indeed, they also provide an unprecedented method of gaining information on whether there are more than three generations of neutrinos, and hence, in the standard model, more than three generations of fermions. Thus, without the necessity of boosting the energy of PEP or PETRA or building LEP, one *may* discover, using only the leptonic decays of the light mesons $\pi^\pm$ and $K^\pm$ (or perhaps F), that $n > 3$.

Since no experiment will ever show that all neutrino masses or leptonic mixing angles are precisely zero, and indeed, existing experiments have not even ruled out the possibility of neutrinos with $m(\nu_i) \gtrsim 100$ MeV for $i \geq 3$, a logically consistent theory of weak leptonic and semileptonic decays (and reactions) must allow for the possibility of nonzero, and perhaps substantial, neutrino masses, together with the associated lepton mixing. The outlines of this generalized theory and some of its implications were given in Ref. 1. As was discussed there and will be treated in greater detail below, a far reaching consequence is that a weak leptonic or semileptonic decay such as $\pi^+ \to \mu^+ \nu_\mu$ is a single, well-defined process only in the one case where $m(\nu_i) = 0$ for all i. In general, it represents the set of *separate, incoherent* decay modes $\pi^+ \to \mu^+ \nu_i$, $i = 1, \ldots, k$, involving the subset of the

n ν_i's allowed by phase space. Because neither the total number of neutrinos, n, nor their masses $m(\nu_i)$, $i=1,\ldots,n$, are known (although there are upper limits on the latter for $i \leq 3$), one is thus forced to reanalyze the entirety of weak leptonic and semileptonic decays within the context of the generalized theory. In this paper we shall perform this task for the leptonic decays of pseudoscalar mesons.

We shall work within a version of the Weinberg-Salam $SU(2)_L \times U(1)$ electroweak gauge group[4] which is generalized[5] to allow for neutrino masses and mixing, and which includes n generations of fermions. In the minimal version of this model there are no right-handed components for neutrinos, which feature precludes the existence of Dirac neutrino masses, and also no Higgs triplets, which precludes Majorana neutrino masses. In our generalized version of the model we shall allow for both right-handed singlet neutrino fields and Higgs triplets of the appropriate weak hypercharge, and thus for both Dirac and Majorana neutrino masses. It should be remarked that the generalized theory of weak decays and resulting tests given in Ref. 1 do not require the framework of the $SU(2)_L \times U(1)$ electroweak gauge group. Accordingly, although this group is well established at the present time as the basis for the standard theory of electroweak interactions in the relevant range of energies, we shall in various places point out what, if any, differences there would be in the applications of our generalized analysis of weak decays if there existed (at phenomenologically allowed levels) $V+A$, S, or P charged weak couplings.

With the neutrino gauge-group eigenstates and mass eigenstates denoted by ν_{l_a} and ν_i, as above, the relation between them is specified by the equation

$$\nu_{l_a} = \sum_{i=1}^{n} U_{ai}\nu_i, \quad a=1,\ldots,n \tag{1.1}$$

where U is the unitary lepton mixing matrix. This mixing and some of the experimental constraints on it were discussed before in a version of the standard electroweak theory.[5] If $m(\nu_i)=0$ for all i, then it is possible to *define* $U \equiv 1$, i.e., to define the gauge-group eigenstates to be simultaneously mass eigenstates. However, this is no longer possible in general in the case of massive nondegenerate neutrinos.[3] One may use either of two conventions to define the order of the neutrino mass eigenbasis and hence the lepton mixing matrix U: (1) such that U is as nearly diagonal as possible, i.e. (with no sum on a) $|U_{aa}| \geq |U_{ai}|$ if $a \neq i$, or (2) such that the ν_i have monotonically increasing masses, i.e., $i \leq j \Leftrightarrow m(\nu_i) \leq m(\nu_j)$. As in Ref. 1, we shall use the first convention. The orders established by these two conventions are in general different. For ν_i with sufficiently small masses ($i \in \{i_L\}$ according to the classification used before[1]) it could happen, for example, that the neutrino mass eigenstates ν_1 and ν_2 which couple dominantly to e and μ, respectively, have masses which satisfy $m(\nu_1) > m(\nu_2)$, and so forth for ν_3. Of course, the situation in which the ν_i ordered by the first convention also satisfy the inequality of criterion (2) is the more natural one to envisage physically.[6] The second convention will be useful in our discussion of neutrino decays. In order to distinguish the neutrino mass eigenstates so defined, we shall denote them as $\nu_{[i]}$, $[i]=[1],\ldots,[n]$, and the transformation to weak eigenstates as

$$\nu_{l_a} = \sum_{[i]=[1]}^{[n]} U_{a[i]}\nu_{[i]}. \tag{1.2}$$

We must stress at the outset that there is, to our knowledge, nothing which precludes neutrino masses in the range probed by the tests to be discussed here. As was pointed out before,[1] the mass limits, as conventionally stated, on the neutrinos relevant for $M^+ \to l_a^+ \nu_{l_a}$ decay, with $M=\pi,K$, $l_a=e,\mu$, namely "$m(\nu_e)$" < 60 eV (Ref. 7) and "$m(\nu_\mu)$" < 0.57 MeV,[8] both at the 90% confidence level (C.L.) are, strictly speaking, ill defined (hence the quotation marks), since ν_e and ν_μ are *not* mass eigenstates. When properly reinterpreted, these limits are seen obviously to apply only to the dominantly coupled mass eigenstates in ν_{l_a}, $l_a=e,\mu$. They do not constrain the masses $m(\nu_i)$ of those ν_i in $\nu_{e,\mu}$ which are subdominantly coupled, i.e., have $|U_{ai}|^2 \ll 1$, where $a=1,2$. Moreover, the cosmological bounds noted by Cowsick and McClelland[9] and extended by other authors[10] apply only to effectively stable neutrinos, i.e., those with lifetimes $\tau_{\nu_i} \gtrsim \tau_{\text{Universe}} \sim 10^{18}$ sec. In contrast, neutrinos with masses greater than several MeV would decay, with $\tau_{\nu_i} \ll \tau_{\text{Universe}}$ unless the $|U_{ai}|$, $a=1$ and 2, are exceedingly small. It should perhaps be mentioned that if one chose to try to restrict particle-physics possibilities by applying somewhat more model-dependent astrophysical bounds, then a certain range of $m(\nu_i)$ from ~100 eV to ~a few MeV would be disfavored.[11] Although it will be discussed later, it is perhaps appropriate to comment immediately that neutrinos with masses in the range detectable by the tests dealt with here would of course give rise to neutrino oscillations[12] with wavelengths so short that existing or planned experiments would measure only an

average effect. However, the M_{l2} test is capable of observing a massive ν_i, especially for larger values of $m(\nu_i)$, with $|U_{ai}|$ $(a=1,2)$ considerably below the level which could be detected or ruled out by existing or planned neutrino-oscillation experiments.

One can envision several qualitative possibilities for neutrino masses and lepton mixing. The simplest is the conventional one where $m(\nu_i)=0$ for all i, and so $U\equiv 1$. Another is that, even if $n>3$, the largest neutrino mass, $m(\nu_{[n]})\ll m_e$. An alternative case, which is of greatest interest here, is one in which the lightest ν_i's indeed have masses $m(\nu_i)\ll m_e$, but the spectrum extends up into the multi-MeV region. This would not entail any conflict with particle or astrophysical bounds, provided that the corresponding couplings to light leptons $|U_{ai}|^2$ $(a=1,2)$ were reasonably small. We do not mean to advocate one of these scenarios in preference to another. We do wish to emphasize that the last one is subject to a direct experimental check by an extremely sensitive, but not overly difficult, test which has not previously been applied. This test and the associated physics issues will be discussed in this paper. Our viewpoint will be deliberately phenomenological; we are not concerned here with theoretical speculations to try to explain various sizes for neutrino masses, but rather the immediate task of carrying out a generalized analysis of the wealth of well-established data on weak leptonic and semileptonic decays and reactions, from which the fundamental properties of weak interactions have been derived, and, as part of this analysis, proposing and applying new tests for neutrino masses and mixing.

The organization of the remainder of this paper is indicated by the following outline.

II. The M_{l2} test: Foundation and applications.

A. An observation concerning weak (semi) leptonic decays.

B. Neutrino-mass limits.

C. The M_{l2} test.

D. Application of the M_{l2} test to existing data.

E. The complete M_{l2} test including measurement of the lepton polarization.

F. The use of the M_{l2} spectral test as a probe of the number of lepton generations.

III. Constraints on neutrino masses and lepton mixing angles from $B(M^+\to e^+\text{“}\nu_e\text{”})/B(M^+\to\mu^+\text{“}\nu_\mu\text{”})$.

IV. The leptonic decays of heavy charged 0^- mesons.

V. Conclusions.

The subsequent articles in the series will deal with μ and τ decay, heavy-neutrino decays, $(\pi^+,K^+)\to l_a^+\nu_{l_a}\gamma$, K_{l3}, and hyperon decays, nuclear β decay and μ capture, neutrino oscillations (in the general case of heavy neutrinos), neutrinoless double-β decay, and other effects such as changes in the determination of quark mixing angles and changes in the true, as opposed to the apparent, values of certain physical constants such as the μ-decay constant G_μ, the Fermi β-decay constant G_V', the pseudoscalar decay constants f_π and f_K, and the W-boson mass m_W.

II. THE M_{l2} TEST: FOUNDATION AND APPLICATIONS

A. An observation concerning weak (semi)leptonic decays

In this section we shall discuss the general foundations for the new class of tests for neutrino masses and mixing and, in particular, the M_{l2} test. In order to make our treatment self-contained, we shall in part recapitulate the presentation given earlier in Ref. 1.

The observation underlying this new class of tests is that in previous direct searches, i.e., via decays, for neutrino masses it was implicitly assumed that in a decay of the form $X\to Y+l_a^\pm+\overset{(-)}{\nu}_{l_a}$, where $l_a=e$ or μ, X denotes the parent particle, and Y denotes a possibly null set of final-state particles, the $\overset{(-)}{\nu}_{l_a}$ is a definite particle with mass $m(\nu_{l_a})$, which could be nonzero and on which the experiment would set an upper limit. (In practice X and Y are both hadronic.) Examples include leptonic π and K decay (for which $Y=\{\phi\}$), K_{l3} decay, and nuclear β decay. In the context of the present gauge theory of electroweak interactions this is equivalent to assuming that the possibility of defining the neutrino weak-gauge-group eigenstates to be simultaneously mass eigenstates obtains in the case of massive (nondegenerate), as well as massless, neutrinos. However, this assumption is not in general valid. Instead, a decay of the form $X\to Y+l_a^\pm+\overset{(-)}{\nu}_{l_a}$ would actually consist of an incoherent sum of the separate modes $X\to Y+l_a^\pm+\overset{(-)}{\nu}_i$, where i runs over the subset of the n neutrino mass eigenstates allowed by phase space. The branching ratio for the ith mode is modulated by the mixing-matrix factor $|U_{ai}|^2$ as well as a kinematic factor depending on $m(\nu_i)$. A similar comment applies to two other types of weak decays: a nuclear β decay which proceeds via electron capture $(Z,A)+e^-\to(Z-1,A)+\nu_e$ (here $a=1$), and the semileptonic decay of a (heavy) lepton, $l_a\to\nu_a+Y$, where $a\geq 3$. An obvious generalization of this comment applies to the pure leptonic decay of the form $l_a\to\nu_{l_a}l_b\bar{\nu}_{l_b}$ which in general consists of all of the modes $l_a\to\nu_i l_b\bar{\nu}_j$ kinematically

allowed, each with U dependence $|U_{ai}^* U_{bj}|^2$. With appropriate modifications this nomenclature could also be extended to cover the various decay modes of massive neutrinos.

A convenient qualitative classification of the ν_i was introduced in Ref. 1. One of the uses of the system pertains to the question of how large the off-diagonal elements of the matrix U are allowed to be. For given decays such as $X \to Y + l_a^{\pm} + \overset{(-)}{\nu}_a$, $(Z,A) + e^- \to (Z-1,A) + \nu_e$, and $l_a \to \nu_a + Y$, we define the light dominantly and subdominantly coupled (LDC and LSC) ν_i modes as those for which $i \in \{i_L\}$ and $|U_{ai}|^2$ is of order unity, and much less than unity, respectively. The heavy dominantly and subdominantly coupled (HDC and HSC) ν_i modes are similarly defined, but with $i \in \{i_H\}$, as allowed by phase space. For sufficiently light ν_i the constraints on lepton mixing from particle-decay data alone would allow the off-diagonal elements $|U_{ai}|$, $a \neq i$, to be comparable with the diagonal elements $|U_{ai}|$, $a = i$. For this range of $m(\nu_i)$ it is instead the data bounding or observing neutrino oscillations which serves to determine the structure of the matrix U, and in particular how large the off-diagonal matrix elements are allowed to be. However, for $i \in \{i_H\}$ the constraints from decay data and oscillation experiments do imply that, at least for $n = 3$ and, with natural mixing, also for $n > 3$, the $|U_{ai}|$, $a \neq i$, are small compared with the $|U_{ai}|$, $a = i$. That is, while there may be several LDC modes, depending on the eventual outcome of experiments on neutrino oscillations, there can be essentially only one HDC mode for each generation of leptons, namely $i = a$.

B. Neutrino-mass limits

Having made these observations, one is prepared to understand the meaning and limitations of present neutrino-mass limits. Let us recall these limits. In 1972, from a search for an early falloff near the end point of the Kurie plot for the well-measured superallowed β decay $^3\mathrm{H} \to {}^3\mathrm{He} + e^- + \bar{\nu}_e$ with an extremely small Q value of 18.6 keV, Bergkvist reported the limit[7] "$m(\nu_e)$" < 60 eV (90% C.L.) (quotation marks ours[1]). This bound was adopted, and still is used in 1980, as the accepted limit by the Particle Data Group.[14] In 1979, from a study of the same decay, a Canadian group obtained the comparable result "$m(\nu_e)$" < 70 eV (2σ level).[15] In addition, in 1976, again from an analysis of tritium β decay, a Russian experiment claimed that "$m(\nu_e)$" < 35 eV (90% C.L.).[16] This group has recently reported positive evidence for a massive electron neutrino, quoting the bounds 26 eV $\leq$ "$m(\nu_e)$" ≤ 46 eV and 14 eV $\leq$ "$m(\nu_e)$" ≤ 46 eV, both at the 99% C.L., based on two different methods of analyzing their data.[17] The best upper bound quoted for "$m(\nu_\mu)$" arises from a precise measurement of the muon momentum spectrum in $\pi^+ \to \mu^+ \nu_\mu$ decay. It should be noted in passing that this method is self-consistent in the sense that the current determinations of the masses m_{π^+} and m_μ are performed in such a way[18] that they would not change if neutrino masses were nonzero. If this appears to be belaboring the obvious, one should point out that in the presence of such nonzero neutrino masses and lepton mixing many of the fundamental constants such as G_μ, G'_V, f_π, f_K, the quark mixing matrix V, in particular V_{ud} and V_{us} ("$\cos\theta_{\text{Cabibbo}}$" and "$\sin\theta_{\text{Cabibbo}}$" in the old four-quark theory), and the W-boson mass m_W *would differ* from their conventional values determined using the assumption that $m(\nu_i) = 0$ for all i and hence $U \equiv 1$. This will be discussed in detail elsewhere. The most recent[19] and accurate measurement of $|\vec{p}_\mu|$ was carried out by a group at the Swiss Institute for Nuclear Research (SIN), which obtained "$m(\nu_\mu)$" < 0.57 MeV (90% C.L.). Finally, from measurements of the electron spectra in leptonic τ decay, assuming a $V-A$ $\tau\nu_\tau$ vertex (which assumption fit their data), the DELCO collaboration reported the bound "$m(\nu_\tau)$" < 250 MeV (90% C.L.).[13] Mass limits can also be obtained from a study of the two-body decay modes $\tau^- \to \nu_\tau \pi^-$ and $\tau^- \to \nu_\tau \rho^-$. From data taken by the SLAC-LBL collaboration on the first mode the limit "$m(\nu_\tau)$" < 245 MeV (2σ level) is quoted.[20] It would be very valuable to improve this limit in future experiments on τ decay. [See Sec. IV and paper II for further tests for, and constraints on, $m(\nu_3)$ from decays involving F and τ.]

The actual meaning of neutrino-mass limits is the following: For the sets $\{\nu_i\}_a$ defined to consist of dominantly coupled ν_i, i.e., those for which $|U_{ai}|^2 \ll 1$, the following limits hold[7,8,13]:

$$m(\{\nu_i\}_1) < 60 \text{ eV}, \tag{2.1}$$

$$m(\{\nu_i\}_2) < 0.57 \text{ MeV}, \tag{2.2}$$

and

$$m(\{\nu_i\}_3) < 250 \text{ MeV}, \tag{2.3}$$

all at ~90% C.L. The above sets must include, but are not necessarily restricted to, the following members:

$$\{\nu_i\}_a \supset \nu_{j=a}, \quad a = 1,2,3. \tag{2.4}$$

Thus for SC ν_i modes, with $|U_{ai}|^2 \ll 1$, where $a = 1,2,3$, the $m(\nu_i)$ are not constrained to be less than the respective masses c_a, where $c_1 = 60$ eV, $c_2 = 0.57$ MeV, and $c_3 = 250$ MeV. This is a crucial point for our test.

Parenthetically, it should be mentioned that the ultimate outcome of neutrino-oscillation experiments will place strong constraints on whether the sets $\{\nu_i\}_a$ can indeed contain more than just the single members $\nu_{i=a}$.

A final comment is that by enumeration of states it is easy to show that the bounds (2.1)–(2.4) together imply the corresponding bounds on the mass-ordered eigenbasis

$$m(\nu_{[j=a]}) < c_a, \quad a=1,2,3. \tag{2.5}$$

Clearly, (2.1)–(2.5) do not imply that $m(\nu_j) < m(\nu_k)$ if $j<k$, although if this inequality did not hold, then some of the ν_i would have to satisfy stricter bounds than they would if it did hold. For example, consider the illustrative case in which $m(\nu_2)<m(\nu_1)<m(\nu_i)$ for all $i>2$. Then $\nu_{[1]}=\nu_2$ and $\nu_{[2]}=\nu_1$ so that ν_2 would not only have to satisfy (2.2) but the stronger limit (2.1).

C. The M_{l2} test

The first and perhaps most sensitive test based on the observation in Sec. II A makes use of the decays $M^+ \to l_a^+ \nu_{l_a}$, where $M=\pi$ or K and $l_a=e$ or μ.[21] It may be recalled that in the SIN $\pi_{\mu 2}$ experiment it was tacitly assumed that ν_μ was a particle of definite mass and consequently the muon momentum spectrum would consist of a single monochromatic[22] line at $|\vec{p}_\mu| = \lambda^{1/2}(m_\pi{}^2, m_\mu{}^2, \text{“}m(\nu_\mu)\text{”}^2)/(2m_\pi)$, where

$$\lambda(x,y,z) \equiv x^2+y^2+z^2-2(xy+yz+zx). \tag{2.6}$$

Thus the precise measurement of $|\vec{p}_\mu|$ performed in this experiment was considered to yield an upper bound on “$m(\nu_\mu)$”. The same tacit assumption is evident in other experiments on π_{l2} and K_{l2} decay such as the Columbia-Nevis measurement[23] of $B(\pi^+ \to e^+\nu_e)/B(\pi^+ \to \mu^+\nu_\mu)$ and the CERN-Heidelberg K_{l2} experiment.[24,25] In fact, however, if neutrinos are massive (and nondegenerate) the l_a momentum and energy spectra would consist of $k_{M,a}$ monochromatic[22] lines at

$$|\vec{p}_a^{\,(i)}| = \frac{m_M}{2}\lambda^{1/2}(1, \delta_a^M, \delta_i^M) \tag{2.7}$$

or equivalently

$$E_a^{(i)} = \frac{m_M}{2}(1+\delta_a^M-\delta_i^M), \tag{2.8}$$

where

$$\delta_a^M \equiv \frac{m_{l_a}{}^2}{m_M{}^2} \tag{2.9}$$

and

$$\delta_i^M \equiv \frac{m(\nu_i)^2}{m_M{}^2}. \tag{2.10}$$

In Eqs. (2.7)–(2.10) we have used the abbreviations $|\vec{p}_a^{\,(i)}|$ for $|\vec{p}_{l_a}^{\,(i)}|$ and similarly for $E_{l_a}^{(i)}$ and $\delta_{l_a}^M$. Obviously $k_{M,a}$ is equal to the number of ν_i, $i=1,\ldots,n$, for which $m(\nu_i)<m_M-m_a$. To our knowledge, no experiment has specifically searched for this clear signature of massive neutrinos and lepton mixing, and accordingly such a search for additional spectral lines in $|\vec{p}_a|$ and E_a was proposed in Ref. 1.

An illustrative example of a possible momentum spectrum in K_{e2} decay is shown in Fig. 1. The lines represent the spectra in the limit of no l_a energy loss, perfect spectrometer resolution, and infinite statistical accuracy; the smooth enveloping curves schematically represent the spectra which would actually be observed experimentally in the presence of imperfect running conditions and of backgrounds. The values of $|\vec{p}_a|$ and E_a for the conventional case where $m(\nu_i)=0$ for all i are denoted by $|\vec{p}_a|_0$ and $(E_a)_0$. The LDC and any LSC modes would be observed to have essentially these values of $|\vec{p}_a|$ and E_a. Further, it is assumed that $\nu_i=\nu_{[i]}$ and the $|U_{ai}|$, $a=1,2$, $i\neq a$, are small even for $\nu_i \in \{\nu_{i_L}\}$, i.e., for a given a there is only one LDC mode. The dominant line in the spectrum of Fig. 1 is due to the decay $K^+ \to e^+\nu_1$, while at slightly lower $|\vec{p}_e|$ there is a second line of much smaller strength due to the decay $K^+ \to e^+\nu_2$. The separation and height of the LSC line are exaggerated for clarity. In this illustration there are two HSC lines due to the decays $K^+ \to e^+\nu_i$, $i=3,4$. The masses $m(\nu_3)$ and $m(\nu_4)$ are sufficiently large so that these lines are clearly separated from the dominant ν_1 line. The heights of the HSC lines relative to that of the DC line are not exactly to scale; the precise limits on their heights, as functions of the $m(\nu_i)$, will be discussed further for both π_{l2} and K_{l2} decays in this and the next section.

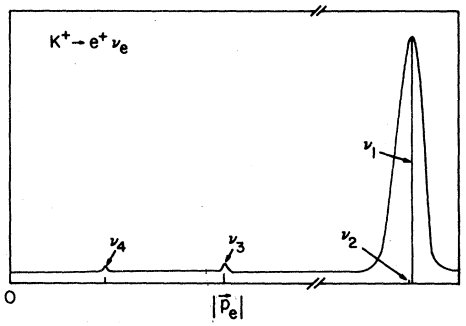

FIG. 1. Schematic charged-lepton momentum spectra for K_{e2} decay. For graphical clarity, parts of the plot are not drawn to scale. See the text for further explanation.

Let us describe this test in greater detail. First, it has the advantage of being purely kinematic, independent of whether other exotic effects, such as very weakly coupled currents with different Lorentz structure than $V-A$, or flavor-changing Higgs bosons are present. Second, the l_a spectrum is discrete, and each HSC ν_i mode is characterized by a monochromatic[22] value of $|\vec{p}_a^{(i)}|$ and $E_a^{(i)}$, so that one can search on an event-by-event basis for HSC ν_i lines. This could never be done in a decay involving three or more particles in the final state, such as K_{l3}, μ, or nuclear β decay, since any HSC ν_i modes present would not be characterized by unique values of momenta or energies of any of the other final-state particles. Third, if an HSC ν_i signal is observed, one can immediately determine independently and unambiguously for each line the corresponding value of $m(\nu_i)$. A very important merit of the test is that this mass determination is independent of the lepton mixing angles. This feature sets the present test apart from other tests for neutrino masses and lepton mixing. For example, by comparing the measured values of the integrated ratios $B(M^+ \to e^+\nu_e)/B(M^+ \to \mu^+\nu_\mu)$ where $M=\pi$ or K, with the values predicted by the conventional $V-A$ theory in which $m(\nu_i)=0$ for all i, one can place certain constraints on possible neutrino masses and lepton mixing. These constraints will be analyzed in Sec. III. However, these ratios reflect the combined effect of all the HSC modes which are present in the respective decays and are incapable of determining $m(\nu_i)$ or $|U_{ai}|$ for any particular HSC ν_i mode. Similarly, neutrino-oscillation experiments can only yield strongly correlated information on the quantities $[m(\nu_i)^2 - m(\nu_j)^2]$ and $U_{bi}^* U_{ai}$ (no sum on i), but not the $m(\nu_i)$ in isolation. (On the other hand, as is well known, neutrino-oscillation experiments have the great advantage of being sensitive to extremely small neutrino masses, far below the minimal level detectable in particle decays.) Fourth, knowing the mass $m(\nu_i)$ and, at this point, assuming that the relevant couplings are $V-A$, one can use simple kinematics to determine the relative coupling strength

$$R_{ai} \equiv \frac{|U_{ai}|^2}{\sum_{j\in\{j_L\}} |U_{aj}|^2} \simeq |U_{ai}|^2 \tag{2.11}$$

for each of the HSC ν_i lines. It is an important feature of our complete test that this assumption need not be made blindly but can be checked by a measurement of the polarization of the l_a^+ from the HSC $M^+ \to l_a^+\nu_i$ decay (see below). It is obvious that the conventional experimental evidence that charged-current leptonic weak interactions are $V-A$, although derived effectively only from data on DC neutrino modes, also implies that $l_a\nu_i$ vertices are $V-A$ for SC ν_i, given the standard gauge-theory framework and the nature of the transformation (1.1). However, one can, at a purely phenomenological level, conceive of a situation in which some of the HSC ν_i lines arose mainly from $V-A$ interactions while others arose dominantly from non-left-handed V,A vertices or S,P vertices.[26] It is in this general phenomenological setting that the full value of the polarization measurement is evident.

The rate for the mode $M^+ \to l_a^+\nu_i$, relative to that for the conventional decay $M^+ \to l_a^+\nu_{l_a}$ where $m(\nu_i)=0$ for all i, is given by

$$\frac{\Gamma(M^+ \to l_a^+\nu_i)}{\Gamma(M^+ \to l_a^+\nu_{l_a})_0} = \frac{|U_{ai}|^2 \rho(\delta_a^M, \delta_i^M)}{\delta_a^M(1-\delta_a^M)^2}, \tag{2.12}$$

where

$$\rho(x,y) = f_{\mathfrak{M}}(x,y)\lambda^{1/2}(1,x,y), \tag{2.13}$$

$$f_{\mathfrak{M}}(x,y) = x+y-(x-y)^2, \tag{2.14}$$

and the function λ was defined in Eq. (2.6). In Eq. (2.13) we have displayed the kinematic rate factor ρ in terms of a part proportional to the matrix element squared, $f_{\mathfrak{M}} \propto |\mathfrak{M}(M^+ \to l_a^+\nu_i)|^2$, and a part, $\lambda^{1/2}(1,\delta_a^M,\delta_i^M)$, proportional to the two-body phase-space factor. What would actually be measured experimentally would be the ratio of the HSC ν_i rate to the sum of light neutrino rates,

$$\frac{\Gamma(M^+ \to l_a^+\nu_i)_{\mathrm{HSC}\,i}}{\sum_{j\in\{j_L\}} \Gamma(M^+ \to l_a^+\nu_j)} \simeq \frac{|U_{ai}|^2 \rho(\delta_a^M, \delta_i^M)}{(\sum_{j\in\{j_L\}} |U_{aj}|^2)\delta_a^M(1-\delta_a^M)^2}. \tag{2.15}$$

However, since the totality of experimental constraints require that for $j \neq a$

$$\sum_{\substack{j\in\{j_H\} \\ j\neq a}} |U_{aj}|^2 \equiv 1 - \sum_{j\in\{j_L\}} |U_{aj}|^2 \ll 1, \tag{2.16}$$

the sum of coupling coefficients in the denominator of the expression on the right-hand side of Eq. (2.15) is quite close to unity. Consequently, this expression is essentially equal to the right-hand side of Eq. (2.12). Note that in the simple case where there is only one DC mode for each a, the sum referred to above would consist of just one dominant term, $|U_{aj}|^2$, $j=a$. For an analysis of the kinematics of HSC ν_i modes in M_{l2} decay, and in particular a comparison with the $m(\nu_i)=0$ case, the following definitions will be useful:

$$\bar{f}_{\mathfrak{M}}(\delta_a^M, \delta_i^M) \equiv \frac{f_{\mathfrak{M}}(\delta_a^M, \delta_i^M)}{f_{\mathfrak{M}}(\delta_a^M, 0)} = \frac{f_{\mathfrak{M}}(\delta_a^M, \delta_i^M)}{\delta_a^M(1-\delta_a^M)}, \tag{2.17}$$

$$\bar{\lambda}^{1/2}(1,\delta_a^M,\delta_i^M)\equiv\frac{\lambda^{1/2}(1,\delta_a^M,\delta_i^M)}{\lambda^{1/2}(1,\delta_a^M,0)}=\frac{\lambda^{1/2}(\delta_a^M,\delta_i^M)}{(1-\delta_a^M)}\,, \tag{2.18}$$

and

$$\bar{\rho}(\delta_a^M,\delta_i^M)\equiv\frac{\rho(\delta_a^M,\delta_i^M)}{\rho(\delta_a^M,0)}=\frac{\rho(\delta_a^M,\delta_i^M)}{\delta_a^M(1-\delta_a^M)^2}\,. \tag{2.19}$$

The behavior of $\bar{f}_{\mathfrak{M}}$, $\bar{\lambda}^{1/2}$, and $\bar{\rho}$, as functions of $m(\nu_i)$, is shown for the decays $\pi^+\to\mu^+\nu_i$, $\pi^+\to e^+\nu_i$, $K^+\to\mu^+\nu_i$, and $K^+\to e^+\nu_i$ in Figs. 2–5, respectively. As is evident in these figures, the kinematic helicity effect acts to enhance $\bar{f}_{\mathfrak{M}}$ as $m(\nu_i)$ increases; for fixed δ_a^M, f increases monotonically from a minimum of $\delta_a^M(1-\delta_a^M)$ at $m(\nu_i)=0$. If $m_{l_a}<m_M/4$, then $f_{\mathfrak{M}}$ will rise to a maximum at $\delta_i^M=\frac{1}{2}+\delta_a^M$, i.e.,

$$m(\nu_i)_{(f_{\mathfrak{M}})_{\max}}=\frac{m_M}{\sqrt{2}}(1+2\delta_a^M)^{1/2} \tag{2.20}$$

and then decrease for larger $m(\nu_i)$. The value of $f_{\mathfrak{M}}$ at this point is

$$(f_{\mathfrak{M}})_{\max}=2\delta_a^M+\tfrac{1}{4}\,. \tag{2.21}$$

If, on the contrary, $m_{l_a}>m_M/4$, then the point (2.20) lies outside of the physical region, so that $f_{\mathfrak{M}}$ will increase monotonically throughout the entire range of allowed values of $m(\nu_i)$. The inequality $m_{l_a}<m_M/4$ is satisfied for the decays $M^+\to e^+\nu_e$, $M=\pi$ or K, and $K^+\to\mu^+\nu_\mu$, but not for the decay $\pi^+\to\mu^+\nu_\mu$. The resulting behavior of $\bar{f}_{\mathfrak{M}}$ is clear from Figs. 2–5. The magnitude of the increase in $f_{\mathfrak{M}}$ is indicated by $(\bar{f}_{\mathfrak{M}})_{\max}$; for $K\to\mu^+\nu_i$ decay this quantity is roughly eight, whereas for the $M^+\to e^+\nu_i$ decays it is approximately equal to $(4\delta_a^M)^{-1}$ and hence is quite large. The exact values of $m(\nu_i)_{(f_{\mathfrak{M}})_{\max}}$ and $(\bar{f}_{\mathfrak{M}})_{\max}$ are listed for reference in Table I. In all of the decays considered, the helicity enhancement of $f_{\mathfrak{M}}$ offsets the monotonic decrease in the phase-space factor $\lambda^{1/2}$, so that the total kinematic rate factor

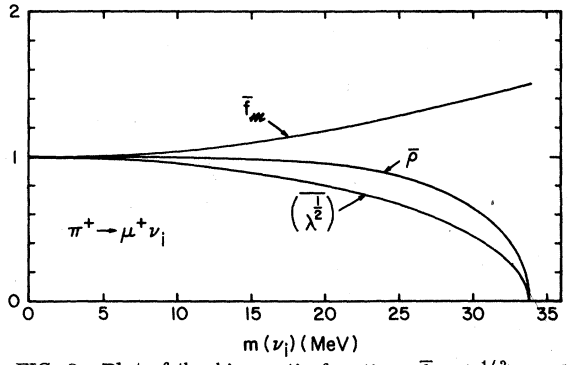

FIG. 2. Plot of the kinematic functions $\bar{f}_{\mathfrak{M}}$, $(\lambda^{1/2})$, and $\bar{\rho}$ for the decay $\pi^+\to\mu^+\nu_i$.

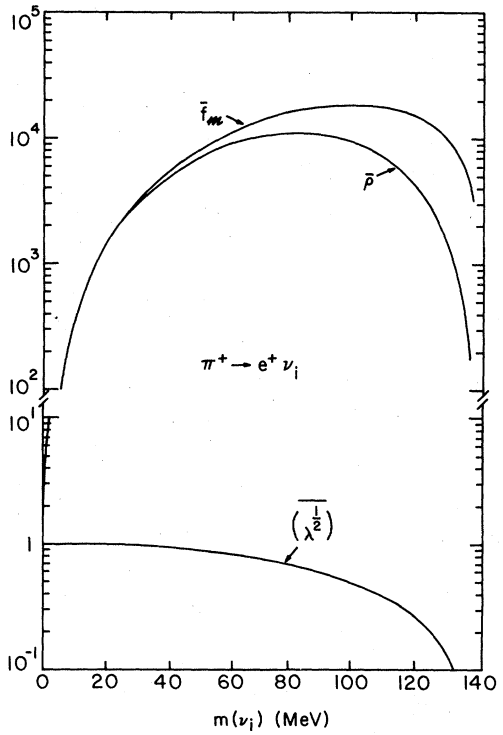

FIG. 3. Same as Fig. 2 but for the decay $\pi^+\to e^+\nu_i$.

ρ increases to a maximum at a nonzero value of $m(\nu_i)$ and then decreases to zero as $m(\nu_i)$ approaches its kinematic limit. As can be seen from Figs. 2 and 3, in $\pi^+\to\mu^+\nu_i$ decay this is a very slight effect, while in $K^+\to\mu^+\nu_i$ decay it is substantial. In the $M^+\to e^+\nu_i$ decays shown in

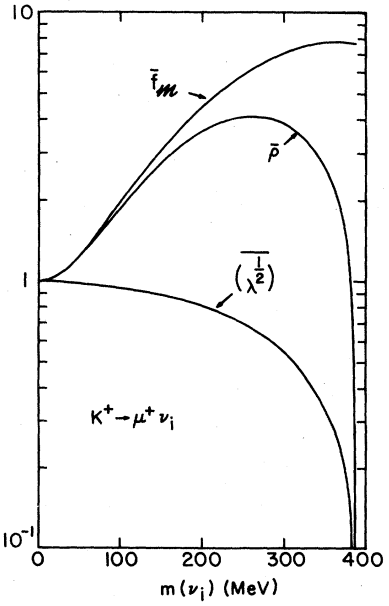

FIG. 4. Same as Fig. 2 but for the decay $K^+\to\mu^+\nu_i$.

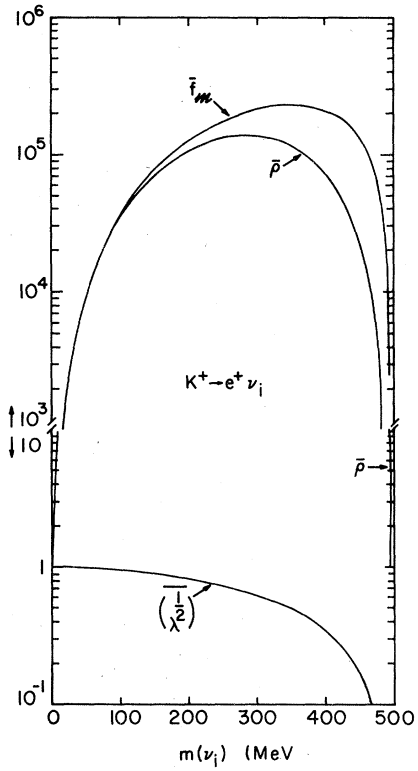

FIG. 5. Same as Fig. 2 but for the decay $K^+ \to e^+ \nu_i$.

Figs. 4 and 5, the drastic increase in $f_{\pi\mu}$ completely overwhelms the decrease in the phase-space factor until $m(\nu_i)$ reaches values quite near to the respective end points. We shall denote the value of $m(\nu_i)$ at which $\bar{\rho}$ reaches its maximum as $m(\nu_i)_{\rho_{max}}$ and the corresponding value of $\bar{\rho}$ as $\bar{\rho}_{max}$. These quantities are listed in Table I for the four decays of interest. Note that a simple expression for $m(\nu_i)_{\rho_{max}}$ applies for the $M^+ \to e^+ \nu_i$ decays, where for $\delta_i^M \gg \delta_e^M$ [which inequality is satisfied in the vicinity of $m(\nu_i)_{\rho_{max}}$], $\rho \simeq \delta_i^M (1 - \delta_i^M)^2$ and hence

$$m(\nu_i)_{\rho_{max}}|_{M^+ \to e^+ \nu_i} \simeq \frac{m_M}{\sqrt{3}} . \tag{2.22}$$

Further discussion of the function $\rho(x, y)$ will be given in Sec. IV. Finally, for later purposes it is useful to list the values of $m(\nu_i)$ at which $\bar{\rho}$ crosses through one on its descent from the maximum to zero. We denote this value by $m(\nu_i)_1$; for the decays $\pi^+ \to \mu^+ \nu_i$ and $K^+ \to \mu^+ \nu_i$, $m(\nu_i)_1 = 4.86$ and 382 MeV, respectively. In the decays $M^+ \to e^+ \nu_i$, $m(\nu_i)_1$ is very close to the respective end points $m_M - m_{l_a}$.

From this analysis of the kinematics of $M^+ \to l_a \nu_i$ decays the great sensitivity of the M_{l2} is evident. A search for HSC spectral lines in M_{l2} decay is not inhibited by kinematic suppression until $m(\nu_i)$ reaches almost its phase-space limit, as a consequence of the helicity enhancement effect together with the slow falloff of the two-body phase-space factor. Indeed, in $K^+ \to \mu^+ \nu_i$ decay and, to an extreme degree, in the $M^+ \to e^+ \nu_i$ decays there is strong kinematic enhancement up to quite large values of $m(\nu_i)$. This property stands in sharp contrast to the situation for three-body decays involving massive neutrinos. For example, in the decay $\mu \to \nu_i e \bar{\nu}_j$ (HSC i, LDC j) for the value $m(\nu_i)/m_\mu = 0.5$ the analogous kinematic rate factor is only ~0.16 of its value at $m(\nu_i) = 0$. (Further details on μ decay are given in paper II.) Because of this feature and the monochromatic nature of the HSC ν_i lines, the test is capable of finding a very small signal. Alternately, if no HSC signal is observed in $M^+ \to l_a^+ \nu_{i_a}$ decay at momentum $|\vec{p}_a^{\,(i)}|$ or energy $E_a^{(i)}$ corresponding to a mass $m(\nu_i)$, with a strength, relative to the dominant light-neutrino peak, greater than $\epsilon(M_{l_{a2}}; m(\nu_i))$ [where the quantity $\epsilon(M_{l_{a2}}; m(\nu_i))$ is determined by the statistics and accuracy of a given $M_{l_{a2}}$ experiment], then one can set a commensurately stringent upper bound on the HSC coupling coefficient of the following form: If

$$m_{min}(M_{l_{a2}}) < m(\nu_i) < m_{max}(M_{l_{a2}}) , \tag{2.23a}$$

then

TABLE I. Maximal values of $\bar{f}_{\pi\mu}$ and the total normalized kinematic rate factor $\bar{\rho}$, together with corresponding values of $m(\nu_i)$, for the decays $M^+ \to l_a^+ \nu_i$, where $M^+ = \pi$, K, and $l_a = e, \mu$. See text for definitions.

Decay	$m(\nu_i)_{(f_{\pi\mu})_{max}}$ (MeV)	$(\bar{f}_{\pi\mu})_{max}$	$m(\nu_i)_{\rho_{max}}$ (MeV)	$\bar{\rho}_{max}$
$\pi^+ \to \mu^+ \nu_i$	$m_\pi - m_\mu = 33.9$ no critical point; $(\bar{f}_{\pi\mu})_{max}$ reached at end point of $m(\nu_i)$	1.50	3.4	1.000 04
$\pi^+ \to e^+ \nu_i$	98.7	1.87×10^4	80.6	1.11×10^4
$K^+ \to \mu^+ \nu_i$	365	7.82	263	4.13
$K^+ \to e^+ \nu_i$	349	2.33×10^5	285	1.38×10^5

$$|U_{ai}|^2 \simeq R_{ai} < \frac{\epsilon(M_{l_a 2}; m(\nu_i))}{\bar{\rho}(\delta_a^M, \delta_i^M)} .$$

In the most conservative application of the test, the quantity $m_{\min}(M_{l_a 2})$ would represent the minimum value of $m(\nu_i)$ such that the HSC ν_i peak at $|\vec{p}_a| = |\vec{p}_a^{(i)}|$ or equivalently $E_a = E_a^{(i)}$ is experimentally resolvable from the dominant light-neutrino peak at $|\vec{p}_a|_0$ or $(E_a)_0$ in the indicated decay. However, as was discussed above, one can, with greater difficulty and caution, search for HSC ν_i peaks lying within the main light-neutrino peak and, if none is found, infer the bound (2.23a) for smaller values of $m_{\min}(M_{l_a 2})$ than the peak resolution value. The constant $m_{\max}(M_{l_a 2})$ could, in a properly designed experiment, approach the kinematic limit $m_M - m_{l_a}$. However, because previous experiments did not recognize the possibility of many spectral lines in M_{l2} decay and hence did not consider the lower ranges of $|\vec{p}_a|$ and E_a to be interesting for this decay, they usually set cuts quite close to $|\vec{p}_a|_0$ or $(E_a)_0$ and in many cases did not even record or analyze events below these cuts. Hence, in most applications of our test to present data, the values of $m_{\max}(M_{l_a 2})$, as determined by these cuts are substantially below $m_M - m_{l_a}$. In a given $M_{l_a 2}$ experiment, the upper limit $\epsilon(M_{l_a 2}; m(\nu_i))$ varies somewhat as a function of the bin in $|\vec{p}_a|$ or E_a, or equivalently in $m(\nu_i)$, which one is testing. However, for our applications to existing data this variation is not too great, and we have made the conservative choice of using a constant $\epsilon(M_{l_a 2})$ equal to the maximum value of $\epsilon(M_{l_a 2}; m(\nu_i))$ over the range of $m(\nu_i)$ specified in (2.23a). The bound (2.23a) can be viewed in two ways: first, if one considers a value of $m(\nu_i)$ which lies in the range covered, then one can use the bound to conclude that the coupling strength of ν_i to l_a, $|U_{ai}|^2$, must be smaller than the indicated expression. Second, if one were to entertain the hypothesis that $|U_{ai}|^2$, HSC i, is larger than the limit given by (2.23a), one could use the bound in its logically equivalent contrapositive form to determine the allowed values of $m(\nu_i)$ consistent with this hypothesis: If

$$R_{ai} > \frac{\epsilon(M_{l_a 2}; m(\nu_i))}{\bar{\rho}(\delta_a^M, \delta_i^M)} , \qquad (2.23b)$$

then there exists no $m(\nu_i)$ in the range $m_{\min}(M_{l_a 2}) < m(\nu_i) < m_{\max}(M_{l_a 2})$.

The ultimate sensitivity of this test is limited by such factors as the e or μ energy loss in the target and by soft bremsstrahlung, the resolution in $|\vec{p}_a|$ or E_a of the detector, and the relevant backgrounds. A background process for $M^+ \to l_a^+ \nu_i$ (HSC i) is the radiative decay $M^+ \to l_a^+ \nu_i \gamma$ (LDC j), where the photon is missed by the detection apparatus. For the decays $K^+ \to l_a^+ \nu_i$ ($a = 1, 2$; HSC i) additional backgrounds arise, respectively, from the decays $K^+ \to \pi^0 l_a^+ \nu_j$ (LDC j), where both photons from the π^0 are missed. Further, for the decay $K^+ \to \mu^+ \nu_i$ (HSC i) there are other backgrounds from the processes $K^+ \to \pi^+ \pi^0$ and, with a smaller branching ratio, $K^+ \to \pi^+ \pi^0 \pi^0$, where the two or four photons from the π^0's are all missed and the π^+ is either misidentified as a μ^+ or (if sufficiently slowed down in the target) actually decays to $\mu^+ \nu_j$ (LDC j). These backgrounds share several common features which can be used effectively to distinguish them from the signal. First, they all involve one or more photons in the final state, so that events due to these processes can be vetoed in an experiment with good photon detection over a large solid angle. Second, they yield continuous $|\vec{p}_a|$ and E_a distributions, in contrast to the monochromatic signal from $M^+ \to l_a^+ \nu_i$ decay. Third, these are approximately calculable and hence, even with imperfect vetoing of photons, they could be subtracted away from the raw event sample (see paper III). Moreover, for a given M and l_a there are ranges of $|\vec{p}_a|$ and E_a where certain of the backgrounds are absent. A different kind of background is present in the search for HSC $M^+ \to e^+ \nu_i$ events. Since $B(M^+ \to \mu^+ \nu_{\mathrm{LDC}\ j}) \gg B(M^+ \to e^+ \nu_{\mathrm{LDC}\ j})$ and since the rate for $M^+ \to e^+ \nu_{\mathrm{HSC}\ i}$ is constrained to be rather small compared to that for $M^+ \to e^+ \nu_{\mathrm{LDC}\ j}$, a search for $M^+ \to e^+ \nu_{\mathrm{HSC}\ i}$ lines with momentum $|\vec{p}_e^{(i)}|$ ($M^+ \to e^+ \nu_i$) in the vicinity of $|\vec{p}_\mu|_0 (M^+ \to \mu^+ \nu_\mu)$ is hindered somewhat by the fact that μ-e misidentification would produce spurious events of this type (and similarly for a search using the energy spectrum in $M^+ \to e^+ \nu_e$ decay). The severity of this background depends on the width of the light-neutrino peaks in the $M^+ \to \mu^+ \nu_\mu$ decays and on the reliability with which the μ-e separation can be performed. Of course past experiments *have* achieved extremely good μ-e separation.[24]

Concerning the question of whether the test would be more advantageously applied to $M^+ \to e^+ \nu_e$ or $M^+ \to \mu^+ \nu_\mu$ decays, several comments are relevant. Since the helicity enhancement of the ith HSC mode is much greater, relative to the LDC mode(s) in the former case, the electron modes offer potentially much greater sensitivity to small coupling coefficients $|U_{1i}|^2$ than do the muon modes to the corresponding coefficients $|U_{2i}|^2$. Also, of course, if $m(\nu_i)$ is sufficiently large, the decay of an $M^+ = \pi^+$ or K^+ into $\mu^+ \nu_i$ may be kinematically forbidden while the decay into $e^+ \nu_i$ is still allowed. On the other

hand, to the extent that lepton mixing is hierarchical, as quark mixing appears to be,[6] i.e., to the extent that $|U_{ai}| > |U_{bj}|$ if $|a-i| < |b-j|$, one would expect that a given HSC mode i would be more weakly coupled in $M^+ \to e^+\nu_i$ than in $M^+ \to \mu^+\nu_i$ decay. Furthermore, since any HSC modes must be small compared to the corresponding LDC modes, and since $B(M^+ \to \mu^+\nu_\mu) \gg B(M^+ \to e^+\nu_e)$, the search for HSC ν_i modes allowed by phase space in the former decay would presumably have the advantage of considerably greater statistics than in the latter. (The exception to this usual situation would occur if $|U_{2i}|^2 \ll |U_{1i}|^2$.)

D. Application of the M_{l2} test to existing data

Although no experiment has specifically searched for additional spectral lines in $|\vec{p}_a|$ or E_a, there are data to which our test can be applied. This task was carried out in Ref. 1. Here we shall elaborate on the resulting bounds and give some further applications. For discussions of the effects of experimental cuts in restricting the ranges of $m(\nu_i)$ over which the search for HSC ν_i peaks can be conducted, it is helpful to have graphs indicating how the various kinematic quantities in M_{l2} decay depend on $m(\nu_i)$. Accordingly, for reference we plot the l_a^+ momentum, energy, kinetic energy $T_a^{(i)}$ (solid curves), and velocity (dotted curve) for the decays $\pi^+ \to \mu^+\nu_i$, $\pi^+ \to e^+\nu_i$, $K^+ \to \mu^+\nu_i$, and $K^+ \to e^+\nu_i$ in Figs. 6–9, respectively. In order to present the results in a uniform manner we have actually plotted the normalized quantities $\bar{p}_a \equiv |\vec{p}_a^{(i)}|/|\vec{p}_a|_0$, and similarly with $\bar{E}_a$ and $\bar{T}_a$ (but not β_a). The horizontal dot-dashed lines represent certain experimental cuts, which will be dealt with below for each experiment individually. Even before proceeding

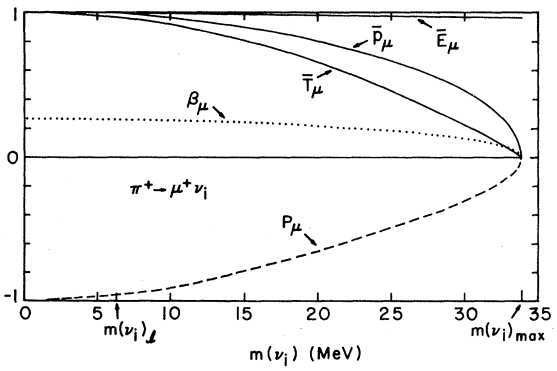

FIG. 6. Kinematic quantities, normalized by their $m(\nu_i)=0$ values and shown as the solid curves, velocity (dotted curve), and polarization (dashed curve) for the μ^+ in the decay $\pi^+ \to \mu^+\nu_i$.

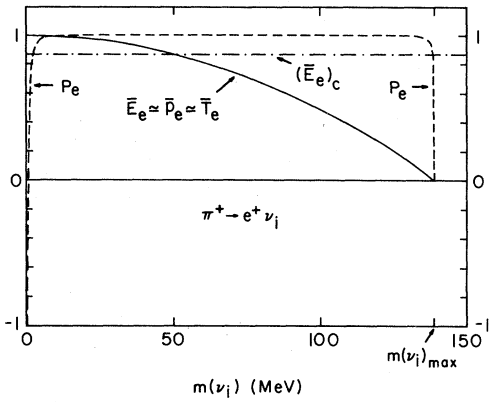

FIG. 7. Kinematic quantities normalized as in Fig. 6 (solid curves) and polarization for the e^+ in the decay $\pi^+ \to e^+\nu_i$. For graphical clarity the dotted line for β_e is omitted; β_e is essentially unity except for $m(\nu_i)$ extremely near its maximum value. The normalized energy cut applied in the experiment of Ref. 23 is shown as the horizontal dot-dashed line.

to consider these experiments, we are compelled to remark on a very striking feature of these graphs, namely, how great a range of $|\vec{p}_a|$ or E_a—essentially everything lying below the lowest horizontal dot-dashed lines—remains to be explored in high-statistics counter experiments.

Let us begin with $\pi^+ \to \mu^+\nu_\mu$ decay and consider the data from the most recent and accurate experiment, by Daum *et al.*[8] at SIN, which utilized a precision magnetic spectrometer to measure $|\vec{p}_\mu|$ in this decay. It should be mentioned that there were previous measurements of $|\vec{p}_\mu|$ or E_μ in $\pi_{\mu 2}$ decay. These included old emulsion experiments[27] and at least one specific bubble-chamber experiment.[28] Since these were generally characterized by rather different operating conditions than the high-precision counter experi-

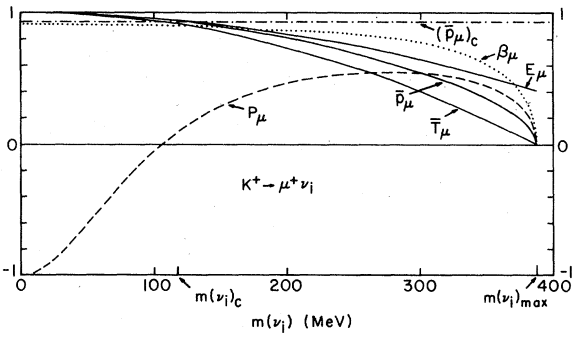

FIG. 8. Normalized kinematic quantities (solid curves), velocity (dotted curve), and polarization (dashed curve) for the μ^+ in the decay $K^+ \to \mu^+\nu_i$. The normalized lower momentum cut applied in the experiment of Ref. 24 is shown as the horizontal dot-dashed line.

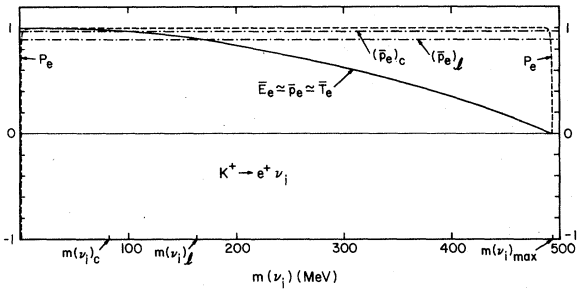

FIG. 9. Normalized kinematic quantities (solid curves) and polarization for the e^+ in the decay $K^+ \to e^+ \nu_i$. For the same reason as in Fig. 7 the dotted curve for the velocity β_e is omitted. The normalized lower momentum cut used in the experiment of Ref. 24, $(\bar{p}_e)_c$, is shown as a horizontal dot-dashed line, corresponding to the value $m(\nu_i) = m(\nu_i)_c$. The normalized lowest value of momentum for which e^+ data was presented in Ref. 23, $(\bar{p}_e)_l$, is indicated by a slightly lower dot-dashed line, corresponding to $m(\nu_i) = m(\nu_i)_l$.

ments, they will be discussed separately later in this section. There was also a counter experiment which used a Ge(Li) detector to measure E_μ (Ref. 29); however, the E_μ spectrum may have contained cuts which were not explicitly stated because they did not significantly affect the measurement reported there, but which could have eliminated possible HSC ν_i events.[29] Finally, there was a magnetic-spectrometer counter experiment by a Liverpool collaboration[30] which was similar to, but had somewhat lesser statistics than, the SIN experiment. We have analyzed the $|\vec{p}_\mu|$ spectrum from this Liverpool experiment and have found, as expected, that the resulting bounds are weaker than, but in agreement with, those which can be extracted from the SIN data. In Fig. 10 we reproduce the data of Daum *et al.*[8] The horizontal axis is, of course, proportional to $|\vec{p}_\mu|$, but no absolute momentum scale was given. Further details concerning this data are contained in Ref. 8. Spectra 1–12 were taken with a spectrometer momentum acceptance quoted as 0.64% [full width at half maximum (FWHM)], which effectively meant that the lowest data point occurred at $|\vec{p}_\mu|_{min}/|\vec{p}_\mu|_0 \simeq 0.98$. Spectra 13–21 were taken with a narrower acceptance of 0.40% (FWHM), or equivalently $|\vec{p}_\mu|_{min}/|\vec{p}_\mu|_0 \simeq 0.99$ for the lowest data point. The value of $|\vec{p}_\mu|_{min}$ for the data with the wider momentum acceptance corresponds to $m(\nu_i)_{max} \simeq 6.4$ MeV; thus it is only possible to search for HSC ν_i modes with $m(\nu_i)$ less than or equal to this value in the SIN data. For clarity the dot-dashed line representing the lowest value of $|\vec{p}_\mu|$ accepted is omitted from Fig. 6, but the equivalent value of $m(\nu_i)$ is marked as $m(\nu_i)_l$,

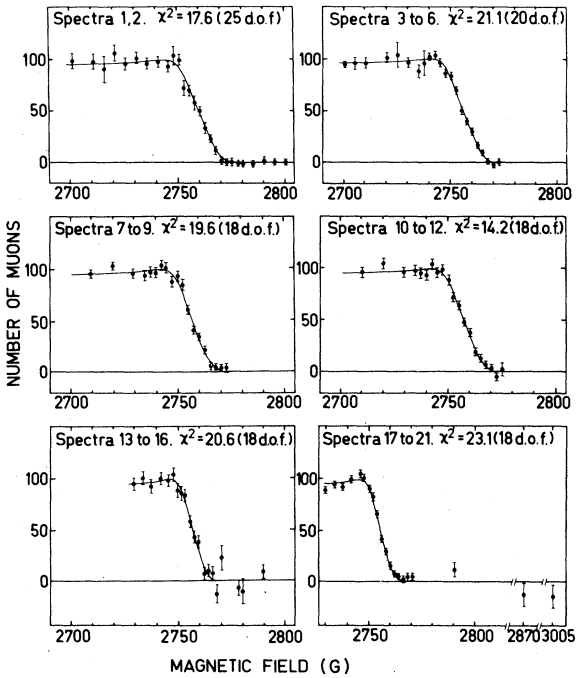

FIG. 10. The μ^+ momentum spectra from the six data-taking periods of the SIN $\pi_{\mu 2}$ experiment of Daum *et al.* (Ref. 8). The vertical axis represents the number of μ^+'s, after background subtraction, normalized to 100 events at the maximum of the theoretical curve. The solid curve is the fitted theoretical curve; the χ^2 values for the fits are shown in the graphs. For further details, see Ref. 8 and the text.

where the subscript "l" stands for "lowest $|\vec{p}_\mu|$." The experimental appearance of the light-neutrino line at $|\vec{p}_\mu|_0$ is a shoulder, with a tail extending below $\sim 0.98\ |\vec{p}_\mu|_0$. An HSC line would thus appear as a second shoulder.

From an analysis of the SIN data we can thus rule out an HSC ν_i signal with strength greater than about ~5% of that of the main light-neutrino peak. A more precise number could be obtained by fitting the data to two ν_i lines, one due to the DC decay $\pi^+ \to \mu^+ \nu_2$ and the other due to the decay $\pi^+ \to \mu \nu_{HSC\ i}$, with four parameters: the values of $m(\nu_2)$ and $m(\nu_i)$ and the heights of the ν_2 and ν_i peaks. One could then test to see if the χ^2 for this two-peak fit was better than that of the conventional one-peak fit. However, this would require a very detailed Monte Carlo simulation of the muon energy loss and spectrometer-resolution smearing, incorporating the specific geometry of the SIN experiment. It would also be necessary to know the precise point-by-point background subtractions. Consequently, this task would seem to be more appropriately performed by the experimentalists than in this work. Ideally, a general analysis of data on $M^+ \to l_a^+ \nu_{l_a}$ decay would begin

with a standard four-parameter fit depending on the masses and heights of not just the DC $M^+ \to l_a^+ \nu_{i=a}$ peak but also a possible weaker light-neutrino peak due to the decay $M^+ \to l_a^+ \nu_j$, where $j=2$ if $a=1$ and $j=1$ if $a=2$. To this one would then add the mass and height of a candidate HSC ν_i peak, thereby obtaining a full six-parameter fitting routine to test for such HSC peaks. However, the simple method used here will suffice for our present purposes. Choosing $m_{\min}(\pi_{\mu 2})$ to be the maximum value of a DC neutrino mass which would be observed by the experiment, and $m_{\max}(\pi_{\mu 2})$ as given above, we then have the following bound: If

$$0.6 \lesssim m(\nu_i) \lesssim 6 \text{ MeV},$$

then (2.24)

$$|U_{2i}|^2 \simeq R_{2i} \lesssim \frac{0.05}{\bar{\rho}(\delta_\mu^\pi, \delta_i^\pi)} .$$

As is evident from Fig. 2, over this range of $m(\nu_i)$, $\bar{\rho}$ is extremely close to unity, so that the upper bound placed on R_{2i} is essentially constant at ~0.05.

Continuing with magnetic-spectrometer experiments, we next apply our test to the CERN-Heidelberg data on $|\vec{p}_a|$ in $K_{l_a 2}$ decay, where $l_a = e$ or μ.[24,25] Before doing this, one should note that there were a number of earlier experiments on $K_{l_a 2}$ decay.[31,32] We have examined the data from the subset[32] of these experiments to which our test can be applied and have found that the constraints which can be derived are weaker than those which follow from the data of Refs. 24 and 25. (This was to be expected, since the CERN-Heidelberg experiment had greater accuracy and statistical weight than previous experiments to which the test could be applied.)

A momentum spectrum from an early version of the experiment which shows the $K_{\mu 2}$ monitor sample is given in the first paper of Ref. 24. Subsequently, in conjunction with a study of the decay $K^+ \to e^+ \nu_e \gamma$,[25] the same group presented an improved $|\vec{p}_\mu|$ spectrum for $K_{\mu 2}$ decay with a much smaller background outside of the main peak. This latest spectrum is reproduced for reference in Fig. 11. The final $|\vec{p}_e|$ spectrum for K_{e2} decay, representing the data from which the value of $B(K^+ \to e^+ \nu_e)/B(K^+ \to \mu^+ \nu_\mu)$ was calculated, was given in the second paper of Ref. 24 and is included here as Fig. 12. This experiment featured very good photon detection in order to veto $K^+ \to l_a^+ \nu_{l_a} \gamma$ and $K^+ \to \pi^0 l_a^+ \nu_{l_a}$ events from the $K_{l_a 2}$ data sets. Its discrimination between μ^+'s and e^+'s by means of a threshold Čerenkov counter has been noted above. The cuts for the μ^+ and e^+ events were

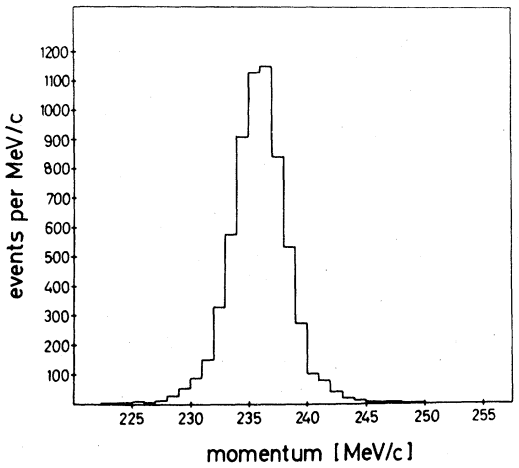

FIG. 11. The μ^+ momentum spectra from the CERN-Heidelberg K_{l2} experiment of Heard *et al.* and Heintze *et al.* (Refs. 24 and 25). (This spectrum was actually given in Ref. 25.)

$$220 < |\vec{p}_\mu| < 252 \text{ MeV} \quad (2.25)$$

and

$$240 < |\vec{p}_e| < 260 \text{ MeV}, \quad (2.26)$$

which bracket the $m(\nu_i)=0$ values given above. The lower momentum cuts, divided by the respective $|\vec{p}_a|_0$ values, are shown as the dot-dashed lines labeled $(\bar{p}_\mu)_c = 0.93$ and $(\bar{p}_e)_c = 0.97$ in Figs. 8 and 9. The value of $m(\nu_i)$ in $K^+ \to \mu^+ \nu_i$ decay which would yield $|\vec{p}_\mu^{(i)}| = |\vec{p}_\mu|_{\text{cut}}$ is 118 MeV, while

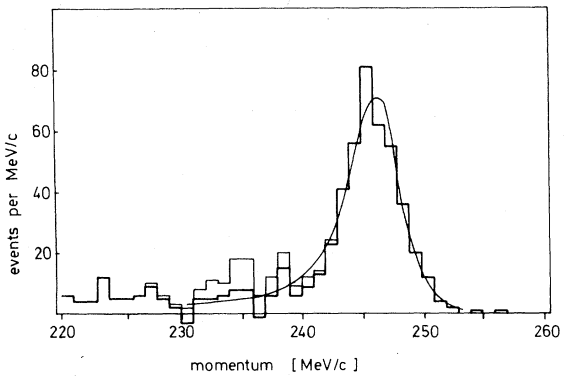

FIG. 12. The e^+ momentum spectrum from the CERN-Heidelberg K_{l2} experiment of Heard *et al.* and Heintze *et al.* (Refs. 24 and 25). (This spectrum was given in the second paper of Ref. 24.) The thin-line histogram represents all of the e^+ events satisfying the trigger and various cuts, while the thick-line histogram represents this event sample after the subtraction of the random background. The smooth curve is the calculated line shape, normalized above 240 MeV/c to the thick histogram.

the analogous value of $m(\nu_i)$ in $K^+ \to e^+ \nu_i$ decay which would yield $|\vec{p}_e^{\,(i)}| = |\vec{p}_e|_{\rm cut}$ is 82 MeV. These values are marked in Figs. 8 and 9, labeled as $m(\nu_i)_c$. No data were presented in Ref. 24 with $|\vec{p}_a| < 220$ MeV. As part of the later analysis of $K^+ \to e^+ \nu_e \gamma$ decay, a $|\vec{p}_e|$ spectrum based on a smaller data set and extending down to 215 MeV was given.[25] Because of the incomplete solid angle coverage and imperfect efficiency of the photon-detection apparatus (lead-glass), there is considerable background in the K_{e2} spectrum. Consequently, we have not used the additional 5-MeV increment in this later data for our bounds on HSC ν_i modes. Moreover, owing to the backgrounds, apparently no K_{l2} data were analyzed below $|\vec{p}_\mu| = 220$ MeV or $|\vec{p}_e| = 215$ MeV.[24,25] The lowest value of $|\vec{p}_\mu| = 220$ MeV coincides with $|\vec{p}_\mu|_{\rm cut}$, but the minimum value $|\vec{p}_e| = 220$ MeV in the data of Ref. 24 lies 20 MeV below $|\vec{p}_e|_{\rm cut}$ and hence is indicated separately on Fig. 9, normalized and labeled as $(\bar{p}_e)_l = 0.89$. The value of $m(\nu_i)$ which would give $|\vec{p}_e^{\,(i)}| = |\vec{p}_e|_l$ in K_{e2} decay is $m(\nu_i)_l = 163$ MeV, as marked in Fig. 9.

The analysis of $K_{\mu 2}$ decay in Ref. 1 relied upon the data in Ref. 24. Here, using the later $K_{\mu 2}$ spectrum of Ref. 25, we can obtain an improved bound. As is evident in Fig. 11, the LDC peak has a low-momentum tail which extends down to ~228 MeV. In order to test for an HSC ν_i peak within this LDC peak it would be necessary to carry out a detailed Monte Carlo fit of the type described above, which would be inappropriate in this work. Instead, we choose the upper end of the momentum range over which to search for such peaks to be the lower edge of the LDC peak at ~228 MeV. We find no evidence for an HSC ν_i peak with a height, at the 1σ level, greater than ~10 events per bin, or 1% of that of the LDC peak, and conclude that if

$$228 > |\vec{p}_\mu^{\,(i)}| > 220 \text{ MeV},$$

i.e.,

$$82 < m(\nu_i) < 118 \text{ MeV}, \tag{2.27}$$

then

$$|U_{2i}|^2 \simeq R_{2i} \lesssim \frac{0.01}{\bar{\rho}(\delta_\mu^K, \delta_i^K)}.$$

The upper bound on R_{2i} in (2.27) varies from 0.01(0.62) to 0.01(0.46) as $m(\nu_i)$ increases from 82 to 118 MeV. Although we shall not try to set a precise bound in the region $|\vec{p}_e| > 228$ MeV, it is clear from Fig. 11 that the data rule out a very sizable HSC peak in this region. To take an example, in the bin $229 \text{ MeV} > |\vec{p}_\mu^{\,(i)}| > 228$ MeV, i.e., $77 \text{ MeV} < m(\nu_i) < 82$ MeV, at the ~1σ level, $R_{2i} \lesssim 0.02/\bar{\rho}(\delta_\mu^K, \delta_i^K) \simeq 0.01$, and so forth for $|\vec{p}_\mu^{\,(i)}| > 229$ MeV.

For K_{e2} decay, from the data shown in Fig. 12 we find that below the LDC peak there is no HSC peak with relative strength greater than about 25% at the 1σ level, and thereby derive the following bound: If

$$240 > |\vec{p}_e^{\,(i)}| > 220 \text{ MeV},$$

i.e.

$$82 < m(\nu_i) < 163 \text{ MeV}, \tag{2.28}$$

then

$$|U_{1i}|^2 \simeq R_{1i} \lesssim \frac{0.25}{\bar{\rho}(\delta_e^K, \delta_i^K)}.$$

Since this is an $M^+ \to e^+ \nu_e$ decay, the bound is, as explained before, extremely stringent; the upper limit varies from $0.25(4.1\times10^{-5})$ to $0.25(1.2\times10^{-5})$ as $m(\nu_i)$ increases from 82 to 163 MeV. Thus one has an explicit example which demonstrates that the M_{l2} test could detect an HSC ν_i coupling coefficient to electrons as small as $|U_{1i}|^2 \sim 4\times10^{-6}$ for a typical mass $m(\nu_i) \sim 160$ MeV. It is clear that in view of this great sensitivity of the test and the fact that usable high-statistics counter data on $K_{l_a 2}$ decay do not extend below $|\vec{p}_a| = 220$ MeV, i.e., covers only about 7 and 11% of the full range of $|\vec{p}_\mu^{\,(i)}|$ and $|\vec{p}_e^{\,(i)}|$, respectively, there is strong motivation for new $K_{l_a 2}$ experiments to search for HSC ν_i peaks in the unexplored lower ranges of $|\vec{p}_a|$. It is, of course, true that certain backgrounds would become more severe at lower $|\vec{p}_a|$; however, in a dedicated experiment with sufficiently good photon detection, particle identification, and momentum resolution this should not preclude such a search, at least over a large fraction of the available range of momenta.

We proceed to consider the Columbia-Nevis experiment by DiCapua *et al.*[23] which determined $B(\pi^+ \to e^+ \nu_e)/B(\pi^+ \to \mu^+ \nu_\mu)$ using energy measurement of the direct and μ-decay positrons, together with a timing technique to separate the former from the latter. Since neither $|\vec{p}_\mu|$ nor E_μ was measured in the Columbia-Nevis π_{l2} experiment, it is not possible to search for $\pi^+ \to \mu^+ \nu_{\rm HSC\ i}$ events in this data. From their total e^+ spectrum due to both $\pi \to e$ and $\pi \to \mu \to e$ events, Di Capua *et al.* separated the pure $\pi \to e$ spectrum by the method just described. The resulting spectrum exhibits noticeable peaks but, unfortunately, is unusable for our test because, as explained in Ref. 23, "All $\cdots$ of these figures (for the total e^+ and individual $\pi \to \mu \to e$ and $\pi \to e$ decays) show a periodic decimal distortion due to a channel-addressing error. No effort was made to remove this error from the data $\cdots$." The peaks re-

ferred to above, and the other structure in the full $\pi \to e$ spectrum, are presumably the effects of this analyzer distortion. For reference, we show the cleanest part of the $\pi \to e$ spectrum from Ref. 23 in Fig. 13 (the full spectrum extends down to channel 10). Unfortunately, no absolute energy scale was given for any of the spectra in Ref. 23. We crudely estimate that this cut occurs at $E_e \sim 55$ MeV.[33] It would obviously be very valuable for the experimentalists to present a new reanalysis of their data with the analyzer distortion removed. We could then meaningfully apply our test to the corrected data.

Finally, let us examine other data to which the M_{l2} test can be applied. Evidently, one of the main drawbacks of the present highest-statistics and highest-precision counter experiments on M_{l2} decays is the fact that they incorporated cuts which severely restrict the ranges of momenta or energies in which one can search for HSC ν_i spectral lines. Accordingly, it is worthwhile to examine data from earlier experiments which did not have such severe cuts.

We consider first the experiment by Hyman *et al.*[28] which specifically studied $\pi^+ \to \mu^+ \nu_\mu$ decay at rest and measured E_μ via the μ^+ range $R_\mu^{(\mathrm{He})}$ in a helium bubble chamber, thereby setting one of the early upper limits on the muon-neutrino "mass", "$m(\nu_\mu)$" < 2.2 MeV (90% C.L.). The data presented in Ref. 28 consist of a peak containing 145 events, centered at $(R_\mu^{(\mathrm{He})})_0 = 1.04$ cm, with a low-energy tail extending down to ~0.96 cm. The published plot is truncated at $R_\mu^{(\mathrm{He})} = 0.78$ cm and shows no further $\pi_{\mu 2}$ events below the peak. The range-momentum relation for the μ^+ in this liquid is approximately[14,28] $R_\mu^{(\mathrm{He})} \propto |\vec{p}_\mu|^{3.6}$. The bound corresponding to less than one event in this range is then the following: If

$$0.96 > R_\mu^{(\mathrm{He})(i)} > 0.78 \text{ cm},$$

i.e.,

$$7 < m(\nu_i) < 13 \text{ MeV}, \tag{2.29}$$

then

$$|U_{2i}|^2 \simeq R_{2i} \lesssim \frac{0.03}{\bar{\rho}(\delta_\mu^\pi, \delta_i^\pi)} \simeq 0.03.$$

Alternatively, one could quote a 90%-confidence-level bound, but the form given above will suffice here. As with the K_{l2} data from the CERN-Heidelberg experiment,[24,25] an important question concerning this bubble-chamber data is whether there were events with $R_\mu^{(\mathrm{He})} < 0.78$ cm at a level above that expected from the radiative decay $\pi^+ \to \mu^+ \nu_\mu \gamma$ where the photon did not convert in the He liquid. However, in view of the low statistics, this data could not provide a very sensitive probe for $\pi^+ \to \mu^+ \nu_{\mathrm{HSC}\,i}$ events.

Let us next consider emulsion experiments which, as a cumulative set, have the advantage of rather high statistics. Early determinations of the muon mass relied upon the measurement, via such emulsion experiments, of the range and momentum of the muon from a decaying pion.[27] There is an approximate empirical relation between the kinetic energy of the muon and its range in the relevant kind of emulsion, of the form $T_\mu/(T_\mu)_0 = [R_\mu/(R_\mu)_0]^{\nu(T_\mu)}$ where $(R_\mu)_0 \simeq 600$ μm, and $\nu((T_\mu)_0) \simeq 0.57$. The exponent ν increases somewhat as T_μ decreases; a useful table is given in Ref. 27. Thus, in an HSC $\pi_{\mu 2}$ decay the muon would be observed to have a smaller range $R_\mu^{(i)}$ than $(R_\mu)_0$. In passing, we note that there is, to our knowledge, no emulsion data with significant statistics on the rare M_{e2} decays, where $M = \pi$ or K, or on $K_{\mu 2}$ decay. This is understandable because of the very small branching ratios for the former decay modes and, independently, because of the large momenta and commensurately large ranges of the l in K_{l2} decay. In the precision measurements by the Berkeley group the main peak was found to have a $\sigma/(R_\mu)_0 = (4.5 \pm 0.1)\%$ and to extend down to $R_\mu \simeq 530$ μm.[27] Muon tracks considerably shorter than $(R_\mu)_0$ have been observed in a number of experiments.[27,34,35] There are two conventional sources of these events. The first is pion decay in flight, where the muon is emitted backwards relative to the direction of motion of the pion. The second is the radiative decay $\pi^\pm \to \mu^\pm \overset{(-)}{\nu}_\mu \gamma$, where the photon is not detected. Two specific studies of anomalously short-range muon tracks from $\pi_{\mu 2}$ decays have been carried out.[34,35] In the first, out of a total of 11 841 $\pi_{\mu 2}$ decays, Fry found eight events with

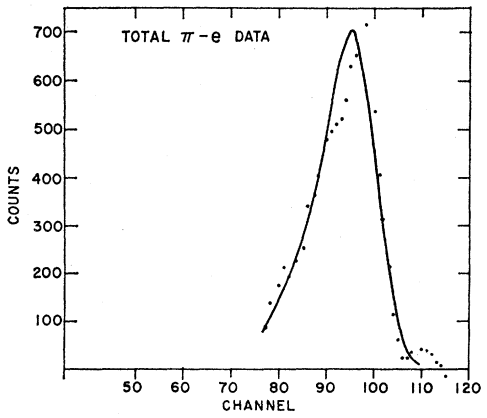

FIG. 13. The e^+ energy spectrum from the Columbia-Nevis $\pi_{e2}/\pi_{\mu 2}$ experiment of Di Capua *et al.* (Ref. 23). See this reference and the text for further details.

$R_\mu < 480$ μm ($T_\mu \lesssim 3.6$ MeV) which could not be explained by π decay in flight.[34] It is interesting that of these eight events there were clusters at certain values of R_μ. This clustering was not commented upon in Ref. 34. From these events, together with a correction for the emulsion thickness, a total branching ratio for events with $R_\mu < 480$ μm was quoted, viz. $(3.3 \pm 1.3) \times 10^{-4}$.[34] It was concluded that this was consistent with the number expected from the radiative decay, and no further attempt was made to adduce any other possible explanations for these eight events. Later, in order to study the radiative decay $\pi^\pm \to \mu^\pm \overset{(-)}{\nu}_\mu \gamma$, Castagnoli and Muchnik examined a total of 93 045 $\pi \to \mu \to e$ events.[35] The signature for a radiative π decay consisted of a $\pi \to \mu$ decay where the track stopped in the emulsion, had a range substantially shorter than $(R_\mu)_0$, and could not have been due to π decay in flight. For experimental reasons pertaining to the size of the emulsion plates and microscope field, an initial cut was applied to retain only events in which the projected muon range was $< 425 \pm 20$ μm. To compare with the theoretical predictions[36] for $\pi^\pm \to \mu^\pm \overset{(-)}{\nu}_\mu \gamma$ decay, the data were presented in the form of an "integral-range" spectrum, with most bins ~50 μm wide. Since the data will be used for our bounds we reproduce this spectrum in Fig. 14. The function $F(R)$ (where $R \equiv R_\mu$) is defined as the partial branching ratio for observed events with muon ranges less than or equal to R, i.e.,

$$F(R_\mu) \equiv F(R_\mu)_{\rm exp} \equiv \frac{1}{\Gamma(\pi^\pm \to \mu^\pm \nu_\mu)} \int_0^{R_\mu} dR'_\mu \frac{\partial E_\mu}{\partial R'_\mu} \frac{d\Gamma}{dE_\mu} \times (\pi^\pm \to \mu^\pm + \cdots)_{\rm exp} . \quad (2.30)$$

[The theoretical calculations of $F(R)$ assumed that these events arose from the radiative decay $\pi^\pm \to \mu^\pm \overset{(-)}{\nu}_\mu \gamma$ and that "$m(\nu_\mu)$" = 0.] As can be seen from the graph, the points at $R_\mu = 225$ and 305 μm are ~1σ high, and for $R_\mu > 435$ μm, the experimental results are much higher than the theoretical predictions. The authors concluded that for $R_\mu < 435$ μm their data agreed with the theory and attributed the discrepancy for $R_\mu > 435$ μm to (a) a possible underestimation of straggling effects; (b) a possible inaccuracy in the correction which was applied for geometrical bias; and (c) a possible anomalously large contribution of structure-dependent terms in the $\pi^\pm \to \mu^\pm \nu_\mu \gamma$ decay amplitude. Like Fry, they did not comment on any clustering of events and did not adduce any other physics explanations for their events. The differential structure of the data is better revealed if one plots the recorded events as a function of R_μ; we have done this in Fig. 15 for the combined data from these two experiments.[34,35] The eight events from Ref. 34 occur at $R_\mu = 120$, 185, 290, 416, 430, 441, 470, and 470 μm; the other 32 events are from Ref. 35. No anomalous events were recorded in Refs. 34 or 35 with

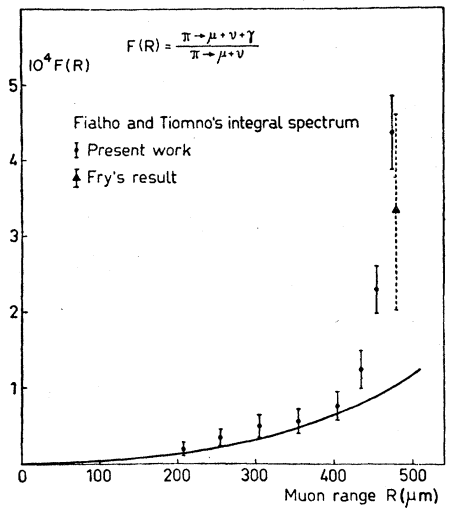

FIG. 14. The muon-integral-range spectrum from the emulsion experiment of Castagnoli and Muchnik (Ref. 35) for the decay(s) $\pi \to \mu^+ \ldots$, where the ellipsis represents one or more undetected neutral particles. As indicated, the triangular point with dashed error bar represents an integral-range value from the data of W. Fry (Ref. 34). The data from Ref. 35 consist of 26 definitely reliable events, together with 6 events labeled as "dubious." The data from Ref. 34 consist of 8 events. The solid curve is the corrected theoretical spectrum for the radiative decay calculated by G. Fialho and J. Tiomno (Ref. 36). See Refs. 34–36 and the text for the definition of $F(R)$ and further details. The authors of Refs. 34 and 35 *interpreted* this data as being due to the radiative decay $\pi^\pm \to \mu^\pm (\overset{(-)}{\nu})_\mu \gamma$, but, as is pointed out in the text, since they did not actually observe the photon which was assumed to have been emitted, this interpretation is not, in general, conclusive.

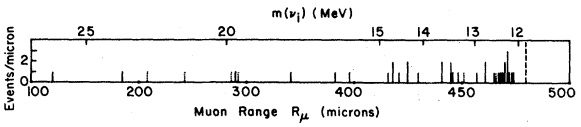

FIG. 15. Differential muon-range distribution, compiled from the emulsion data of Refs. 34 and 35. The 8 events from Ref. 34 are listed in the text; the remaining 32 are from Ref. 35. Of the latter, the 6 dubious ones are distinguished with dotted marks. The dashed line indicates roughly the position in actual muon range R_μ where the cuts applied in Ref. 35 precluded further analysis of events. The upper horizontal axis indicates the value of $m(\nu_i)$ which would lead to the observed R_μ in the decay $\pi^\pm \to \mu^\pm (\overset{(-)}{\nu})_i$.

$R_\mu < 120$ μm, and in both analyses events with $R_\mu \gtrsim 480$ μm were excluded by the event-selection criteria. Hence, we have truncated the graph on the low end at 100 μm and on the high end at 500 μm. Note the clustering of events, in particular around $R_\mu \simeq 471$ μm.

We have several comments to make about this data. In Refs. 34 and 35 the authors only observed the muon track, *not* the photon. Thus the signature for the alleged $\pi^\pm \to \mu^\pm \overset{(-)}{\nu}_\mu \gamma$ events did not include the requirement that the photon be detected.[37] Rather, starting from the tacit assumption that $\pi_{\mu 2}$ decay consisted of a decay into two particles, each of definite mass [with "$m(\nu_\mu)$" = 0] and that the $\pi_{\mu 2}$ spectrum thus consisted of just a single peak, these authors inferred that the short muon range implied the presence of a photon. However, in the case of massive neutrinos and lepton mixing this assumption and the inference based on it are not in general valid. Hence, it is necessary to reinterpret the results of these experiments. One must say that in general the events observed are due to the set of radiative decays $\pi^\pm \to \mu^\pm \overset{(-)}{\nu}_i \gamma$, which must certainly occur, and, *in addition*, to possible decay modes of the form $\pi^\pm \to \mu^\pm \nu_i$, HSC i. Among the radiative decays, those with LDC ν_i will, of course, be predominant. To be logically consistent, an experiment that intends to measure a radiative decay such as $\pi^\pm \to l_a^\pm \overset{(-)}{\nu}_{l_a} \gamma$, $K^\pm \to l_a^\pm \nu_{l_a} \gamma$, where $l_a = e$ or μ, must observe the photon; it is not sufficient to record events with $|\vec{p}_{l_a}| < |\vec{p}_{l_a}|_0$. This implies that the results quoted for $\Gamma(\pi^\pm \to \mu^\pm \overset{(-)}{\nu}_\mu \gamma)$ in Refs. 34 and 35 are not conclusive, nor is the listing, based on Ref. 35, included in Ref. 14. A similar comment applies for one part of the CERN-Heidelberg experiment which sought to observe the structure-dependent, negative-photon-helicity contribution to $K^+ \to e^+ \nu_e \gamma$ decay by measuring events which had $|\vec{p}_e| < |\vec{p}_e|_0$ and did *not* have a coincident photon (see paper III).[25] Thus, it is possible that the clustering evident in Fig. 15 and/or the fact that the integral range distribution in Fig. 14 falls above the model predictions in certain intervals of R_μ are heretofore unrecognized indications of HSC $\pi_{\mu 2}$ decays. It is straightforward to determine which values of $m(\nu_i)$ would correspond to given values of $R_\mu^{(i)}$. If, for example, one were to interpret the peak at $R_\mu^{(i)} \simeq 471$ μm as an HSC ν_i peak in $\pi_{\mu 2}$ decay, it would correspond to $m(\nu_i) \simeq 12$ MeV and a branching ratio, relative to the dominant peak, of order a few times 10^{-5}. Since $\bar{\rho}(\delta_\mu^\pi, \delta_i^\pi) = 0.99$ for $m(\nu_i) = 12$ MeV, this branching ratio is also approximately equal to $R_{2i} \simeq |U_{2i}|^2$. It should be noted in passing that, to our knowledge, no single constraint or set of constraints from other data would forbid such values of $m(\nu_i)$ and R_{2i}. However, just as one cannot validly assign these events with $|\vec{p}_\mu| < |\vec{p}_\mu|_0$ to the radiative decay $\pi^\pm \to \mu^\pm \nu_\mu \gamma$ since no photon was observed, so also one cannot with certainty assert that even clustered events represent an HSC ν_i $\pi_{\mu 2}$ decay since there could well have been an undetected photon present.[37]

Leaving open the possibility that some of the events shown in Fig. 15 are HSC ν_i $\pi_{\mu 2}$ decays, we can use this emulsion data to set quite stringent upper bounds on the branching ratios and corresponding values of R_{2i} for such decays. The Berkeley data on the muon-range distribution in $\pi_{\mu 2}$ decay was presented in the form of a graph covering the range $420 < R_\mu < 700$ μm. The main peak contains ~560 events and, as noted before, extends down to $R_\mu \simeq 530$ μm. No events were shown with $R_\mu < 516$ μm. Thus, as at the 1 event level we infer the following bound: If

$$516 > R_\mu^{(i)} > 480 \ \mu\text{m},$$

i.e.,

$$10 \lesssim m(\nu_i) \lesssim 12 \ \text{MeV}, \tag{2.31}$$

then

$$|U_{2i}|^2 \simeq R_{2i} \lesssim \frac{0.01}{\bar{\rho}(\delta_\mu^\pi, \delta_i^\pi)} \simeq 0.01 .$$

For $R_\mu < 480$ μm a much better bound can be obtained because of the specific high-statistics studies of Refs. 34 and 35. For this we take the 1σ upper limit on the integral-range spectrum of Fig. 14 and subtract the calculated radiative contribution to obtain a 1σ upper limit on a possible HSC ν_i $\pi_{\mu 2}$ increment $[\Delta F(R_\mu)_{\text{HSC}\,\nu_i}]_{1\sigma\,\max}$. That is,

$$[\Delta F(R_\mu)]_{1\sigma\,\max} \equiv F(R_\mu)_{\text{exp}} + \sigma_F - F(R_\mu)_{\text{rad}}^{\text{thy}}, \tag{2.32}$$

where σ_F denotes the one-standard-deviation error in the experimental measurement of $F(R_\mu)$, and $F(R_\mu)_{\text{rad}}^{\text{thy}}$ is the theoretical calculation of $F(R_\mu)$ due to the decay $\pi^\pm \to \mu^\pm \overset{(-)}{\nu}_\mu \gamma$. Since for the HSC ν_i modes

$$\frac{d\Gamma}{dR_\mu}(\pi^\pm \to \mu^\pm \overset{(-)}{\nu}_i) = \Gamma(\pi^\pm \to \mu^\pm \overset{(-)}{\nu}_i)\delta(R_\mu - R_\mu^{(i)}) \tag{2.33}$$

the observed spectrum of short-range muons will be given by

$$F(R_\mu)_{\text{exp}} = F(R_\mu)_{\text{rad}} + \sum_{i=1}^{n} B(\pi^\pm \to \mu^\pm \overset{(-)}{\nu}_i)\theta(R_\mu - R_\mu^{(i)}). \tag{2.34}$$

Hence, assuming that there is a negligible error in the theoretical calculation of the radiative

spectrum,[36] i.e., that $F(R_\mu)_{\rm rad}=F(R_\mu)^{\rm thy}_{\rm rad}$, it follows that

$$[\Delta F(R_\mu)]_{1\sigma\,\max}=\sigma_F+\sum_{i=1}^{n} B(\pi^\pm\to\mu^{\pm}\overset{(-)}{\nu}_i)\theta(R_\mu-R_\mu^{(i)})\,. \tag{2.35}$$

Thus, *a fortiori*, the contribution of any particular HSC ν_i mode with $R_\mu^{(i)}<R_\mu$ is bounded above according to

$$B(\pi^\pm\to\mu^{\pm}\overset{(-)}{\nu}_i)<[\Delta F(R_\mu)]_{1\sigma\,\max}\,. \tag{2.36}$$

Consequently, the resultant 1σ level upper bound on the coupling strength of such an HSC mode has the following general form: If

$$R_\mu>R_\mu^{(i)}>0\,,$$

i.e.,

$$m(\nu_i)_{R_\mu}<m(\nu_i)<m_{\pi^+}-m_\mu\,,$$

then

$$R_{2i}<\frac{[\Delta F(R_\mu)]_{1\sigma\max}}{\bar\rho\,(\delta_\mu^\pi,\delta_i^\pi)}\,. \tag{2.37}$$

The resulting bounds are shown in Fig. 16. The solid line indicates the 1σ level upper bound on $B(\pi^+\to\mu^+\nu_{{\rm HSC}\,i})$ as a function of $R_\mu^{(i)}$ or equivalently $m(\nu_i)$, while the dotted curve represents the corresponding bound on R_{2i}. The vertical dashed line indicates approximately the value of R_μ (480 μm) beyond which events were excluded by the selection criteria of Refs. 34 and 35.

Finally, since we have obtained several upper bounds on R_{2i} from the application of the $M_{\mu 2}$ spectral test, it is useful to present them in a unified manner to show their relative sizes and the different ranges of $m(\nu_i)$ to which they apply.

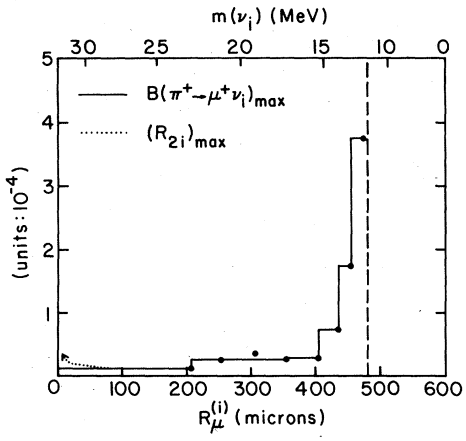

FIG. 16. Upper bounds on the branching ratio $B(\pi^+\to\mu^+\nu_i)$ and relative coupling strength R_{2i} as functions of muon range $R_\mu^{(i)}$ or equivalently, $m(\nu_i)$ from our analysis of the emulsion data of Refs. 34 and 35.

This is done in Fig. 17. The upper bounds (a), (b), and (c) are, respectively, from the SIN data (2.24), the Argonne bubble-chamber experiment (2.29), and the emulsion data (2.31) [and (2.37) and Fig. 16], all on $\pi_{\mu 2}$ decay, or more precisely $\pi\to\mu+$(undetected neutrino and possibly also photon). The upper limit (d) comes from the CERN-Heidelberg data on $K_{\mu 2}$ decay (2.27). For clarity the bounds are shown separately; however, where the mass ranges covered by two bounds overlap [as is the case with the bounds (b) and (c1)], the resultant upper bound is of course given by the minimum of the two. As is obvious from our analysis, in the regions $m(\nu_i)\lesssim 0.6$ MeV, $6\lesssim m(\nu_i)\lesssim 7$ MeV, and $34\lesssim m(\nu_i)\lesssim 82$ MeV, although no upper limits are drawn, it is not implied that there are none. Rather, these would require either putting limits on possible HSC ν_i peaks within the main LDC $\pi_{\mu 2}$ and $K_{\mu 2}$ peaks, which is best performed by the experimentalists themselves, or an application

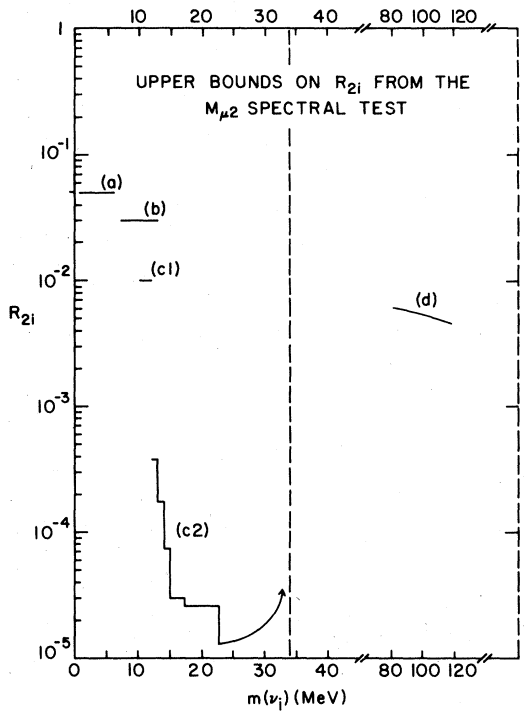

FIG. 17. The combined set of upper bounds on the relative coupling strength R_{2i} derived from the application of the M_{i2} spectral test to existing data. Segment (a) represents the bound (2.24) from the SIN $\pi_{\mu 2}$ data of Ref. 8; (b) the bound (2.29) from the Argonne bubble-chamber data of Ref. 28; (c1), the bound (2.31) from the Berkeley emulsion data of Ref. 27; (c2), the bound given by (2.37) and Fig. 16 from the emulsion data of Refs. 34 and 35; and (d), the bound (2.27) from the CERN-Heidelberg $K_{\mu 2}$ data of Refs. 24 and 25. See Ref. 25.

of the integral $B(M^+ \to e^+\nu_e)/B(M^+ \to \mu^+\nu_\mu)$ constraints, which will be carried out in Sec. III. (In fact, as will be seen, although the integral branching ratio constraints on R_{1i} are very stringent, those on R_{2i} do not improve upon the upper bounds from the differential spectral test.) As for the region $m(\nu_i) \gtrsim 118$ MeV, the size of R_{2i} is weakly limited by various indirect constraints to be discussed later, but the $M_{\mu 2}$ (here the $K_{\mu 2}$) spectral test does not place any useful upper bound on R_{2i}.

Concerning upper bounds on R_{1i}, inasmuch as the application of the M_{e2} test yielded only the single limit (2.28) on this quantity, we shall not give a plot of this limit. For R_{1i} the integrated-branching-ratio constraint provides very severe upper bounds over a large range of $m(\nu_i)$, as will be shown in Sec. III.

E. The complete M_{l2} test including measurement of the lepton polarization

The full M_{l2} test proposed in Ref. 1 consists not only of a careful scan of the $|\vec{p}_a|$ or E_a spectrum to search for the discrete lines from possible HSC modes $M^\pm \to l_a^\pm \nu_i$, where $M = \pi$ or K and $l_a = e$ or μ, but also a measurement of the polarization of the $l_a^\pm$.[21] In the rest frame of the $M^\pm$ this polarization is completely longitudinal. For the general case of $M^\pm \to l_a^\pm \overset{(-)}{\nu}_i$ decay we denote this polarization by $P_{l_a^\pm}^{(i)}(M_{l_a 2})$. The test would thus proceed as follows. If an HSC ν_i peak is observed at momentum $|\vec{p}_a^{\,(i)}|$ or energy $E_a^{(i)}$ one can immediately determine the mass $m(\nu_i)$. Next, assuming that this peak is sufficiently removed from the LDC peak, one can, by momentum selection, pick out on an event-by-event basis, the $l_a^\pm$'s from $M^\pm \to l_a^\pm \nu_{\text{HSC}\,i}$ decay and channel them to the apparatus to measure their polarization. In principle, one can determine the $l_a^\pm$ polarization individually for each HSC ν_i line which satisfies the above separation criterion. Knowing $m(\nu_i)$ and assuming standard $V-A$ couplings, one has a definite prediction for this polarization (see below), which can thus be checked to verify the consistency of the assumption or, if the $V-A$ prediction is violated, to investigate the Lorentz structure of the couplings responsible for the HSC ν_i events. On the other hand, if the line-separation criterion is not satisfied, then one could only perform the polarization measurement on a statistical basis, and it would be much more difficult since the HSC events would presumably comprise only a small fraction of the total sample.

With standard $V-A$ charged-current couplings for the $l_a\nu_i$ vertex, the $l_a^\pm$ polarization is given by

$$P_{l_a^\pm}^{(i)}(M_{l_a 2}) = \frac{\mp(\delta_a^M - \delta_i^M)\lambda^{1/2}(1, \delta_a^M, \delta_i^M)}{f_{\mathfrak{M}}(\delta_a^M, \delta_i^M)}, \qquad (2.38)$$

where one may recall the definitions given in Eqs. (2.6), (2.9), (2.10), and (2.14). The antisymmetry of the l_a^+ (or l_a^-) polarization as a function of δ_a^M and δ_i^M, or equivalently m_{l_a} and $m(\nu_i)$, follows from general principles; in somewhat figurative language, the lighter lepton has its "preferred" helicity, and hence the heavier one is forced to have a "dispreferred" helicity. The polarization $P_{l_a^+}^{(i)}$ is plotted as a function of $m(\nu_i)$ (as the dashed curve) in Figs. 6–9 for the decays $\pi^+ \to \mu^+\nu_i$, $\pi^+ \to e^+\nu_i$, $K \to \mu^+\nu_i$, and $K^+ \to e^+\nu_i$, respectively. Obviously the same graphs apply, with a change in sign of the polarization, to the corresponding M^- decays. For nonzero values of $m(\nu_i)$, $P_{l_a^+}^{(i)}$ differs strikingly from its $m(\nu_i) = 0$ value of -1. As $m(\nu_i)$ increases from zero, $P_{l_a^+}^{(i)}$ rises, at first monotonically. It will cross through zero and assume positive values as $m(\nu_i)$ equals and then exceeds m_{l_a}; this is possible if and only if $m_{l_a} \leq m_M/2$, respectively. The inequality $m_{l_a} < m_M/2$ is true of M_{e2} and $K_{\mu 2}$, but not $\pi_{\mu 2}$, decay. Assuming that this condition is satisfied, $P_{l_a^+}^{(i)}$ ascends through positive values and reaches a maximum at $\delta_i^M = (1 - \delta_a^M)/3$, i.e.,

$$m(\nu_i)_{\text{pol crit}} = \frac{m_M}{\sqrt{3}}(1 - \delta_a^M)^{1/2}. \qquad (2.39)$$

At this point,

$$(P_{l_a^\pm}^{(i)})_{\text{crit}} = \pm \frac{(1 - 4\delta_a^M)^{3/2}}{(1 + 8\delta_a^M)(1 - \delta_a^M)^{1/2}}. \qquad (2.40)$$

For reference, the values of $m(\nu_i)_{\text{pol crit}}$ and $(P_{l_a^+}^{(i)})_{\text{crit=max}}$ are listed in Table II. It might be noted that in the M_{e2} decays $m(\nu_i)_{\text{pol crit}} \simeq m(\nu_i)_{\rho\,\text{max}}$. The magnitude of the polarization, $|P_{l_a^\pm}^{(i)}(M_{l_a 2})|$ goes to zero as $m(\nu_i) \to m(\nu_i)_{\text{max}}$. That is must do so is clear analytically, since Eq. (2.38) can alternatively be expressed as $P_{l_a^\pm}^{(i)}(M_{l_a 2}) = \mp f_P(\delta_a^M, \delta_i^M)\beta_{l_a}^{(i)}$, where $\beta_{l_a}^{(i)}$ is the ve-

TABLE II. Critical values of the lepton polarization $(P_{l_a^+}^{(i)})_{\text{crit=max}}$ and corresponding values of $m(\nu_i)_{\text{pol crit}}$ for the decays $M^+ \to l_a^+\nu_i$ where $M = \pi$, K and $l_a = e, \mu$. See text for definitions.

Decay	$m(\nu_i)_{\text{pol crit}}$ (MeV)	$(P_{l_a^+}^{(i)})_{\text{crit=max}}$
$\pi^+ \to \mu^+\nu_i$	none	no critical point; maximum of zero reached at end point of $m(\nu_i)$
$\pi^+ \to e^+\nu_i$	80.6	$1 - 1.81 \times 10^{-4}$
$K^+ \to \mu^+\nu_i$	278	0.553
$K^+ \to e^+\nu_i$	285	$1 - 1.44 \times 10^{-5}$

locity of l_a and $f_P(\delta_a^M, \delta_i^M)$ is a function which can be read off from Eq. (2.38) and approaches a finite constant as $m(\nu_i) \to m(\nu_i)_{\max}$.

A useful feature of the polarization test is that for small $m(\nu_i)$, $P_{l_a^\pm}^{(i)}$ is controlled by the ratio $[m(\nu_i)/m_{l_a}]^2$ rather than $[m(\nu_i)/m_M]^2$ and hence can be sensitive to values of $m(\nu_i) \ll m_M$. For example in π_{e2} decay, for $m(\nu_i)=1$ MeV, even though $m(\nu_i) \ll m(\nu_i)_{\max}$ and the kinematic rate factor $\bar{\rho}$ has only increased from 1 to ~4.8, far below its eventual maximum of $\sim 2\times 10^4$, the polarization $P_{e^+}^{(i)}$ has already changed drastically from −1 to +0.56. Thus, while it was emphasized earlier that the M_{l2} test, unlike tests using three-body decays, is very sensitive to *large* $m(\nu_i)$ because the helicity enhancement offsets or overwhelms the decrease in the phase-space factor until $m(\nu_i)$ approaches the kinematic limit, it should also be stressed that the full test is quite sensitive to values of $m(\nu_i)$ which are very *small* compared to the Q value of the decay. Specifically, even if $m(\nu_i) \ll m_M - m_{l_a}$, one could still use the test to detect the ν_i line if $m(\nu_i) \gtrsim m_{l_a}$ [as would be true for a wide range of $m(\nu_i)$ in the M_{e2} decays], since there would be a gross change in $P_{l_a}^{(i)}$.

It is an important feature of the complete M_{l2} test that one does not have to make the assumption of $V-A$ charged-current couplings blindly for a given ν_i line, but can check it by measuring the polarization of the $l_a^\pm$ in $M^\pm \to l_a^{\pm(-)}\nu_i$ decay. To analyze how one can perform this check we shall examine the $l_a^\pm$ polarization which would result if the couplings dominantly responsible for such an HSC ν_i decay were not $V-A$. It may be recalled[26] that for an HSC ν_i decay mode the relative strength of non-$V-A$ interactions can be much larger than for the LDC mode(s), as long as the overall strength of the former is sufficiently small relative to that of the latter. We thus consider all of the couplings which could contribute to HSC ν_i M_{l2} decay, namely S, P, V, and A. Note that any (leptonic or hadronic) tensor couplings that might be present would give zero contribution because of the lack of enough independent momenta:

$$\langle 0|\bar{\psi}_{q'}\sigma_{\alpha\beta}(a+b\gamma_5)\psi_q|M\rangle = 0$$

and

$$[\bar{\psi}_{l_a}\sigma_{\alpha\beta}(c_T^{(i)}+c_{T'}^{(i)}\gamma_5)\psi_{\nu_i}]p_M^\alpha\langle 0|J_{(V,A)}^\beta|M\rangle = 0\,.$$

For this general case the amplitude for the decay $M^+ \to l_a^+\nu_i$ can be written in the form[38]

$$\mathrm{Amp}(M^+ \to l_a^+\nu_i) = \kappa_{(V,A)}^{(i)}[\bar{v}_{l_a}\not{p}_M(c_V^{(i)}+c_A^{(i)}\gamma_5)u_{\nu_i}] + m_M\kappa_{(S,P)}^{(i)}[\bar{v}_{l_a}(c_S^{(i)}+c_P^{(i)}\gamma_5)u_{\nu_i}] \tag{2.41}$$

and similarly for $M^- \to l_a^-\bar{\nu}_i$ decay, where the constants $\kappa_{(V,A)}^{(i)}$ and $\kappa_{(S,P)}^{(i)}$ contain all of the dependence on dimensionless coupling constants, intermediate-vector- or -scalar-boson masses, and the respective hadronic matrix elements, with the parent-meson four-momentum p_M factored out in the (V,A) case term and, to keep the dimensions of $\kappa_{(V,A)}^{(i)}$ and $\kappa_{(S,P)}^{(i)}$ the same, a factor of m_M extracted from the latter. With no loss of generality, for each individual $M^\pm \to l_a^\pm\nu_i$ decay, one can define $\kappa_{(V,A)}^{(i)}$ and $\kappa_{(S,P)}^{(i)}$ to be real, shifting any phases to the $c_Z^{(i)}$, $Z=V$, A, S, and P. Finally, the notation emphasizes the fact that $\kappa_{(V,A)}^{(i)}$, $\kappa_{(S,P)}^{(i)}$, and $c_Z^{(i)}$ are in general different for different i; they also generally depend on M and l_a, but to avoid awkward notation this dependence is not indicated explicitly. (Examples of various $c_Z^{(i)}$'s will be mentioned later.) The polarization of the $l_a^\pm$ in the decay $M^\pm \to l_a^\pm\nu_i$ is then given by

$$P_{l_a^\pm}^{(i)} = \pm\frac{N_{l_a}^{(i)}(M_{l_a2})}{D_{l_a}^{(i)}(M_{l_a2})}\,, \tag{2.42a}$$

where

$$N_{l_a}^{(i)}(M_{l_a2}) = \lambda^{1/2}(1,\delta_a^M,\delta_i^M)\{\kappa_{(V,A)}^{(i)2}\,\mathrm{Re}(c_V^{(i)}c_A^{(i)*})(\delta_a^M-\delta_i^M) - \kappa_{(S,P)}^{(i)2}\,\mathrm{Re}(c_S^{(i)}c_P^{(i)*}) + \kappa_{(V,A)}^{(i)}\kappa_{(S,P)}^{(i)}[\mathrm{Re}(c_V^{(i)}c_P^{(i)*}-c_A^{(i)}c_S^{(i)*})(\delta_a^M)^{1/2} - \mathrm{Re}(c_V^{(i)}c_P^{(i)*}+c_A^{(i)}c_S^{(i)*})(\delta_i^M)^{1/2}]\}, \tag{2.42b}$$

$$D_{l_a}^{(i)}(M_{l_a2}) = \kappa_{(V,A)}^{(i)2}\left[\left(\frac{|c_V^{(i)}|^2+|c_A^{(i)}|^2}{2}\right)f_{\mathfrak{M}}(\delta_a^M,\delta_i^M) - (|c_V^{(i)}|^2-|c_A^{(i)}|^2)(\delta_a^M\delta_i^M)^{1/2}\right] + \kappa_{(S,P)}^{(i)2}\left[\left(\frac{|c_S^{(i)}|^2+|c_P^{(i)}|^2}{2}\right)(1-\delta_a^M-\delta_i^M) - (|c_S^{(i)}|^2-|c_P^{(i)}|^2)(\delta_a^M\delta_i^M)^{1/2}\right] + \kappa_{(V,A)}^{(i)}\kappa_{(S,P)}^{(i)}[\mathrm{Re}(c_V^{(i)}c_S^{(i)*}+c_A^{(i)}c_P^{(i)*})(\delta_i^M)^{1/2}(1+\delta_a^M-\delta_i^M) + \mathrm{Re}(-c_V^{(i)}c_S^{(i)*}+c_A^{(i)}c_P^{(i)*})(\delta_a^M)^{1/2}(1+\delta_i^M-\delta_a^M)]\,. \tag{2.42c}$$

For the pure (V,A) case Eq. (2.42) reduces to

$$P^{(i)}_{l_a^\pm}(M_{l_a 2})_{(V,A)} = \frac{\pm \rho^{(i)}_{VA}\cos\varphi^{(i)}_{VA}(\delta^M_a - \delta^M_i)\lambda^{1/2}(1,\delta^M_a,\delta^M_i)}{\frac{1}{2}(\rho^{(i)\,2}_{VA}+1)f_{\mathfrak{M}}(\delta^M_a,\delta^M_i) - (\rho^{(i)\,2}_{VA}-1)(\delta^M_a\delta^M_i)^{1/2}}, \tag{2.43}$$

where

$$\rho^{(i)}_{VA} \equiv \left|\frac{c^{(i)}_V}{c^{(i)}_A}\right| \tag{2.44a}$$

and

$$\varphi^{(i)}_{VA} \equiv \arg\left(\frac{c^{(i)}_V}{c^{(i)}_A}\right). \tag{2.44b}$$

[In writing Eq. (2.43), we have assumed that $c^{(i)}_A \neq 0$; the cases in which $c^{(i)}_V$ or $c^{(i)}_A$ vanish are trivial.] The general (V,A) expression for the polarization (2.43) is, like the $(V-A)$ one in Eq. (2.42), antisymmetric in the variables δ^M_a and δ^M_i, or equivalently m_{l_a} and $m(\nu_i)$. For fixed M, l_a, and ν_i, the magnitude of the polarization is a maximum for the purely chiral cases $c^{(i)}_V = \pm\, c^{(i)}_A$; here

$$|P^{(i)}_{l_a^\pm}(M_{l_a 2})_{(V,A)}|_{\max} = |P^{(i)}_{l_a^\pm}(M_{l_a 2})_{(V\pm A)}| = \frac{|\delta^M_a - \delta^M_i|\,\lambda^{1/2}(1,\delta^M_a,\delta^M_i)}{f_{\mathfrak{M}}(\delta^M_a,\delta^M_i)}. \tag{2.45}$$

If $c^{(i)}_V \neq \pm\, c^{(i)}_A$, because of a difference in magnitudes, $|c^{(i)}_V| \neq |c^{(i)}_A|$ (which may be CP-conserving), or a (CP-violating) difference in phases, or both, then the magnitude of the polarization is reduced commensurately [except at the point $m(\nu_i) = m_{l_a}$, if this is in the physical region, where it vanishes, independent of $c^{(i)}_V$ and $c^{(i)}_A$]. As can be seen from the denominator of the right-hand side of Eq. (2.45), the kinematic rate factor for the (V,A) case differs from that for the pure $V-A$ (or $V+A$) case; in particular, the dependence on lepton masses in $|\mathfrak{M}(M^\pm \to l_a^\pm \nu_i)|^2$ is given by this full denominator multiplied by $|c^{(i)}_A|^2$ rather than just $f_{\mathfrak{M}}(\delta^M_a,\delta^M_i)$.

For the pure (S,P) case

$$P^{(i)}_{l_a^\pm}(M_{l_a 2})_{(S,P)} = \frac{\pm \rho^{(i)}_{SP}\cos\varphi^{(i)}_{SP}\lambda^{1/2}(1,\delta^M_a,\delta^M_i)}{\frac{1}{2}(\rho^{(i)2}_{SP}+1)(1-\delta^M_a-\delta^M_i) - (\rho^{(i)2}_{SP}-1)(\delta^M_a\delta^M_i)^{1/2}}, \tag{2.46}$$

where

$$\rho^{(i)}_{SP} \equiv \left|\frac{c^{(i)}_S}{c^{(i)}_P}\right| \tag{2.47a}$$

and

$$\varphi^{(i)}_{SP} \equiv \arg\left(\frac{c^{(i)}_S}{c^{(i)}_P}\right). \tag{2.47b}$$

Observe that the (S,P) expression (2.46) for the charged-lepton polarization is symmetric in the variables m_{l_a} and $m(\nu_i)$ if both $c^{(i)}_S$ and $c^{(i)}_P$ are symmetric or antisymmetric functions of these variables. In contrast, Eq. (2.46) is antisymmetric in these two variables if one of $c^{(i)}_{S,P}$ is symmetric while the other is antisymmetric. A "typical" charged-Higgs-boson–lepton vertex might have the dependence on lepton masses given by $c^{(i)}_S \propto [m_{l_a} - m(\nu_i)]$ and $c^{(i)}_P \propto [m_{l_a} + m(\nu_i)]$, so that $P^{(i)}_{l_a^\pm}(M_{l_a 2})_{(S,P)}$ would, like $P^{(i)}_{l_a^\pm}(M_{l_a 2})_{(V,A)}$, be an antisymmetric function of m_{l_a} and $m(\nu_i)$.[39] As with (V,A) couplings, the maximum magnitude of the polarization occurs for the purely chiral choice $c^{(i)}_S = \pm\, c^{(i)}_P$:

$$|P^{(i)}_{l_a^\pm}(M_{l_a 2})_{(S,P)}|_{\max} = |P^{(i)}_{l_a^\pm}(M_{l_a 2})_{(S\pm P)}| = \frac{\lambda^{1/2}(1,\delta^M_a,\delta^M_i)}{1-\delta^M_a-\delta^M_i}. \tag{2.48}$$

It is easy to prove the following important property: for fixed M, for all δ^M_a and δ^M_i,

$$|P^{(i)}_{l_a^\pm}(M_{l_a 2})_{(S,P)}|_{\max} \geq |P^{(i)}_{l_a^\pm}(M_{l_a 2})_{(V,A)}|_{\max}, \tag{2.49}$$

where the equality holds nontrivially only at the point $m(\nu_i) = 0$.

Let us proceed to discuss how one would obtain information about the Lorentz structure of the effective HSC ν_i interaction from experiment polarization measurements. As was implied in our previous analysis, the lepton polarization is, in principle, experimentally accessible for both $e^\pm$ and $\mu^\pm$ decay modes. Regarding the actual measurement, for both $e^\pm$ and $\mu^\pm$ decay modes one could use the various techniques which have been employed successfully to determine the polarization of the e in μ decay, while for the latter, in the case of a μ^+, one would also have the option of stopping the μ^+ and measuring the angular distribution of the e^+ from its decay. However, because $B(M^\pm \to e^\pm \overset{(-)}{\nu}_{\mathrm{LDC}\,i}) \ll B(M^\pm \to \mu^\pm \overset{(-)}{\nu}_{\mathrm{LDC}\,j})$ and in each case $B(M^\pm \to l_a^\pm \overset{(-)}{\nu}_{\mathrm{HSC}\,r}) \ll B(M^\pm \to l_a^\pm \overset{(-)}{\nu}_{\mathrm{LDC}\,s})$, $l_a = e$ or μ, one faces a much more severe problem of statistics if one wishes to measure $P^{(i)}_{e^\pm}(M_{e2})$. This problem may be surmountable with the extremely high pion-beam fluxes available at the meson factories LAMPF (Los Alamos Meson Physics Facility), TRIUMF (Triuniversity Meson Facility), and SIN. Secondly, for our purposes it is crucial to be able to combine the polarization measurement with the search for HSC peaks in the $|\vec{p}_a|$ or E_a spectrum. Since for the highest precision the latter would require stopping the meson, and since one must maximize the rate at which the mesons decay, relative to

the rate at which they interact, one would favor the use of M^+'s rather than M^-'s. Restricting one's measurements to the M^+ decays would not incur the loss of any information about the Lorentz structure of the couplings since $P^{(i)}_{l_a^+}(M^+_{l_a 2}) = -P^{(i)}_{l_a^-}(M^-_{l_a 2})$ for an arbitrary mixture of these couplings. (However, we shall keep the notation general.)

From the measurement of $|\vec{p}^{(i)}_a|$ or $E^{(i)}_a$ for the HSC ν_i line in any one of the eight decays $M^\pm \to l_a^\pm \overset{(-)}{\nu}_i$, where $M = \pi$ or K and $l_a = e$ or μ, one can determine $m(\nu_i)$ and thus can predict the position of this ith line in all of the other seven decays where it is allowed by phase space (the charge-conjugate modes being trivial).[40] Further, given the assumption of $V-A$ couplings, one has definite predictions for the $l_a^\pm$ polarization in all of the eight allowed $M^\pm \to l_a^\pm \overset{(-)}{\nu}_i$ decay modes. If for those modes where it can be measured, $P^{(i)}_{l_a^\pm}(M_{l_a 2})_{\rm exp}$ agreed with these predictions, it would provide very strong support for this assumption of $V-A$ couplings. It is true that even if the predictions agreed with the experimental measurements it would not, strictly speaking, prove the validity of the above assumption. This is due to the fact that, as a consequence of the inequality (2.46), any value of $P^{(i)}_{l_a^\pm}(M_{l_a 2})_{(V-A)}$ can be reproduced by $P^{(i)}_{l_a^\pm}(M_{l_a 2})_{(S,P)}$ for appropriate choices of $c_S^{(i)}$ and $c_P^{(i)}$. Recall that these choices can be made separately for each triplet (M, a, i) since, although it is suppressed in the notation, $c_S^{(i)}$ and $c_P^{(i)}$ depend in general on M and l_a as well as i. However, one would be justified in regarding this as an extremely unlikely conspiracy, especially if for a given i, measurements of $P^{(i)}_{l_a^\pm}(M_{l_a 2})$ for different M's and l_a's all agreed with the $V-A$ predictions. If, on the other hand, the measured values $P^{(i)}_{l_a^\pm}(M_{l_a 2})_{\rm exp}$ did not agree with these predictions, then in general one could only conclude that the couplings were some mixture of S, P, V, and A. However, depending on the actual value of $P^{(i)}_{l_a^\pm}(M_{l_a 2})_{\rm exp}$, one may be able to restrict the Lorentz structure of these couplings further. This is a result of the fact that although any value of $P^{(i)}_{l_a^\pm}(M_{l_a 2})_{(V,A)}$ can be reproduced by $P^{(i)}_{l_a^\pm}(M_{l_a 2})_{(S,P)}$ for appropriate choices of $c_S^{(i)}$ and $c_P^{(i)}$, there are values of $P^{(i)}_{l_a^\pm}(M_{l_a 2})_{(S,P)}$ which cannot be reproduced by $P^{(i)}_{l_a^\pm}(M_{l_a 2})_{(V,A)}$ for any choices of $c_V^{(i)}$ and $c_A^{(i)}$. Specifically, if $P^{(i)}_{l_a^\pm}(M_{l_a 2})_{\rm exp} = 0$, to within experimental accuracy, then, assuming that $m(\nu_i) \neq m_{l_a}$, one can conclude, to the given degree of accuracy, that the couplings are pure (S, V) or (P, A). If

$$0 < |P^{(i)}_{l_a^\pm}(M_{l_a 2})_{\rm exp}| \leq |P^{(i)}_{l_a^\pm}(M_{l_a 2})_{(V,A)}|_{\rm max}\,, \qquad (2.50)$$

then one cannot determine for an individual $M^\pm \to l_a^\pm \overset{(-)}{\nu}_i$ decay what combination of S, P, V, and A the couplings are, except that, of course, they cannot be pure (S, V) or pure (P, A). Note that it does not help to combine data on the ν_i line with different parent mesons M and charged leptons l_a, since the $c_Z^{(i)}$ are in general nontrivial functions of M and a. However, if

$$|P^{(i)}_{l_a^\pm}(M_{l_a 2})_{(V,A)}| < |P^{(i)}_{l_a^\pm}(M_{l_a 2})_{\rm exp}| \leq |P^{(i)}_{l_a^\pm}(M_{l_a 2})_{(S,P)}|_{\rm max}\,, \qquad (2.51)$$

then one can conclude that the couplings for this HSC ν_i mode cannot be pure (V, A). To illustrate these remarks, we show in Figs. 18 and 19 the values of $|P^{(i)}_{\mu^\pm}(\pi_{\mu 2})|_{\rm max}$ and $|P^{(i)}_{\mu^\pm}(K_{\mu 2})|_{\rm max}$ for the (V, A) and (S, P) cases. It is evident that for a fixed $m(\nu_i)$, especially, in the vicinity of m_μ for $K_{\mu 2}$ decay, there is a substantial range of values of $P^{(i)}_{\mu^\pm}(M_{\mu 2})_{\rm exp}$ for which one could exclude pure (V, A) couplings. In M_{e2} decays, for most values of $m(\nu_i)$ it would be much more difficult to use this method because, except near $m(\nu_i) = m_e$, $|P^{(i)}_{e^\pm}(M_{e2})_{(V,A)}|_{\rm max}$ is quite close to $|P^{(i)}_{e^\pm}(M_{e2})_{(S,P)}|_{\rm max}$. Owing to this fact, we shall not present graphs analogous to Figs. 18 and 19 for these M_{e2} decays.

Although in general the couplings involved in M_{l2} decay will violate CP, the only measurable quantities in this decay are CP-conserving. It is true that in the presence of CP violation partial decay rates for conjugate modes may differ, as is the case with $K^+ \to \pi^+\pi^+\pi^-$ and its charge-conjugate decay. But because there are no hadronic or even electromagnetic final-state phase shifts for the $l_a^\pm \overset{(-)}{\nu}_i$ final state, CPT invariance guarantees that $\Gamma(M^+ \to l_a^+ \nu_i) = \Gamma(M^- \to l_a^- \bar{\nu}_i)$, as was implied in our previous notation. Note that for fixed $|c_Z^{(i)}|$, $Z = S, P, V$, and A, the actual value of $\Gamma(M^\pm \to l_a^\pm \overset{(-)}{\nu}_i)$, which is proportional to $D^{(i)}_{l_a}(M_{l_a 2})\lambda^{1/2}(1, \delta_a^M, \delta_i^M)$, does depend on whether CP is conserved, through the factors

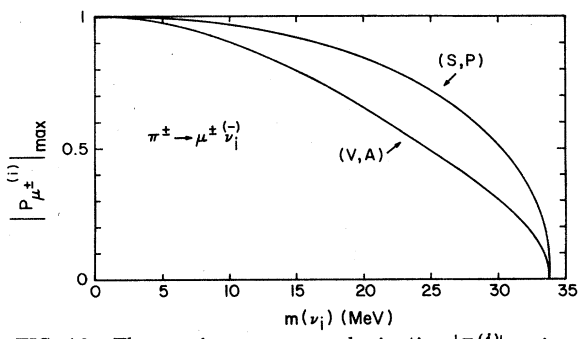

FIG. 18. The maximum muon polarization $|P^{(i)}_{\mu^\pm}|_{\rm max}$ in the decays $\pi^\pm \to \mu^\pm (\overset{(-)}{\nu})_i$ for the cases of pure (V, A) and pure (S, P) couplings.

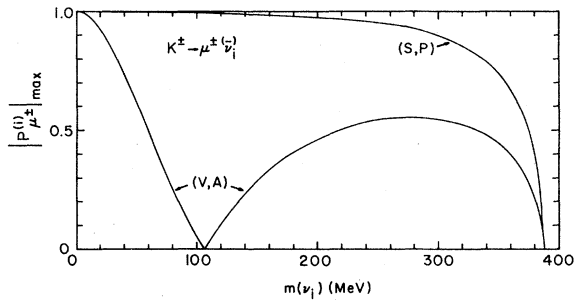

FIG. 19. Same as Fig. 18, but for the decays $K^+ \to \mu^\pm(\overline{\nu})_i$.

$\mathrm{Re}(\pm c_V^{(i)} c_S^{(i)*} + c_A^{(i)} c_P^{(i)*})$ in Eq. (2.42c). But since one does not know the values of the $|c_Z^{(i)}|$ for any given decay mode, this dependence is unobservable. Note also that this effect is strictly absent if the couplings are pure (V,A) or pure (S,P), regardless of whether CP is conserved by the respective $c_{V,A}^{(i)}$ or $c_{S,P}^{(i)}$. Similar comments apply to the charged-lepton polarization. Here one may first remark that if the effective interaction is purely chiral, $V \pm A$ or $S \pm P$, then even if U or its (S,P) analog is complex, this has no effect on $P_{l_a^\pm}^{(i)}(M_{l_a 2})$. For the general case [and also for the pure (S,P) or (V,A) cases, in contrast with the rate], for fixed $|c_Z^{(i)}|$, $P_{l_a^\pm}^{(i)}(M_{l_a 2})$, although CP conserving, does depend on whether CP is violated, through the various real parts of products of $c_Z^{(i)}$'s and $c_{Z'}^{(i)*}$'s. But again, one has no operational way of using this fact to test for CP violation.

Let us give a simple example which will illustrate these comments for the (V,A) case. Consider[26] a (generally non-left-right-symmetric) $\mathrm{SU}(2)_L \times \mathrm{SU}(2)_R \times \mathrm{U}(1)$ theory. In such a theory there would be different quark- and lepton-mixing matrices for the left- and right-handed fermions: $(q_a)_\chi = \sum_{i=1}^n V_{ai}^{(\chi)} (q_i)_\chi$ and $(\nu_a)_\chi = \sum_{i=1}^n U_{ai}^{(\chi)} (\nu_i)_\chi$, where $\chi = L$ or R, and a and i label the gauge group and mass eigenstates, respectively. For our illustrative example we shall assume that there is no $W_L - W_R$ mixing; it would be straightforward to incorporate this if one wished. The partial effective strengths of the left- and right-handed interactions, before multiplication by the appropriate quark and/or lepton mixing matrices, are given by $(G_\chi/\sqrt{2}) \equiv (g_\chi^2/8 m_{W_\chi}^2)$. Well known experimental data restrict the strength of the right-handed effective interaction for the LDC neutrinos, but allow it to be comparable to, or indeed larger than, the strength of the left-handed interaction for HSC ν_i modes, provided that these are sufficiently small relative to the LDC modes.[26,41] Then for the decay $M^+(q(\frac{2}{3})_r \overline{q}(-\frac{1}{3})_s) \to l_a^+ \nu_i$,

$$\kappa_{(V,A)}^{(i)} c_{(A)}^{(i)} = f_M \left(\mp \frac{G_L}{\sqrt{2}} V_{rs}^{(L)*} U_{ai}^{(L)*} + \frac{G_R}{\sqrt{2}} V_{rs}^{(R)*} U_{ai}^{(R)*} \right). \tag{2.52}$$

Observe that whereas for the $V-A$ case the quark-mixing-angle dependence factors out in the comparison of the rate for the ν_i HSC decay mode with that for the LDC mode(s) in Eqs. (2.21)–(2.15), so that one can determine $|U_{ai}|^2 \simeq R_{2i}$ or set an upper limit on it via the method of Eq. (2.23), this cancellation would not occur for the general (V,A) case, and hence one would not be able to determine or bound the lepton-mixing-matrix coefficients in the same manner. This is of course to be expected, since instead of the one complex unknown in each decay mode, U_{ai}, there would then be three: $U_{ai}^{(L)}$, $U_{ai}^{(R)}$, and $V_{rs}^{(R)}$. Observe also that any CP violation would be a combination of the violation in the quark and lepton sectors. One could also consider the effect of charged-Higgs-boson couplings, but this example will suffice.

Unfortunately, there is, to our knowledge, no published data to which the combined test can be applied. It is true that several experiments have been conducted to measure the polarization of the muon in $\pi_{\mu 2}$ decay. Following early work by Alikhanov *et al.*,[42] a CERN experiment determined the helicity of the μ^- from $\pi_{\mu 2}^-$ decay in flight by measuring the asymmetry in the muon-scattering cross section in polarized iron.[43] However, this experiment did not present any reconstructed $|\vec{p}_\mu|$ spectrum in the rest frame of the π^-, nor did it give the inferred longitudinal polarization of the μ^- in the π^- rest frame as a function of $|\vec{p}_\mu|$. Instead, only the resultant mean of all $\pi_{\mu 2}$ events was reported: $P_{\mu^-} = 1.17 \pm 0.32$.[43] A similar experiment by a Columbia-Nevis group measured P_{μ^-}, again with pion decays in flight, and obtained the result $P_{\mu^-} = +1$ with a ~30% uncertainty.[44] As in the CERN work, no reconstructed $|\vec{p}_\mu|$ momentum spectrum or twofold distribution of events as functions of $|\vec{p}_\mu|$ and P_{μ^-} was reported. Of course, this is to be expected, because such distributions would have appeared not to have any direct physical interest, given the tacit assumptions made in these experiments that $\pi_{\mu 2}$ decay yielded only two particles, each of definite mass. Similarly, one might inquire about the status of any measurements of P_{μ^+} in $K_{\mu 2}$ decay. The answer is that in the CERN-Heidelberg data $K_{\mu 2}$ data certain measurements of the energies of e^+'s from the decays of μ^+'s could be used indirectly to infer a rough value for P_{μ^+}, at least for the integrated event sample.[45] It would be interesting to reanalyze this data to obtain, if possible, a twofold distribution in both $|\vec{p}_\mu|$ and

P_{μ^+}. Finally, there is, to our knowledge, no published data on P_e in π_{e2} or K_{e2} decay, a situation that could have been foreseen because of the very small branching ratios for these rare decay modes and the tacit assumption that since "$m(\nu_e)$" = "$m(\nu_\mu)$" = 0, $P_{e^+}(M_{e2}) = P_{\mu^+}(M_{\mu 2})$ and similarly $P_{e^-}(M_{e2}) = P_{\mu^-}(M_{\mu 2})$.

F. The use of the M_{l2} spectral test as a probe of the number of lepton generations

The observation underlying this section is very simple but also very powerful. The logic proceeds in well-defined steps: first, in order for a massive neutrino line to be observed by the M_{l2} spectral test, it must have

$$m(\nu_i) > m(\{\nu_j\}_1)_{\max} = 60 \text{ eV} \tag{2.53}$$

[see (2.1) for the notation] and hence cannot be ν_1. Second, if it is observed to have

$$m(\nu_i) > m(\{\nu_j\}_2)_{\max} = 0.57 \text{ MeV}, \tag{2.54}$$

then, at the relevant confidence level, it cannot be ν_2. [This confidence level rapidly approaches unity as a function of the difference $m(\nu_i) - 0.57$ MeV.] This second condition will presumably be satisfied, if an HSC ν_i is observed at all, given the width and line shape of the LDC peak in M_{l2} decays and the difficulty of detecting an HSC ν_i peak which is unresolved from this LDC peak. Hence, assuming that an HSC ν_i line is detected, and that it satisfies the inequality (2.54), one has immediately proved that $i \geq 3$. For obvious reasons one cannot claim to have observed ν_3 itself. Next, if

$$m(\nu_i) > m(\{\nu_j\}_3)_{\max} \simeq 250 \text{ MeV}, \tag{2.55}$$

it follows that i must be greater than 3; that is, one has discovered not just a massive neutrino but a fourth generation of neutrinos. Within the standard theory of weak interactions this means that one has immediately established that there are $n \geq 4$ generations of leptons and of quarks. The condition (2.55) can, of course, not be met in π_{l2} decay but could be satisfied in the leptonic decays of $K^\pm$ and heavier charged pseudoscalar mesons such as the F, and so forth for b- and t-flavored mesons.

Let us then state the general generational bound which follows from the M_{l2} spectral test. Assume that one observes

$$k_1 \text{ lines with } m(\{\nu_j\}_2)_{\max} < m(\nu_i) < m(\{\nu_j\}_3)_{\max} \tag{2.56}$$

and

$$k_2 \text{ lines with } m(\nu_i) > m(\{\nu_j\}_3)_{\max} . \tag{2.57}$$

Then the number of neutrino types and hence, in the standard theory, the number of lepton and of quark generations, n, satisfies the lower bound

$$n \geq \max \begin{cases} k_1 + k_2 + 2 , \\ k_2 + 3 . \end{cases} \tag{2.58}$$

One should perhaps pause to remark on the great power of this result. Given only the very minimal assumption that the number of charged leptons is equal to the number of neutrinos, one has the potential of using the old and supposedly well-studied decays of $\pi^\pm$ and $K^\pm$ mesons (as well as the decays of heavier charged 0^- mesons) in a new way to gain information which may not be attainable with an upgraded PEP or PETRA and maybe not even with LEP itself; namely, to set a lower bound greater than 3 on the number of lepton generations. In the standard model, this is also the same lower bound on the number of quark generations. Of course, the M_{l2} spectral test may very well yield only null results, as indeed the search for new quarks and charged leptons at LEP may, but that is not the point; one should realize the *potential* that this test has for yielding information about n, as well as about the $m(\nu_i)$ and $|U_{ai}|$. The test requires no new accelerators but rather only a careful and precise experiment on leptonic π and K decay (and, ideally also the leptonic decays of F and heavier mesons), analyzed within an appropriately generalized theory of weak decays. It is clear that this feature of the test provides added motivation for one to perform it.

III. CONSTRAINTS ON NEUTRINO MASSES AND LEPTON MIXING ANGLES FROM $B(M^+ \to e^+ \text{ "}\nu_e\text{"})/B(M^+ \to \mu^+ \text{ "}\nu_\mu\text{"})$

We next proceed to discuss the constraints on possible HSC neutrino modes which can be obtained from the ratio of branching ratios:

$$R_M = \frac{B(M^+ \to e^+ \text{ "}\nu_e\text{"})}{B(M^+ \to \mu^+ \text{ "}\nu_\mu\text{"})} , \tag{3.1}$$

where $M = \pi$ or K, and the notation "ν_{l_a}" expresses the fact that the experiments do not observe the gauge-group eigenstates ν_{l_a} but instead, indirectly, the mass eigenstates ν_i which, in the case of interest, are different.[3] Thus, as was stressed before in Ref. 1, the quantity $B(M^+ \to l_a^+ \text{ "}\nu_{l_a}\text{"})$ is not fully defined without a precise specification of the cuts that were used to select the l_a^+"ν_{l_a}" events. Indeed, if an HSC ν_i had sufficiently large mass that the corresponding $|\vec{p}_a^{\,(i)}|$ or $E_a^{(i)}$ fell below their respective cuts, this mode would not even have been counted as part of the $l_a^+ \nu_{l_a}$ event sample. Moreover, for

sufficiently large $m(\nu_i)$ either or both of the decays $M^+ \to \mu^+ \nu_i$ and $M^+ \to e^+ \nu_i$ might be kinematically forbidden. The constraints from the measurement of R_M complement those derived above from a search for HSC peaks in the charged-lepton spectra in $M^+ \to l_a \nu_{l_a}$ decays. The latter apply with greatest sensitivity for $m(\nu_i)$ such that the corresponding $|\vec{p}_a^{\,(i)}|$ or $E_a^{(i)}$ are outside the main light-neutrino peak, whereas, in contrast, the measurement of R_M only places stringent bounds on the couplings $|U_{ai}|$, $a=1,2$, of those ν_i with $m(\nu_i)$ such that ν_i events are included in at least one of the l_a^+"ν_{l_a}" samples.

General constraints on lepton mixing in the standard three-doublet $SU(2)_L \times U(1)$ model were discussed previously.[5] The R_M constraints arise from the agreement between the measured values of R_π and R_K and the theoretical predictions of these ratios in the usual $V-A$ theory with radiative corrections incorporated. In Ref. 5 the general constraints were applied to a specific case in which $m(\nu_1)=m(\nu_2)=0$ and $m(\nu_3)$ is sufficiently heavy that the decays $M^+ \to l_a^+ \nu_3$, where $M=\pi$, K, and $l_a=e$, μ, are kinematically forbidden. Subsequently, Kolb and Goldman considered R_K in the case where $m(\nu_i)$ and $m(\nu_2)$ are assumed to be of order a few eV and $m(\nu_3)$ is such that the above decays into ν_3 could occur.[46] However, they failed to take into account the experimental cuts which were used to define the $M^+ \to e^+$"ν_e" and $M^+ \to \mu^+$"ν_μ" events. As will be seen from our analysis, when these cuts are correctly incorporated the bounds are changed substantially from those presented in Ref. 46.

The general expression for R_M, as calculated to lowest order in the standard electroweak gauge theory and applied to a particular experiment, is

$$R_M = \frac{\sum_{i=1}^{n} |U_{1i}|^2 \rho(\delta_e^M, \delta_i^M) \theta_{e\,\mathrm{cut}}^{(M)}}{\sum_{i=1}^{n} |U_{2i}|^2 \rho(\delta_\mu^M, \delta_i^M) \theta_{\mu\,\mathrm{cut}}^{(M)}} , \tag{3.2}$$

where of course the sums run over only the respective subsets of all n ν_i which satisfy the requirement $m_M > m_{l_a} + m(\nu_i)$. The $\theta_{l_a\,\mathrm{cut}}^{(M)}$ represent the combination of cuts used to define the M_{e2} and $M_{\mu 2}$ events. Thus, in the Columbia-Nevis π_{l2} experiment[23] $\theta_{e\,\mathrm{cut}}^{(\pi)} = \theta(E_e - E_{e\,\mathrm{cut}}^{(\pi)}) = \theta[m(\nu_i)_{\mathrm{cut}}^{(\pi e)} - m(\nu_i)]$ for each i, where $E_{\mathrm{cut}}^{(\pi)} \simeq 55$ MeV, and equivalently $m(\nu_i)_{\mathrm{cut}}^{(\pi e)} \simeq 65$ MeV. The function $\theta(x)=1$ if $x>0$ and 0 if $x \leq 0$. Finally, $\theta_{\mu\,\mathrm{cut}}=1$ since no cuts were imposed on the primary muon momentum or energy, which were not measured. For the CERN-Heidelberg K_{l2} experiment[24] $\theta_{e\,\mathrm{cut}}^{(K)} = \theta(|\vec{p}_e| - |\vec{p}_e|_{\mathrm{cut}}^{(Ke)}) = \theta[m(\nu_i)_{\mathrm{cut}}^{(Ke)} - m(\nu_i)]$ and similarly with μ, where $|\vec{p}_e|_{\mathrm{cut}}^{(K)} = 240$ MeV, i.e., $m(\nu_i)_{\mathrm{cut}}^{(Ke)} \simeq 82$ MeV, and $|\vec{p}_\mu|_{\mathrm{cut}}^{(K)} = 220$ MeV, i.e., $m(\nu_i)_{\mathrm{cut}}^{(K\mu)} \simeq 118$ MeV. In addition there were cuts to exclude events with excessively large momenta; however, these are not relevant to the application of Eq. (3.2). Finally, there were effectively cuts on β_e and β_μ due to the Čerenkov counters used to separate e^+'s from μ^+'s, but the effects of these were subsumed in the above $|\vec{p}_{e,\mu}|$ cuts.

In the case where $m(\nu_i)=0$ for all i, R_M reduces to

$$R_M^{(0)} = \frac{\delta_e^M (1-\delta_e^M)^2}{\delta_\mu^M (1-\delta_\mu^M)^2} . \tag{3.3}$$

More generally, if the neutrino masses are nonzero but $m(\nu_i) \ll m_e$ for all i, then the kinematic rate factors $\rho(\delta_a^M, \delta_i^M)$ in Eq. (3.2) are essentially equal for each i and hence, because of the unitarity of U, $R_M \simeq R_M^{(0)}$, independent of the lepton-mixing angles. Thus, for this case, $0 < m(\nu_i) \ll m_e$, the nonzero neutrino masses would not cause an experimentally detectable change in R_M from the value $R_M^{(0)}$, and so the experimental measurements of R_M could not be used to restrict the $|U_{ai}|$, $a=1,2$. Of course, this is not to say that there would not be any restrictions, but only that they would arise from other sources—nuclear β decay for $m(\nu_i)$ down to 10–100 eV and data bounding or observing neutrino oscillations, which is sensitive to substantially lower $m(\nu_i)$.

We briefly review the experimental measurements of R_M. As discussed above, R_π was measured by a Columbia-Nevis experiment; updating their original result by using the presently accepted value for the π^+ lifetime, one obtains[23] $R_\pi^{(\mathrm{exp})} = (1.274 \pm 0.024) \times 10^{-4}$. Combining this result in the usual least-squares manner with an earlier measurement by a Chicago experiment[47] yields[14] $R_\pi^{(\mathrm{exp})} = (1.267 \pm 0.023) \times 10^{-4}$. The lowest-order $V-A$ prediction, assuming that $m(\nu_i)=0$ for all i, is given by Eq. (3.3) with $M=\pi$: $R_\pi^{(0)} = 1.2836 \times 10^{-4}$. Incorporating radiative corrections (RC),[48] one obtains $R_\pi^{(0;RC)} = 1.233 \times 10^{-4}$, whence

$$\overline{R}_\pi^{(\mathrm{exp})} \equiv \frac{R_\pi^{(\mathrm{exp})}}{R_\pi^{(0;\mathrm{RC})}} = 1.028 \pm 0.019 . \tag{3.4}$$

(For the Columbia-Nevis experiment alone, $\overline{R}_\pi^{(\mathrm{exp})} = 1.033 \pm 0.019$.)

The most recent measurement of R_K was performed by a CERN-Heidelberg experiment, which obtained[24] $R_K^{(\mathrm{exp})} = (2.45 \pm 0.11) \times 10^{-5}$. The weighted mean of all experiments yields[14] $R_K^{(\mathrm{exp})} = (2.425 \pm 0.14) \times 10^{-5}$. The lowest-order $V-A$ prediction is $R_K^{(0)} = 2.5690 \times 10^{-5}$. Because the (structure-dependent term in the) radiative correction is uncertain, we shall write $R_K^{(0;\mathrm{RC})} = R_K^{(0)}(1 \pm \delta_K^{(\mathrm{RC})})$, where $\delta_K^{(\mathrm{RC})}$ represents this uncertainty and might be as large as ~0.05. Then

$$\bar{R}_K^{(\exp)} \equiv \frac{R_K^{(\exp)}}{R_K^{(0;\,\mathrm{RC})}} = 0.944 \pm \Delta\bar{R}_K^{(\exp)}, \tag{3.5}$$

where $\Delta\bar{R}_K^{(\exp)} = 0.055$ for $\delta_K^{(\mathrm{RC})} = 0$ and 0.07 for $\delta_K^{(\mathrm{RC})} = 0.05$. (The CERN-Heidelberg experiment alone gives $\bar{R}_K^{(\exp)} = 0.954 \pm \Delta\bar{R}_K^{(\exp)}$, where $\Delta\bar{R}_K^{(\exp)} = 0.043$ for $\delta_K^{(\mathrm{RC})} = 0$ and 0.06 for $\delta_K^{(\mathrm{RC})} = 0.05$.[48]) Evidently, $\bar{R}_\pi^{(\exp)}$ is only consistent with unity at approximately the 1.5σ level. In view of the uncertainty in the (structure-dependent part of the) radiative correction for $R_K^{(0;\,\mathrm{RC})}$, it is doubtful whether one can use $\bar{R}_K^{(\exp)}$ as reliably as $\bar{R}_\pi^{(\exp)}$ to test e-μ weak universality or to constrain neutrino masses and mixing angles. However, it is amusing to mention here a result which will emerge from our analysis to be given below: for certain ranges of $m(\nu_i)$ and $|U_{ai}|$, $a = 1, 2$; HSC i, which are allowed by other phenomenological constraints, $\bar{R}_\pi$ is slightly greater than unity, while $\bar{R}_K$ is slightly less than one. Indeed, it is conceivable that the deviations of $\bar{R}_\pi$ and $\bar{R}_K$ from unity are hitherto unrecognized indications of the presence of HSC neutrino modes in π_{l2} and K_{l2} decays.

The R_M constraint on neutrino masses and lepton mixing can be written in the form

$$\left|\bar{R}_M^{(\mathrm{RC})} - \bar{R}_M^{(\exp)}\right| \leq \epsilon(R_M), \tag{3.6}$$

where $\epsilon(R_M)$ is a measure of the uncertainty in the determination of $R_M^{(\exp)}$. It is reasonable to take

$$\epsilon(R_M) = \sigma_M, \tag{3.7}$$

where σ_M is the one-standard-deviation error in the measurement of $R_M^{(\exp)}$. In (3.6)

$$\bar{R}_M^{(\mathrm{RC})} \equiv \frac{R_M^{(\mathrm{RC})}}{R_M^{(0;\,\mathrm{RC})}}. \tag{3.8}$$

As before, the superscript (RC) signifies that the quantity contains order-α radiative corrections. It is easy to see that to our order of accuracy the radiative corrections to the ratio $\bar{R}_M^{(\mathrm{RC})}$ are negligible. Denote the radiatively corrected total rate for $M^+ \to l_a^+ \nu_i$ as

$$\Gamma^{(\mathrm{RC})}(M^+ \to l_a^+ \nu_i) \equiv \Gamma_0(M^+ \to l_a^+ \nu_i)[1 + \Delta(\delta_a^M, \delta_i^M)]. \tag{3.9}$$

Then the conventional result is

$$R_M^{(0;\,\mathrm{RC})} = R_M^{(0)}(1 + \Delta_M), \tag{3.10a}$$

where the correction

$$\Delta_M \equiv \Delta(\delta_e^M, 0) - \Delta(\delta_\mu^M, 0) \tag{3.10b}$$

was calculated by Kinoshita.[48] Now

$$\bar{R}_M^{(\mathrm{RC})} = \frac{\sum_{i\in\{i_L\}} |U_{1i}|^2 + \sum_{i\in\{i_H\}} |U_{1i}|^2 \bar{\rho}(\delta_e^M, \delta_i^M)\theta_{e\,\mathrm{cut}}^{(M)}\,[1 + \Delta(\delta_e^M, \delta_i^M) - \Delta(\delta_e^M, 0)]}{\sum_{i\in\{i_L\}} |U_{2i}|^2 + \sum_{i\in\{i_H\}} |U_{2i}|^2 \bar{\rho}(\delta_\mu^M, \delta_i^M)\theta_{\mu\,\mathrm{cut}}^{(M)}\,[1 + \Delta(\delta_\mu^M, \delta_i^M) - \Delta(\delta_\mu^M, 0)]}. \tag{3.11a}$$

Clearly, the difference between $\bar{R}_M^{(\mathrm{RC})}$ and

$$\bar{R}_M^{(0)} = \frac{\sum_{i\in\{i_L\}} |U_{1i}|^2 + \sum_{i\in\{i_H\}} |U_{1i}|^2 \bar{\rho}(\delta_e^M, \delta_i^M)\theta_{e\,\mathrm{cut}}^{(M)}}{\sum_{i\in\{i_L\}} |U_{2i}|^2 + \sum_{i\in\{i_H\}} |U_{2i}|^2 \bar{\rho}(\delta_\mu^M, \delta_i^M)\theta_{\mu\,\mathrm{cut}}^{(M)}} \tag{3.11b}$$

is a second-order correction, since the $|U_{ai}|^2$, $a = 1, 2$; $i \in \{i_H\}$, are forced by the totality of experimental data (if not always by the individual R_π or R_K constraints alone) to be quite small, whereas equivalently $\sum_{i\in\{i_L\}} |U_{ai}|^2$ is nearly equal to one. To a very good approximation we may therefore state the R_M constraint as

$$\left|\bar{R}_M - \bar{R}_M^{(\exp)}\right| \leq \epsilon(R_M). \tag{3.12}$$

In order to determine the bounds on an HSC neutrino mode we shall consider the simple case of $n-1$ light neutrinos and one HSC mode, labeled i. (The minimal and currently most interesting special case is $n = 3$, $i = 3$.) Then

$$\bar{R}_M = \frac{1 + |U_{1i}|^2[\bar{\rho}(\delta_e^M, \delta_i^M)\theta_{e\,\mathrm{cut}}^{(M)} - 1]}{1 + |U_{2i}|^2[\bar{\rho}(\delta_\mu^M, \delta_i^M)\theta_{\mu\,\mathrm{cut}}^{(M)} - 1]} \tag{3.13}$$

and the constraint (3.12) can be written explicitly as

$$\frac{\left|1 - \bar{R}_M^{(\exp)} + |U_{1i}|^2[\bar{\rho}(\delta_e^M, \delta_i^M) - 1] - |U_{2i}|^2[\bar{\rho}(\delta_\mu^M, \delta_i^M) - 1]\right|}{1 + |U_{1i}|^2[\bar{\rho}(\delta_\mu^M, \delta_i^M) - 1]} \leq \epsilon(R_M). \tag{3.14}$$

It is worth recalling that the R_M bound can be expressed in two logically equivalent ways: "If $m(\nu_i) = m_0$, then only those values of $|U_{1i}|$ and $|U_{2i}|$ which satisfy (3.14) are allowed" or, in contrapositive form, "if $|U_{1i}|$ or $|U_{2i}|$ lies outside of the range allowed for a given $m(\nu_i) = m_0$ by (3.14) then $m(\nu_i) \neq m_0$. Moreover, it must be stressed that we are concerned here *only* with the implications of the R_M constraint. Although the R_π and R_K constraints alone (and, at the 2σ level, together) would allow rather large values of $|U_{1i}|$ and/or $|U_{2i}|$ (HSC i) for certain ranges of $m(\nu_i)$, we do *not* mean to imply that there are not other experimental constraints which would preclude

such large values of HSC mixing coefficients. Indeed, there are: for example, neutrino oscillations of the HSC type, which would be spatially approximately uniform, in contrast to the possible oscillations inferred in Ref. 12. But it seems worthwhile at least to clarify precisely what bounds the R_M constraint alone places on the $|U_{ai}|$, $a=1,2$; HSC i, and that is the purpose of this section.

Since the experimental conditions are somewhat different for the π_{l2} and K_{l2} measurements, we shall discuss the corresponding applications of this general constraint separately. We consider $\bar{R}_\pi$ first and for illustrative purposes plot this ratio schematically as a function of $m(\nu_i)$ in Fig. 20, using the cuts of the Columbia-Nevis experiment. As $m(\nu_i)$ increases from zero, the helicity enhancement effect raises $\bar{\rho}(\delta_e^M, \delta_i^M)$ much faster than $\bar{\rho}(\delta_\mu^M, \delta_i^M)$ and consequently, unless $|U_{1i}| \ll |U_{2i}|$, $\bar{R}_\pi$ increases above one. This behavior is illustrated in Fig. 20. Two curves are shown, corresponding to two different values of $|U_{1i}|$, labeled in order of increasing magnitude by (a1) and (a2). The larger the value of $|U_{1i}|$, the more rapid the rise in $\bar{R}_\pi$ as a function of $m(\nu_i)$. The experimental value (3.4) is shown as the dot-dashed line, together with the tolerance limits $\bar{R}_\pi^{(\mathrm{exp})} \pm \epsilon(R_\pi)$, plotted for $\epsilon(R_\pi)=\sigma_\pi$ as dashed lines. The ranges of $m(\nu_i)$ within this interval for which the two different values of $|U_{1i}|$ represented by

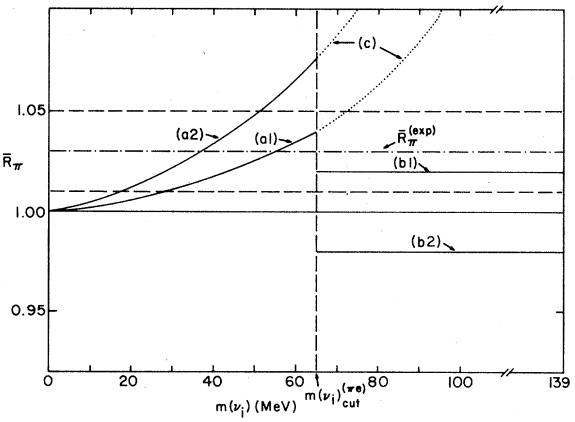

FIG. 20. Schematic plot of various possible qualitative behaviors (solid curve) of the ratio $\bar{R}_\pi$ in the case of one HSC ν_i. The central value of $\bar{R}_\pi^{(\mathrm{exp})}$ is indicated by the dot-dashed line, while the 1σ upper and lower values of this ratio are represented by the adjacent horizontal dashed lines. The vertical dashed line roughly indicates the value of $m(\nu_i)^{(\pi e)}_{\mathrm{cut}}$ corresponding to the energy cut applied in the data of Ref. 23. For explanations of the possible behaviors described by the sets of curves (a) and (b), and the significance of the dotted set of curves (c), see the text.

curves (a1) and (a2) are allowed or forbidden are evident from the graph. The size of $|U_{2i}|$ also influences $\bar{R}_\pi$, but for fixed $m(\nu_i)$, its effect is much smaller than that of $|U_{1i}|$. For $0 < m(\nu_i) < 4.9$ MeV, $\bar{\rho}(\delta_\mu^\pi, \delta_i^\pi)$ is greater than, but extremely close to, one; recall from Sec. II that $\bar{\rho}(\delta_\mu^\pi, \delta_i^\pi)_{\max}$ occurs at $m(\nu_i)=3.4$ MeV and is equal to 1.000 04. For $4.9 < m(\nu_i) < 33.9$ MeV, $\bar{\rho}(\delta_\mu^\pi, \delta_i^\pi)$ decreases smoothly from one to zero. As $m(\nu_i)$ increases beyond $m(\nu_i)^{(\pi e)}_{\mathrm{cut}}$, $\theta_{e\,\mathrm{cut}}^{(\pi)}$ falls to zero, and for larger values of $m(\nu_i)$, $\bar{R}_\pi = (1-|U_{1i}|^2)/(1-|U_{2i}|^2)$, independent of $m(\nu_i)$. In an actual experiment this falloff would be somewhat smeared out because of the imperfect resolution with which $|\vec{p}_a|$ or E_a are measured. In Fig. 20 two possible values of $\bar{R}_\pi$ are shown in this region, labeled by (b1) and (b2), corresponding to $|U_{1i}| < |U_{2i}|$ and $|U_{1i}| > |U_{2i}|$, respectively. Note that if, as in Ref. 46, one had failed to take account of the experimental cuts, then one would have obtained the erroneous dotted curves labeled (c). For $m(\nu_i)$ in region (a) $\bar{R}_\pi$ does place a stringent upper bound on $|U_{1i}|$, together with a weaker upper bound on $|U_{21}|$ over part of this interval.

Consider first the range

$$0 < m(\nu_i) < m(\nu_i)_1^{(\pi e)} = 4.9 \text{ MeV}. \tag{3.15}$$

In this interval the coefficient function $[\bar{\rho}(\delta_\mu^\pi, \delta_i^\pi) - 1]$ of $|U_{2i}|^2$ in Eq. (3.13) is positive. (The coefficient function $[\bar{\rho}(\delta_e^K, \delta_i^K) - 1]$ of $|U_{1i}|^2$ in Eq. (3.13) is always positive unless $m(\nu_i)$ is extremely close to the kinematic limit, 33.9 MeV.) Hence, for fixed $m(\nu_i)$ and $|U_{1i}|$, an increase in $|U_{2i}|$ decreases $\bar{R}_\pi$. Thus, for fixed $m(\nu_i)$, the maximum allowed value of $|U_{1i}|$ increases as a function of $|U_{2i}|$, although, as will be seen, this effect is quite small. The subset of the unit square in the $|U_{1i}|^2$, $|U_{2i}|^2$ plane which is allowed by the constraint (3.14) for a typical value of $m(\nu_i)$ in the interval (2.15), $m(\nu_i)=3$ MeV, is shown schematically in Fig. 21(a). We include this figure only for illustration, since it is the intersection of the regions allowed by the R_π and R_K constraints which is of physical interest. For clarity the scale of the $|U_{1i}|^2$ axis is greatly magnified relative to that of the $|U_{2i}|^2$ axis. The dashed area corresponds to the allowed region for $\epsilon(R_\pi)=\sigma_\pi$, while the dotted area applies for the more lenient assignment $\epsilon(R_\pi)=2\sigma_\pi$ (roughly a 95%-confidence-level limit). Before stating the bounds analytically we introduce some nomenclature. First, the terms "upper bound" and "lower bound" on $|U_{bi}|$ will be taken to mean "upper bound less than unity" and "lower bound greater than zero" on $|U_{bi}|$. Second, since there may or may not be an upper or lower bound on $|U_{bi}|$, $b=1,2$, depending on the values of other parameters, we shall often give such

bounds in the form

$$|U_{bi}|^2 \leq \min\{1, f\}_a \tag{3.16a}$$

and

$$|U_{bi}|^2 \geq \max\{0, g\}_a , \tag{3.16b}$$

where f and g are generic functions. The subscript a stands for "allowed" and indicates that if $f<0$ or $g>1$ there are no solutions for $|U_{1i}|$ and $|U_{2i}|$ which satisfy Eq. (3.14). As is evident from Fig. 21(a), $|U_{1i}|$ has an upper bound for all $|U_{2i}|$; it is given by

$$|U_{1i}|^2 \leq \frac{\bar{R}_\pi^{(\exp)} - 1 + \epsilon(R_\pi) + |U_{2i}|^2[\bar{\rho}(\delta_\mu^\pi, \delta_i^\pi) - 1][\bar{R}_\pi^{(\exp)} + \epsilon(R_\pi)]}{\bar{\rho}(\delta_e^\pi, \delta_i^\pi) - 1} . \tag{3.17}$$

Since $[\rho(\delta_\mu^\pi, \delta_i^\pi) - 1] \leq 5\times 10^{-4}$ while $[\bar{R}_\pi^{(\exp)} - 1 + \epsilon(R_\pi)] = 0.05$ [if one takes $\epsilon(R_\pi) = \sigma_\pi$], the second term in the numerator of the right-hand side of Eq. (3.16) is negligible compared to the first. Hence, the upper bound on $|U_{1i}|$ is almost independent of $|U_{2i}|$ for this range of $m(\nu_i)$. There may also be a lower bound on $|U_{1i}|$:

$$|U_{1i}|^2 \geq \max\left\{0, \frac{\bar{R}_\pi^{(\exp)} - 1 - \epsilon(R_\pi) + |U_{2i}|^2[\bar{\rho}(\delta_\mu^\pi, \delta_i^\pi) - 1][\bar{R}_\pi^{(\exp)} - \epsilon(R_\pi)]}{\bar{\rho}(\delta_e^\pi, \delta_i^\pi) - 1}\right\}_a . \tag{3.18}$$

For $\epsilon(R_\pi) = \sigma_\pi$ this is a nontrivial bound. It is easily seen that the constraint (3.16) by itself yields no upper bound on $|U_{2i}|$. Of course such an upper bound is imposed by the totality of experimental data relevant to possible HSC neutrino modes; however, we are examining only the implications of the R_M constraint here. To a very good approximation, $|U_{2i}|$ also has no lower bound. Strictly speaking, there exists an extremely narrow range of values of $|U_{1i}|$ for which there is such a lower bound, given by

$$|U_{2i}|^2 \geq \max\left\{0, \frac{1 - \bar{R}_\pi^{(\exp)} - \epsilon(R_\pi) + |U_{1i}|^2[\bar{\rho}(\delta_e^\pi, \delta_i^\pi) - 1]}{[\bar{\rho}(\delta_\mu^\pi, \delta_i^\pi) - 1][\bar{R}_\pi^{(\exp)} + \epsilon(R_\pi)]}\right\}_a , \tag{3.19}$$

namely the range

$$\frac{\bar{R}_\pi^{(\exp)} - 1 + \epsilon(R_\pi)}{\bar{\rho}(\delta_e^\pi, \delta_i^\pi) - 1} \leq |U_{1i}|^2 \leq \frac{\bar{R}_\pi^{(\exp)} - 1 + \epsilon(R_\pi) + [\bar{\rho}(\delta_\mu^\pi, \delta_i^\pi) - 1][\bar{R}_\pi^{(\exp)} + \epsilon(R_\pi)]}{\bar{\rho}(\delta_e^\pi, \delta_i^\pi) - 1} . \tag{3.20}$$

Consider next the region

$$4.9 \text{ MeV} < m(\nu_i) \leq m(\nu_i)_{\text{cut}}^{(\pi e)} . \tag{3.21}$$

Here $\bar{\rho}(\delta_\mu^\pi, \delta_i^\pi) < 1$, so that for fixed $m(\nu_i)$ and $|U_{1i}|$, an increase in $|U_{2i}|$ increases $\bar{R}$; consequently, the maximum allowed value of $|U_{1i}|$ is a decreasing function of $|U_{2i}|$, in contrast to the situation in the interval (3.15). For $m(\nu_i)$ in the interval (3.21) the allowed region can be either of two types, shown for representative masses in Figs. 21(b) and 21(c). Observe that for $\epsilon(R_\pi) = \sigma_\pi$ (represented as before by the dashed area) the immediate neighborhood of the origin is forbidden. $|U_{1i}|$ has the upper bound

$$|U_{1i}|^2 \leq \min\left\{1, \frac{\bar{R}_\pi^{(\exp)} - 1 + \epsilon(R_\pi) - |U_{2i}|^2[1 - \bar{\rho}(\delta_\mu^\pi, \delta_i^\pi)][\bar{R}_\pi^{(\exp)} + \epsilon(R_\pi)]}{\bar{\rho}(\delta_e^\pi, \delta_i^\pi) - 1}\right\}_a . \tag{3.22}$$

Here the second term in the numerator of the expression on the right-hand side of (3.22) is not in general negligible compared to the first. The absolute maximum value $|U_{1i}|_{\text{abs max}}$ occurs for $|U_{2i}| = 0$. For sufficiently small $|U_{2i}|$ there can also be a lower bound on $|U_{1i}|$:

$$|U_{1i}|^2 \geq \max\left\{0, \frac{\bar{R}_\pi^{(\exp)} - 1 - \epsilon(R_\pi) - |U_{2i}|^2[1 - \bar{\rho}(\delta_\mu^\pi, \delta_i^\pi)][\bar{R}_\pi^{(\exp)} - \epsilon(R_\pi)]}{\bar{\rho}(\delta_e^\pi, \delta_i^\pi) - 1}\right\}_a . \tag{3.23}$$

$|U_{2i}|$ may have an upper bound:

$$|U_{2i}|^2 \leq \min\left\{1, \frac{\bar{R}_\pi^{(\exp)} - 1 + \epsilon(R_\pi) - |U_{1i}|^2[\bar{\rho}(\delta_e^\pi, \delta_i^\pi) - 1]}{[1 - \bar{\rho}(\delta_\mu^\pi, \delta_i^\pi)][\bar{R}_\pi^{(\exp)} + \epsilon(R_\pi)]}\right\}_a . \tag{3.24}$$

As with $|U_{1i}|_{\text{abs max}}$, the absolute maximum value allowed for $|U_{2i}|$ is reached at $|U_{1i}| = 0$. The condition that $|U_{2i}|_{\text{abs max}}$ be less than unity is $\bar{\rho}(\delta_\mu^\pi, \delta_i^\pi) < [\bar{R}_\pi^{(\exp)} + \epsilon(R_\pi)]^{-1}$. For $\epsilon(R_\pi) = \sigma_\pi$ and $2\sigma_\pi$ this condition is satisfied for $m(\nu_i) \gtrsim 20$ and 21 MeV, respectively. In the interval (3.21) there is no lower bound on $|U_{2i}|$. Thus for $4.9 < m(\nu_i) \lesssim 20$ MeV the allowed region has the qualitative form illustrated with the particular value $m(\nu_i) = 10$ MeV in Fig. 21(b), while for $20 \text{ MeV} \lesssim m(\nu_i) < m(\nu_i)_{\text{cut}}^{(\pi e)}$ it has the form illustrated with $m(\nu_i) = 35$ MeV in Figs. 21(c1) and 21(c2).

Finally, if

$$m(\nu_i) > m(\nu_i)_{\text{cut}}^{(\pi e)} , \tag{3.25}$$

then (3.14) reads simply

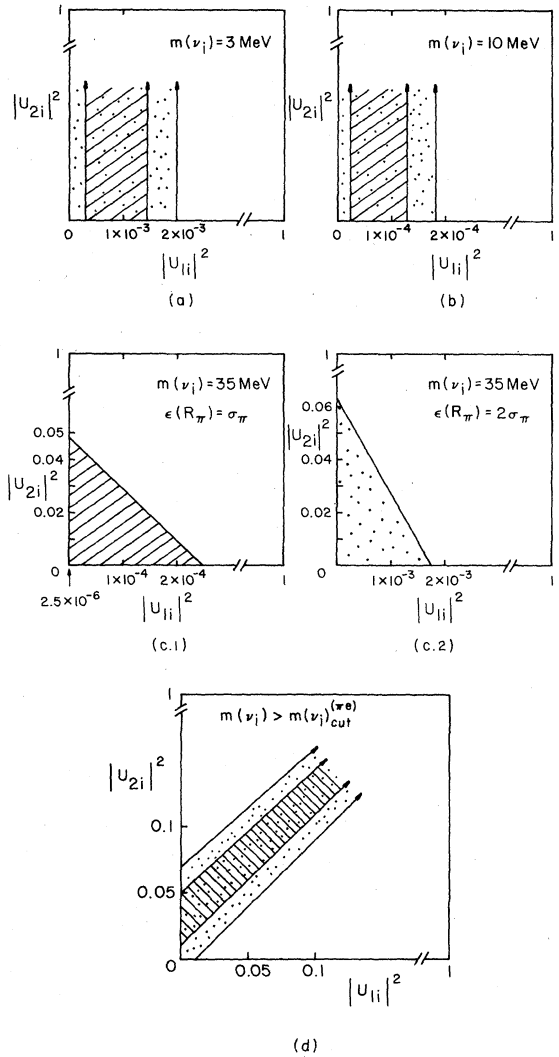

FIG. 21. Schematic plot showing the shapes of the regions in the $|U_{1i}|^2-|U_{2i}|^2$ parameter space allowed, for various values of $m(\nu_i)$, by the R_π constraint *by itself*. The diagonally slashed regions represent the bound (3.12) with $\epsilon(R_\pi)=\sigma_\pi$, while the dotted regions correspond to the same bound but with $\epsilon(R_\pi)=2\sigma_\pi$. The value [or, in the case of graph (d), the range of values] of $m(\nu_i)$ which applies for each graph is indicated on the figure.

$$\left|\frac{1-|U_{1i}|^2}{1-|U_{2i}|^2}-\bar{R}_\pi^{(\exp)}\right|\leq\epsilon(R_\pi) \tag{3.26}$$

independent of the actual value of $m(\nu_i)$, so long as it satisfies (3.25). The locus of solutions to this inequality is the diagonal strip shown schematically in Fig. 21(d). The constraint (3.14) also yields the bound (3.26) for $M=\pi$ or K if $m(\nu_i)>m_M-m_e$, independent of the experimental cuts in that case. It was this special case to which the general R_M constraint was applied in Ref. 5, and the result (3.26) was noted there.

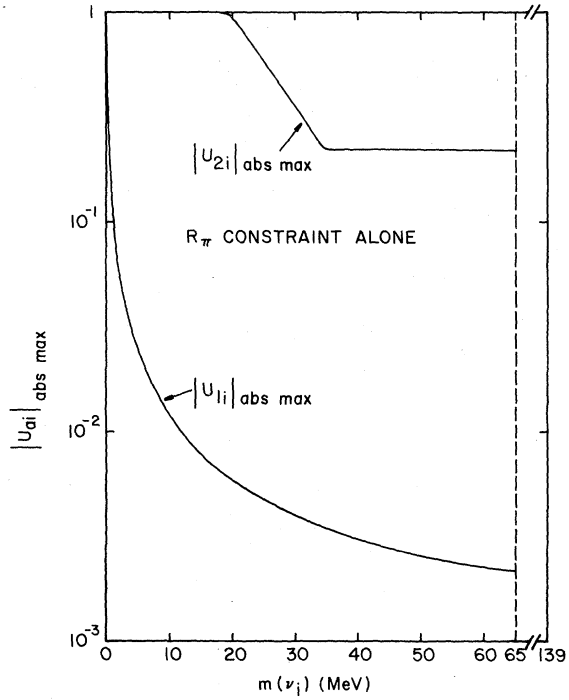

FIG. 22. The maximum values of the coupling coefficients $|U_{1i}|$ and $|U_{2i}|$ allowed, for $\epsilon(R_\pi)=\sigma_\pi$, by the R_π constraint in the case of one HSC ν_i, plotted as functions of $m(\nu_i)$. See the text for further details.

The values of $|U_{1i}|_{\text{abs max}}$ and $|U_{2i}|_{\text{abs max}}$ are plotted in Fig. 22 as functions of $m(\nu_i)$ for the cuts used in the Columbia-Nevis π_{l2} experiment. Note that for $m(\nu_i)>4.9$ MeV these values cannot occur simultaneously.

We next proceed to consider the $\bar{R}_K$ constraint. This is slightly more complicated than that for $\bar{R}_\pi$ because $\theta^{(K)}_{\mu\,\text{cut}}$ is a nontrivial function of $|\vec{p}_\mu|$. The behavior of $\bar{R}_K$ as a function of $m(\nu_i)$ is shown schematically in Fig. 23 for various choices of $|U_{ai}|$, $a=1,2$, and for the cuts used in the CERN-Heidelberg experiment. Observe that the coefficient functions $[\bar{\rho}(\delta_a^K,\delta_i^K)\theta^{(K)}_{l_a\,\text{cut}}-1]$ of the $|U_{ai}|$, $a=1,2$, in Eq. (3.13) with $M=K$ are both positive for $m(\nu_i)$ less than the respective $m(\nu_i)^{(Kl_a)}_{\text{cut}}$, for $l_a=e$, μ, and drop to -1 at these values of $m(\nu_i)$. *Apriori*, the cuts might have been sufficiently lenient that one or both of the $\theta^{(K)}_{l_a\,\text{cut}}$ functions remained equal to one all the way up to the respective neutrino masses $m(\nu_i)_1^{(Kl_a)}$ at which $\bar{\rho}(\delta_a^K,\delta_i^K)$ dropped below one. However, this is not the case in existing experiments; for K_{e2} decay, as mentioned above, $m(\nu_i)^{(Ke)}_{\text{cut}}=82$ MeV while $m(\nu_i)^{(Ke)}$ is extremely close to the kinematic limit, 493.2 MeV. Similarly, in $K_{\mu2}$ decay, $m(\nu_i)^{(K\mu)}_{\text{cut}}=118$ MeV, while $m(\nu_i)_1^{(K\mu)}=382$ MeV. Moreover,

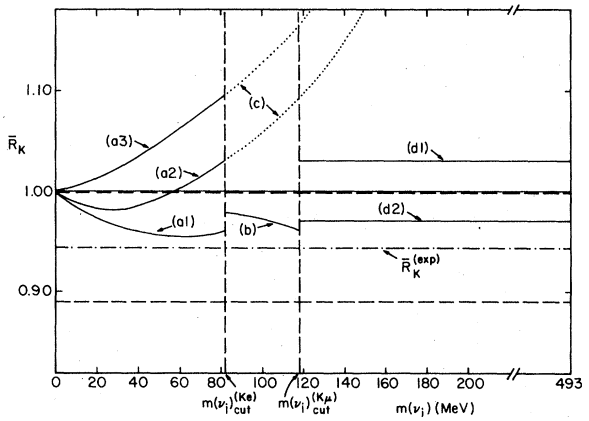

FIG. 23. Schematic plot of various possible qualitative behaviors (solid curves) of the ratio $\bar{R}_K$ in the case of one HSC ν_i. The central value of $\bar{R}_K^{(exp)}$ is indicated by the dot-dashed line, while the 1σ upper and lower values of this ratio are represented by the adjacent horizontal dashed lines. The vertical dashed lines represent the values of $m(\nu_i)_{cut}^{(K_{l2}a)}$ corresponding to the cuts applied to the data of Ref. 24 to define the $K^+ \to e^+ \text{“}\nu_e\text{”}$ and $K^+ \to \mu^+ \text{“}\nu_\mu\text{”}$ event samples. See the text for further explanation of the possible behaviors represented by the sets of curves (a), (b), and (d), and the significance of the set of curves (c).

$m(\nu_i)_{cut}^{(Ke)} > m(\nu_i)_{cut}^{(K\mu)}$; we shall assume this inequality in our general discussion in order for it to be directly applicable to the CERN-Heidelberg experiment from which the numerical values of these cuts were taken. Given these initial remarks, let us analyze the behavior of $\bar{R}_K$ and present the resulting bounds. We consider first the region $0 \leq m(\nu_i) \leq m(\nu_i)_{cut}^{(Ke)}$. As $m(\nu_i)$ increases from zero, $\bar{R}_K$ will rise monotonically above one if $|U_{1i}| \geq |U_{2i}|$; this situation is illustrated schematically in curve (a1) of Fig. 23. If $|U_{1i}|/|U_{2i}|$ is sufficiently less than unity, then $\bar{R}_K$ will begin by decreasing below one. If there exists a value of $m(\nu_i)$ less than $m(\nu_i)_{cut}^{(Ke)}$ such that $|U_{1i}|^2[\bar{\rho}(\delta_e^K, \delta_i^K) - 1] = |U_{2i}|^2[\bar{\rho}(\delta_\mu^K, \delta_i^K) - 1]$, then $\bar{R}_K$ will reach a minimum and curve upward again, crossing unity at this value of $m(\nu_i)$. This case is illustrated in curve (a2) of Fig. 23. If $|U_{1i}| \ll |U_{2i}|$, then the value of $m(\nu_i)$ which would yield the above equality among coefficient functions might be greater than $m(\nu_i)_{cut}^{(Ke)}$; in this case $\bar{R}_K$ would remain below unity throughout the range $0 < m(\nu_i) < m(\nu_i)_{cut}^{(Ke)}$. This third case is shown as curve (a3). As $m(\nu_i)$ increases past $m(\nu_i)_{cut}^{(Ke)}$, $\theta_{e\,cut}^{(K)} \to 0$ and $\bar{R}_K$ drops to $(1 - |U_{1i}|^2)/\{1 + |U_{2i}|^2[\bar{\rho}(\delta_\mu^K, \delta_i^K) - 1]\}$. This is less than unity for all $m(\nu_i)_{cut}^{(Ke)} < m(\nu_i) < m(\nu_i)_{cut}^{(K\mu)}$ and $|U_{ai}|$, $a = 1, 2$, and decreases as a function of $m(\nu_i)$. The behavior of $\bar{R}_K$ in this interval is illustrated by curve (b) of Fig. 23. The dotted curves labeled (c) indicate the spurious further growth in $\bar{R}_K$ which one would predict if one neglected the experimental cuts. Finally, for $m(\nu_i) > m(\nu_i)_{cut}^{(K\mu)}$ $\bar{R}_K$ takes on the value $(1 - |U_{1i}|^2)/(1 - |U_{2i}|^2)$, as shown by the lines (d1) and (d2) for $|U_{1i}| < |U_{2i}|$ and $|U_{1i}| > |U_{2i}|$, respectively.

Analytic expressions for the bounds on $|U_{ai}|^2$ from the R_K constraint can be derived in a manner similar to that for the R_π constraint; we omit the details for brevity. It is straightforward to take the intersection of the regions allowed by the R_π and R_K bounds to derive resultant overall allowed regions for particular values of $m(\nu_i)$. However, it is important to remember the uncertainty in the radiative correction for R_K. Especially in view of this, one might take the more cautious position of using the 95%-confidence-level errors for $\bar{R}_\pi^{(exp)}$ and $\bar{R}_K^{(exp)}$, which would allow not only the conventional $V-A$ theory with $m(\nu_i) = 0$ for all i but also a wider range of possible values of $|U_{1i}|$ and $|U_{2i}|$ for a given $m(\nu_i)$.

Before comparing the bounds on $|U_{ai}|$ from the R_M constraint with those obtained in Sec. II from the application of the M_{l2} spectral test, one should emphasize that the constraint and test are on somewhat different logical footings and yield different information about possible HSC ν_i decay modes. The spectral test is direct and is capable of being used to discover HSC ν_i lines in the charged-lepton spectrum. It can be applied on an event-by-event basis and can be used to determine $m(\nu_i)$ and, with the testable assumption of $V-A$ couplings, $R_{ai} \simeq |U_{ai}|^2$ for each of these lines, separately. If such an HSC ν_i decay should be observed in any one of the various M_{la2} decays, one could predict where to search for it in each of the other decays in which it would be kinematically allowed to occur. In contrast, the R_M constraint is not capable of proving the existence of an HSC ν_i decay, much less of determining $m(\nu_i)$ or R_{ai} for such a mode. Even if a statistically significant deviation of $\bar{R}_M^{(exp)}$ from unity should eventually be established and the radiative corrections were calculable with sufficient accuracy for this deviation to be used to gain information about the relevant weak interactions, this effect would be due to all of the HSC ν_i contributions present, as well as possible other new phenomena (see below) and could not, without further input, be utilized to investigate any particular ν_i mode. In the absence of any positive HSC ν_i signal, however, both the spectral and branching-ratio tests yield useful bounds on R_{ai}.

In passing, it is interesting to comment on precisely what information the R_M measurement does provide about weak interactions and, in particular, about possible charged-Higgs-boson con-

tributions to M_{l2} decay. Historically, the agreement between $R_\pi^{(\exp)}$ and $R_K^{(\exp)}$, and the predictions of the $V-A$ theory with radiative corrections played a key role in providing support for this theory and for the universality of $e\nu_e$ and $\mu\nu_\mu$ couplings incorporated in it. Indeed, it is often stated in the literature that this agreement confirms that the relevant couplings are $V-A$ and, furthermore, proves weak e-μ universality to the respective experimental levels of accuracy. In fact, however, both statements are incorrect, even in the conventional theoretical context of massless neutrinos, and hence no lepton mixing. To show this, we consider for simplicity the case where the charged-current couplings are of the pure (V,A) form. Then

$$(\bar{R}_M^{(0)})_{(V,A);m_\nu=0}=\frac{|c_V^{(e\nu_e)}|^2+|c_A^{(e\nu_e)}|^2}{|c_V^{(\mu\nu_\mu)}|^2+|c_A^{(\mu\nu_\mu)}|^2}. \quad (3.27)$$

Thus the experimental finding that $\bar{R}_M^{(\exp)}=1$ to the 1.5σ and $\sim 1\sigma$ levels for $M=\pi$ and K, respectively, does not prove e-μ weak universality, which is the statement that[49]

$$c_V^{(e\nu_e)}=c_V^{(\mu\nu_\mu)} \quad (3.28a)$$

and

$$c_A^{(e\nu_e)}=c_A^{(\mu\nu_\mu)}, \quad (3.28b)$$

but rather only the substantially weaker condition that

$$|c_V^{(e\nu_e)}|^2+|c_A^{(e\nu_e)}|^2=|c_V^{(\mu\nu_\mu)}|^2+|c_A^{(\mu\nu_\mu)}|^2 \quad (3.29)$$

to within the respective experimental uncertainties. Further, as is clear from Eq. (3.27), the R_M measurement, *by itself*, gives no information on whether the couplings are $V-A$ or not. It is, of course, true that the measured[42-44] μ^- polarization in $\pi_{\mu 2}^-$ decay demonstrates this to $\sim 30\%$ accuracy, and a combination of data, the most precise of which comes from μ and nuclear β decays, establishes the $V-A$ nature of leptonic weak-charged-current couplings and the property of e-μ universality to reasonably high precision. But when analyzing what constraints $\bar{R}_M^{(\exp)}$ provides concerning possible new phenomena such as neutrino masses and mixing, it is well to specify precisely what information it yielded in the conventional case.

In the more general context of nonzero neutrino masses and $U\neq 1$, it is necessary to redefine the meaning of e-μ weak universality. We restrict this redefinition to (V,A) couplings, since the (S,P) couplings due to Higgs-fermion interactions are naturally proportional to the fermion masses and hence would intrinsically violate e-μ universality. We first note that a very weak definition would be $\sum_{i=1}^n |U_{1i}|^2=\sum_{j=1}^n |U_{2j}|^2$, which of course is automatically satisfied in the standard electroweak theory. A stronger form of the definition would be $\sum_{i\in\{i_L\}}|U_{1i}|^2=\sum_{j\in\{j_L\}}|U_{2j}|^2$, which corresponds more closely to the meaning that the conventional definition would have if directly reinterpreted in the more general context of interest here. The strict requirement that $|U_{1i}|=|U_{2i}|$ for all i would be an unnatural one to use for the generalized definition since it does not correspond to the effective meaning of the old e-μ universality property and, indeed, is strongly violated if U is close to the identity. Thus, one may say that, even before considering the effects of Higgs-boson couplings, e-μ weak universality is naturally and generally violated if $m(\nu_i)\neq 0$ for some i and $U\neq 1$. However, this (tree-level[49]) violation may, *a priori*, be arbitrarily small. In contrast, as is well known, Higgs-boson couplings would also, and intrinsically, violate this universality of couplings. Just as in the conventional framework the agreement between the $V-A$ theory and the experimental measurements of R_π and R_K could not, by itself, prove e-μ weak universality, so also, *a fortiori*, it could not prove this in the more general case of nonzero neutrino masses and lepton mixing. The ratio $\bar{R}_M$ could equal unity to within the experimental accuracy even if the most reasonable definition given above did not hold, i.e., even if $\sum_{i\in\{i_L\}}|U_{1i}|^2\neq\sum_{j\in\{j_L\}}|U_{2j}|^2$, as long as the HSC contributions compensated for this inequality, so that

$$\sum_{i\in\{i_L\}}|U_{1i}|^2+\sum_{\text{HSC }i}|U_{1i}|^2\bar{\rho}(\delta_e^M,\delta_i^M)\theta_{e\,\text{cut}}^{(M)}=\sum_{j\in\{j_L\}}|U_{2j}|^2+\sum_{\text{HSC }j}|U_{2j}|^2\bar{\rho}(\delta_\mu^M,\delta_j^M)\theta_{\mu\,\text{cut}}^{(M)}$$

to the required precision. It is certainly true that this compensation could justifiably be considered conspiratorial, but it is nevertheless possible. Conversely, even if $\sum_{i\in\{i_L\}}|U_{1i}|^2=\sum_{j\in\{j_L\}}|U_{2j}|^2$, $\bar{R}_M$ would in general differ from unity. Hence, in the general context of $m(\nu_i)\neq 0$ and $U\neq 1$, it would be difficult to use an experimental measurement of $\bar{R}_M$ to test even a redefined form of e-μ weak universality. For an experiment seeking to test e-μ universality by measuring R_M, a necessary first step would be to set its own upper limit on possible HSC ν_i decay modes both inside and below the dominant light-neutrino peak. Subject to the reasonable assumption of the absence of anomalously strongly coupled charged Higgs bosons (see below), it could then establish a consequent upper limit on the deviation from effective e-μ weak universality as defined, say in terms of the quantity $(\sum_{i\in\{i_L\}}|U_{1i}|^2-\sum_{j\in\{j_L\}}|U_{2j}|^2)$. Historically, the measurement of R_π and R_K yielded a very stringent upper limit on the possible admixture of (S,P)

charged weak couplings. However, it is worthwhile to observe that a certain type of (S,P) coupling evades this upper limit. Consider a general interaction Lagrangian of the form

$$\mathcal{L}_I = \frac{g}{2\sqrt{2}}\,\bar{\psi}_{f_2}\gamma_\alpha(c_V^{(f_2f_1)} + c_A^{(f_2f_1)}\gamma_5)\psi_{f_1}W^\alpha + \frac{g}{2\sqrt{2}}\,\bar{\psi}_{f_2}(c_S^{(f_2f_1)} + c_P^{(f_2f_1)}\gamma_5)\psi_{f_1}\varphi + \text{H.c.}, \tag{3.30}$$

where ψ_{f_1} and ψ_{f_2} are two generic fermion fields and W and ϕ denote the charged vector and scalar boson fields. If the (S,P) couplings have the form

$$c_S^{(f_2f_1)} = \lambda(m_{f_2} - m_{f_1})c_V^{(f_2f_1)} \tag{3.31a}$$

and

$$c_P^{(f_2f_1)} = \lambda(m_{f_2} + m_{f_1})c_A^{(f_2f_1)}, \tag{3.31b}$$

where λ is an arbitrary constant, then, independent of the values of $m(\nu_i)$ and U, the presence of these (S,P) couplings does not change R_M or $P_{l_{\frac{1}{a}}}^{(i)}(M_{l_a2})$ from their (V,A) values. Hence, in particular, in the conventional framework with $m(\nu_i)=0$ and $U=1$, the experimental finding that $R_M=1$ to a given degree of accuracy does not, *by itself*, rule out (S,P) couplings of arbitrarily large magnitude, provided that they have the form given in Eq. (3.31).[50] However, having made this observation, one should add that, although the relations (3.31) are not unmotivated in certain models, typically $\lambda \sim m_W^{-1}$, so that even if present at full characteristic strength, the charged-Higgs-boson exchange would make negligible contributions to the amplitude for M_{l_a2} decay. This fact is important for our use of the R_M constraint to derive correlated bounds on $m(\nu_i)$ and R_{ai} since, *a priori*, a deviation of $\bar{R}_M^{(\text{exp})}$ from unity could not be taken to suggest the existence of HSC ν_i decay modes, even assuming that the radiative corrections were sufficiently accurately calculable, unless one could demonstrate that such a deviation could not be caused by other phenomena such as charged-Higgs-boson exchange. Thus for a given HSC ν_i decay mode, while a Higgs-boson contribution might be present, it would generally only be significant, relative to the regular W term, where both were extremely small.

From the point of view of planning experiments to search for HSC ν_i M_{l_a2} decays it is of immediate interest to know what upper bounds are implied by our above analysis of existing data on the branching ratios for these decays, relative to the dominant light-neutrino modes. Having obtained a set of correlated upper limits on the $|U_{ai}|^2 \simeq R_{ai}$ as functions of $m(\nu_i)$, it is now straightforward to answer this question, since

$$B_{H/L}[M_{l_a2}; m(\nu_i)] = R_{ai}\,\bar{\rho}(\delta_a^M, \delta_i^M), \tag{3.32}$$

where the subscript H/L refers to HSC modes relative to the sum of L(D+S)C modes. $B_{H/L}(\pi_{\mu 2}; m(\nu_i))_{\max}$ arises from the $\pi_{\mu 2}$ spectral test and accordingly is graphed in Fig. 16 as the dotted line (which coincides with the solid line except near the end point at 33.9 MeV). The upper bound on $B_{H/L}(\pi_{e2}; m(\nu_i))$ is presented in Fig. 24. The vertical dashed lines indicate where the limit from the R_π constraint ceases to apply and where the bound from the K_{e2} spectral test starts to apply. Because of the uncertainties in the radiative corrections for R_K and hence for $\epsilon(R_K)$, we have chosen not to graph the upper bounds due to the R_K constraint. It is straightforward to derive these from the various equations presented in this section, given as input a choice for $\delta_K^{(RC)}$ and thus $\epsilon(R_K)$. We emphasize that although no upper limit is drawn in the region $65 \lesssim m(\nu_i) \lesssim 82$ MeV, the R_K constraint does yield such a limit, albeit a model-dependent one. The upper bound on $B_{L/H}(K_{\mu 2}; m(\nu_i))$ is plotted in Fig. 25. For $m(\nu_i) \lesssim 34$ MeV it arises from the $\pi_{\mu 2}$ spectral test; for $m(\nu_i) \in (34\text{ MeV}, 65\text{ MeV})$ from the R_π constraint, and for $m(\nu_i) \in (85\text{ MeV}, 118\text{ MeV})$ from the $K_{\mu 2}$

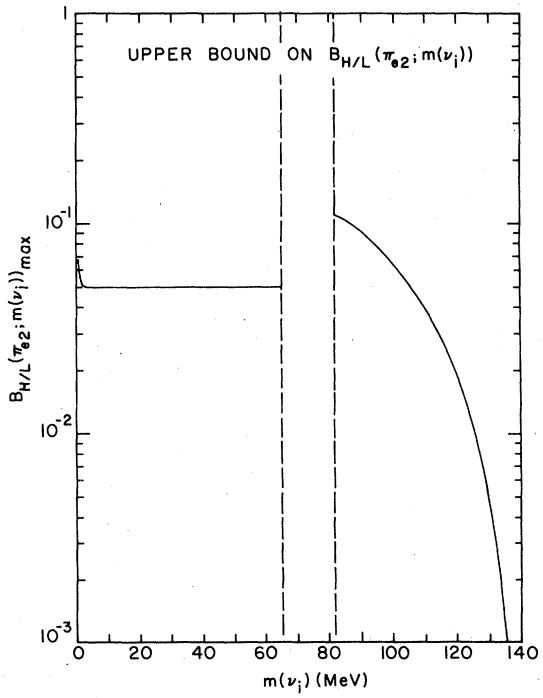

FIG. 24. The upper bound on the ratio of HSC to the sum of light-neutrino branching ratios for π_{e2} decay, $B_{H/L}(\pi_{e2}; m(\nu_i))$. See the text for definitions and further explanation.

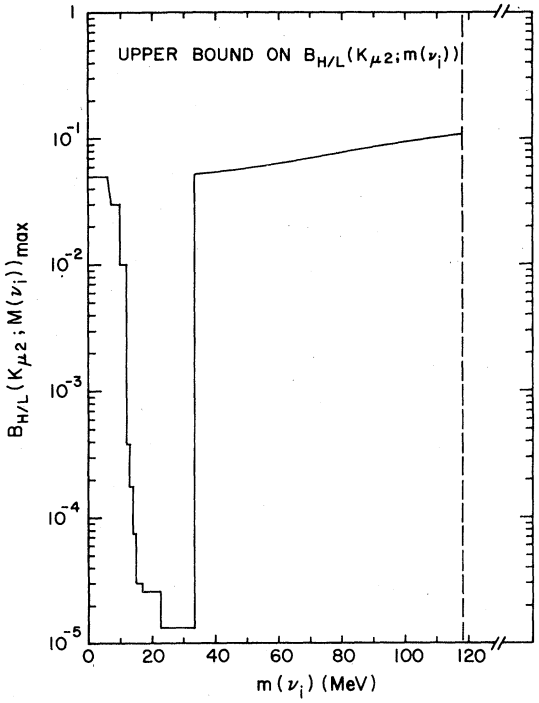

FIG. 25. Same as Fig. 24 but for $K_{\mu 2}$ decay. See also Ref. 25.

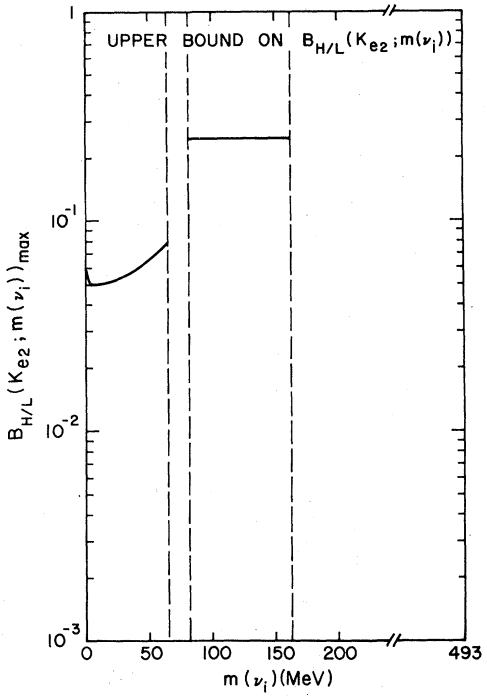

FIG. 26. Same as Fig. 24 but for K_{e2} decay.

spectral test. In the interval $m(\nu_i) \in$ (65 MeV, 82 MeV) the bound (3.26) from the R_π constraint, together with a (model-dependent) value of $|U_{1i}|_{max}^2$ from the R_K constraint, places an upper limit on the relative branching ratio, not plotted in Fig. 25. (See also Ref. 25.) Finally, $B_{L/H}(K_{e2};m(\nu_i))_{max}$ is presented in Fig. 26. It relies upon the R_π constraint for $m(\nu_i) \lesssim 65$ MeV and the direct K_{e2} spectral test for $m(\nu_i) \in$ (82 MeV, 163 MeV). In the region $m(\nu_i) \in$ (65 MeV, 82 MeV) the model-independent upper bound from the R_K constraint should be recalled; however, for $m(\nu_i) > 163$ MeV neither the spectral test nor the R_M bounds yields any useful upper limit on $B_{H/L}(K_{e2};m(\nu_i))$.

IV. THE LEPTONIC DECAYS OF HEAVY CHARGED 0^- MESONS

The application of the general theory to the leptonic decays of heavy charged 0^- mesons is somewhat more complicated than for light mesons, but again yields a number of striking and testable predictions. Indeed, such mesons may serve as unprecedented sources for the production and study of heavy neutrinos.

These complications stem partly from the unavailability of beams of heavy mesons and the low production rates, via e^+e^- annihilation, relative to the copious production of π's and K's in fixed-target accelerator experiments. In particular, although there are "factories" for the production of the light new-flavored 0^- mesons, such as the $\psi''(3.770)$ for the D's, the mesons with maximal leptonic branching ratios are heavier, as will be shown below, and for them one cannot expect such convenient sources. Furthermore, whereas one can stop π's and K's in an absorber to study their decays, heavy mesons have sufficiently short lifetimes that they will decay in flight. However, if the center-of-mass energy $\sqrt{s}$ is not too far above threshold for the production of a given heavy meson, it will have a relatively low velocity, and, independently of this, one can tag the three-momentum of one M^* in a pair by measuring the decay products of the other member of the pair, so that the decay in flight does not necessarily present a serious problem. The branching ratios of the dominant leptonic decay modes of heavy mesons are substantially smaller than those of the dominant modes $\pi_{\mu 2}$ and $K_{\mu 2}$ of the light mesons. Finally, there is another complication which arises from the fact that in the leptonic decays of heavy mesons some, such as those involving the τ lepton, will be cascade decays.

The rate for the decay $M^+(q_r(\frac{2}{3})\bar{q}_s(-\frac{1}{3})) \to l_a^+\nu_i$ is modulated by the quark-mixing-matrix factor $|V_{rs}|^2$. Experiments on V-suppressed versus V-allowed nonleptonic D decays and experiments on the (x_{vis} dependence of) charm-induced dilepton production in deep-inelastic ν_μ and $\bar{\nu}_\mu$ reactions have shown that $|V_{cd}/V_{cs}|^2 \equiv |V_{21}/V_{22}|^2 \sim |V_{us}/V_{ud}|^2$

$\equiv |V_{12}/V_{11}|^2$, which latter ratio is known[51] to be ~0.05. From an analysis of constraints on quark-mixing angles arising from the $K^0 \leftrightarrow \bar{K}^0$ transition and the $K_L \to \mu^+\mu^-$ decay rate, one can infer that $|V_{ub}/V_{cb}|^2 \equiv |V_{13}/V_{23}|^2 \ll 1$ and, more generally, that, barring finely tuned cancellations, quark mixing should be hierarchical, as defined before.[6] This finding that $|V_{23}/V_{23}|^2 \ll 1$ has recently received experimental support.[6] It is reasonable to expect that this V dependence will continue to hold for the t-flavored mesons. Note, however, that although one has a rough measure of $|V_{21}|$ and $|V_{22}|$ individually from ν_μ and $\bar{\nu}_\mu$ reactions, the theoretical and experimental result that $|V_{13}/V_{23}|^2 \ll 1$ does not fix the precise magnitude of either $|V_{13}|$ or $|V_{23}|$ individually. Now, since leptonic decays must involve the factor $|V_{rs}|^2$, whereas the dominant semileptonic and nonleptonic decays will only involve $\max\{|V^*_{rm}V_{sn}|^2\} = |V^*_{r,m=r}V_{s,n=s}|^2 \simeq 1$, the branching ratio $B(M^+(q_r\bar{q}_s) \to l_a^+\nu_i)$ is maximized if $r=s$. It follows that the heavy 0^- mesons of primary interest here are F, $M^+(c\bar{b})$, and $M^+(t\bar{b})$. Unfortunately, one will note that, for a given heavy flavor f, these are not the lightest f-flavored mesons, and for increasing $m(q_f)$ they become progressively heavier relative to these lightest f-flavored mesons. A consequence which was alluded to above is that, to the extent that there exist q_f-onium resonances which are just above threshold for the production of bare f-flavored hadrons, and hence serve as factories for the lowest-lying states, such as the $1\,^3D_1$ $\psi''(3.770)$ for D mesons or the $4\,^3S_1\Upsilon$ (10.55) for the low-lying 0^- B mesons,[52] these will not yield the mesons with optimal leptonic branching ratios. Although this is certainly a disadvantage, it may not be too serious. Consider, for example, the lowest-lying heavy meson of interest here, namely the F. In order to study leptonic F decays, one could tag one of the F's, say the F^+, produced in the $e^+e^- \to F^+F^-$ reaction by observing a V-allowed nonleptonic decay of its partner F^-, such as $F^- \to \pi^-\eta$. One could then search for events in which, besides the hadron system whose charge and mass reconstruct to those of the F^-, there is a single e^+ or μ^+. As we will show, there may also be spectacular events in which, besides the hadrons which reconstruct to the F^-, and the single e^+ or μ^+, there is a high-energy particle pair, which would usually be $e^-\pi^+$ and sometimes e^-e^+ if $n=3$, but could include $e^\mp\mu^\pm$, $\mu^-\mu^+$, $\mu^-\pi^+$, etc., if $n>3$. This pair would have a production vertex which in general, and especially if $n=3$, would be separated by some distance from the e^+e^- interaction point. It would also have a substantial invariant mass, which in the $l_a^-l_a^+$ case would show that it was not due to the conversion of a photon.

In the conventional theory of the leptonic decay of a heavy 0^- meson M^+, even in the V-favored case, the $e^+\nu_e$ and $\mu^+\nu_\mu$ modes have very small branching ratios because of the usual kinematic suppression. For the c- and $\bar{b}$-flavored mesons, the dominant leptonic decay mode is clearly $M^+ \to \tau^+\nu_\tau$. This is also true for the t-flavored meson $M^+(t\bar{q}_s)$ unless there exists an l_4 with $m_{l_4} < m(M^+(t\bar{q}_s))$ such that (in the conventional theory) $\delta_{l_4}^{Mt}(1-\delta_{l_4}^{Mt})^2 > \delta_\tau^{Mt}(1-\delta_\tau^{Mt})^2$. The actual rate, and hence branching ratio, are not precisely calculable, since, even if $|V_{rs}|$ is known approximately, the heavy-pseudoscalar-meson decay constant f_M is not. Estimates in various models do indicate that f_M is an increasing function of m_M.[53] In the case of the lowest-lying heavy mesons of interest here, the F, a rough number for the branching ratio $B(F^+ \to \tau^+\nu_\tau)$ can be obtained as follows.[54] The inputs for the calculation of $\Gamma(F^+ \to \tau^+\nu_\tau)$ in the conventional theory are m_τ, which has been measured to high precision, $|V_{22}|$, which is reasonably well known,[6] m_F, for which there are some measurements reported,[55,56] and f_F, which is not known. The original observation of the F reported by the DASP collaboration at DORIS yielded the value[55] $m_F = 2.03 \pm 0.06$ GeV, which we shall use here. This value is consistent, to within the errors, with the ones reported recently by emulsion experiments.[56] As for f_F, a conservative estimate would be that $f_F \simeq f_K \simeq f_\pi$. Next, one may use the quark-model estimate

$$\Gamma_{\rm tot}(F) \sim \Gamma_{\rm tot}(c) \simeq (|V_{21}|^2 + |V_{22}|^2) G_F^2 m_c^5 (192\pi^3)^{-1}(2+3\lambda),$$

where λ represents an effective strong-interaction enhancement of nonleptonic charm decays and is chosen to give the average observed semileptonic branching ratio $(\frac{1}{2})(B(D^+ \to e^+X) + B(D^0 \to e^+X)) \sim 0.1$. When sufficiently accurate measurements of the F lifetime become available from emulsion or bubble-chamber experiments one will be able to replace this estimate with an experimental value, but the preliminary measurements[56] have a large enough spread that we shall continue to use the quark-model result. Then

$$B(F^+ \to \tau^+\nu_\tau)_{\substack{m(\nu_i)=0\,\forall i \\ m_F = 2.03\ \text{GeV}}} \simeq 1.8\% \left(\frac{\tau_F}{4.2\times 10^{-13}\ \text{sec}}\right)\left(\frac{f_F}{f_\pi}\right)^2. \tag{4.1}$$

Unfortunately, even when m_F and τ_F are more accurately measured, this branching ratio will still be uncertain because of the lack of knowledge of f_F. The observed leptonic final state from the F^+ will consist of $(e^+$ of $\mu^+) + \cdots$, where the ellipsis represents the undetected (anti)neutrino(s). (We concentrate here on the leptonic decay modes

of the τ, since they provide signatures which are more free of hadronic backgrounds than those due to the semileptonic modes.) Hence, it is clear that one must contend with a rather small effective leptonic branching ratio $B(F^+ \to (e^+ \text{ or } \mu^+) + \cdots)$. Since the effective branching ratio above is evidently not reliably calculable, a more useful quantity to consider is the ratio of integrated single e^+ to μ^+ events, N_e^F/N_μ^F. In the conventional theory this ratio *can* be reliably predicted to be

$$\left(\frac{N_e^F}{N_\mu^F}\right)_{\substack{m(\nu_i)=0\,\forall i \\ m_F = 2.03 \text{ GeV}}} = \frac{B(F^+ \to e^+\nu_e) + B(F^+ \to \tau^+\nu_\tau)B(\tau^+ \to \bar{\nu}_\tau e^+\nu_e)}{B(F^+ \to \mu^+\nu_\mu) + B(F^+ \to \tau^+\nu_\tau)B(\tau^+ \to \bar{\nu}_\tau \mu^+\nu_\mu)} \simeq 0.72, \tag{4.2}$$

where we have used $B(\tau^+ \to \bar{\nu}_\tau e^+\nu_e) \simeq B(\tau^+ \to \bar{\nu}_\tau \mu^+\nu_\mu) \simeq 0.175$. In the conventional theory the ratio $B(\tau^+ \to \bar{\nu}_\tau e^+\nu_e)/B(\tau^+ \to \bar{\nu}_\tau \mu^+\nu_\mu)$ is predicted to be 1.03, which agrees, to within errors, with the experimental results[14] $B(\tau^+ \to \bar{\nu}_\tau e^+\nu_e) = (17 \pm 1.1)\%$ and $B(\tau^+ \to \bar{\nu}_\tau \mu^+\nu_\mu) = (17.9 \pm 1.5)\%$. Note that in the numerator of Eq. (4.2) the direct decay is completely negligible, while in the denominator the direct decay constitutes about 30% of the total. A more detailed prediction of this theory concerns the momentum spectra for such single e^+ and μ^+ events from leptonic F^+ decay. These spectra depend on the angles of production of the F^+F^- pair relative to the e^+e^- beam axis and of the τ^+ relative to the F^+ direction of motion, as well as β_F and hence $\sqrt{s}$. Qualitatively, the e^+ momentum spectrum would be determined by the usual differential decay distribution for (three-body) leptonic decay, appropriately twice Lorentz boosted. For $\sqrt{s} \gtrsim 2m_F$ they would peak around 1 GeV and fall off for larger momenta. The μ^+ momentum distribution would consist of a part, comprising about 70% of the total (assuming that $m_F = 2.03$ GeV), which follows the same smooth shape as the e^+ distribution, together with a part, comprising about 30% of the total, which has the shape of a sharper peak. In the rest frame of the F, the latter peak would occur at $|\vec{p}_\mu| = (m_F/2)(1 - \delta_\mu^F)$. Assuming that $n = 3$, with obvious changes in m_M, f_M, and V_{rs}, the same discussion applies to the leptonic decays of heavy $\bar{b}$- or t-flavored mesons. It might be noted that for these heavier mesons, the contribution to N_μ^M from the direct decay $M^+ \to \mu^+\nu_\mu$ would be commensurately smaller than it is for the F. These, then, would be the features of leptonic heavy-meson decay within the conventional theory, or the generalized theory with sufficiently small $m(\nu_i)$ and $|U_{ai}|$, $a \neq i$.

However, aside from this special case, the predictions of the general theory are noticeably different from those of the conventional theory with $m(\nu_i) = 0$ for all i. The rate for leptonic M^+ decay is given by

$$\Gamma(M^+(q_r\bar{q}_s) \to l_a^+\nu_i) = \frac{G_0^2 m_M^3 f_M^2}{8\pi} |V_{rs}|^2 |U_{ai}|^2 \rho(\delta_a^M, \delta_i^M), \tag{4.3}$$

where

$$\frac{G_0}{\sqrt{2}} \equiv \frac{g^2}{8m_W^2} \tag{4.4}$$

and g is the gauge coupling constant for the $SU(2)_L$ factor group in the standard electroweak gauge group.[4] Note that G_0 is *not* in general equal to the "usual" μ-decay constant $G_\mu = G_0^{(\text{apparent})}$ because of the effects of neutrino masses and mixing. However, for our present purposes we may neglect this difference and approximate $G_0 \simeq G_\mu$. We shall define the reduced rate

$$\Gamma_r(M^+(q_r\bar{q}_s) \to l_a^+\nu_i) = |U_{ai}|^2 \rho(\delta_a^M, \delta_i^M). \tag{4.5}$$

It is useful to divide our analysis of heavy-0^--meson leptonic decay into two parts; in the first we shall assume that there are only three generations of fermions, while in the second we shall generalize this to $n \geq 3$.

In the case $n = 3$ the effective reduced rate for $M^+ \to l_a^+ + \cdots$, $a = 1, 2$, is given by

$$\Gamma_r(M^+ \to l_a^+ + \cdots) = \sum_{i=1}^{3} |U_{ai}|^2 \rho(\delta_a^M, \delta_i^M) + B(\tau^+ \to \bar{\nu}_\tau l_a^+ \nu_{l_a}) \sum_{j=1}^{3} |U_{3j}|^2 \rho(\delta_\tau^M, \delta_j^M), \tag{4.6}$$

where

$$B(\tau^+ \to \bar{\nu}_\tau l_a^+ \nu_{l_a}) = \sum_{i,j=1}^{3} B(\tau^+ \to \bar{\nu}_i l_a^+ \nu_j). \tag{4.7}$$

Since the U dependence of $B(\tau^+ \to \bar{\nu}_i l_a^+ \nu_j)$ is $|U_{3i}U_{aj}^*|^2$, the dominant term in the sum in Eq. (4.7) is $B(\tau^+ \to \bar{\nu}_3 l_a^+ \nu_{j=a})$. Dropping completely negligible terms in Eq. (4.6), we obtain

$$\Gamma_r(M^+ \to e^+ + \cdots) = |U_{13}|^2 \rho(0, \delta_3^M) + B(\tau^+ \to \bar{\nu}_\tau e^+\nu_e)[(1 - |U_{33}|^2)\rho(\delta_\tau^M, 0) + |U_{33}|^2 \rho(\delta_\tau^M, \delta_3^M)] \tag{4.8}$$

and

$$\Gamma_\tau(M^+ - \mu^+ + \cdots) = |U_{22}|^2 \rho(\delta_\mu^M, 0) + |U_{23}|^2 \rho(\delta_\mu^M, \delta_3^M) + B(\tau^+ \to \bar{\nu}_\tau \mu^+ \nu_\mu)[(1 - |U_{33}|^2)\rho(\delta_\tau^M, 0) + |U_{33}|^2 \rho(\delta_\tau^M, \delta_3^M)] , \tag{4.9}$$

where we have taken $\rho(\delta_e^M, \delta_3^M) \simeq \rho(0, \delta_3^M)$ in the first term of Eq. (4.8), since this term can only be non-negligible if $\delta_3^M \gg \delta_e^M$. Let us comment on these results in the lowest-mass case of interest, where $M = F$. First, given the upper limit (2.3), together with the values of the reported measurements of m_F,[55,56] a substantial mass $m(\nu_3)$ would sharply reduce the $F^+ \to \tau^+ \nu_\tau$ decay rate and possibly even cause the dominant contribution to this rate, from the mode $F^+ \to \tau^+ \nu_3$, to vanish. If the off-diagonal lepton-mixing-matrix elements $|U_{ai}|$, $a \neq i$, are extremely small, then this would have the effect of rendering N_e^F utterly negligible and strongly reducing N_μ^F. Their ratio would then be $N_e^F/N_\mu^F \ll 1$, grossly different from the prediction of the conventional theory with $m(\nu_i) = 0\ \forall i$ given in Eq. (4.2). This effect is an obvious one and would have been noticed even if one had neglected lepton mixing. A more subtle effect arises from this mixing, namely that the $M^+ \to e^+ + \cdots$ yield now has a non-negligible direct, as well as cascade, contribution, from the decay $M^+ \to e^+ \nu_3$. Similarly, the $M^+ \to \mu^+ + \cdots$ yield receives a new direct HSC contribution from the decay mode $M^+ \to \mu^+ \nu_3$, in addition to the DC mode $M^+ \to \mu^+ \nu_2$. The branching ratios $B(\tau^+ \to \bar{\nu}_\tau l_a^+ \nu_{l_a})$ would also change somewhat, and their ratio ($a = 1$ versus $a = 2$) would increase very slightly. Thus, for example, considering the dominant modes in each case, the ratio (calculated to zero-loop order) $B(\tau^+ \to \bar{\nu}_3 e^+ \nu_1)/B(\tau^+ \to \bar{\nu}_3 \mu^+ \nu_2)$ would increase by about 0.2% as $m(\nu_3)$ grew from 0 to 200 MeV. Given the constraints on U, the reductions in the main DC cascade contributions to N_e^F and N_μ^F are not compensated by the small HSC mixing terms, so that both of these integrated yields decrease somewhat as $m(\nu_3)$ increases. Since the absolute sizes of $B(F^+ \to l_a^+ + \cdots)$ or, equivalently, in a given experiment, $N_{l_a}^F$, $l_a = e$ or μ, cannot be predicted very reliably, it is not clear that one can gain much information about $m(\nu_3)$ from the absolute size of the lepton yield. The following numerical examples will serve to give a quantitative measure of these effects for the case $n = 3$, $M = F$. Consider the value $m(\nu_3) = 200$ MeV. For this value of $m(\nu_3)$ neither the spectral test nor the branching-ratio constraint puts useful limits on $|U_{a3}|$, $a = 1, 2$. The R_K constraint [in the specific form of Eq. (3.26) with $\pi \leftrightarrow K$] does imply a certain upper bound on the ratio $(1 - |U_{13}|^2)/(1 - |U_{23}|^2)$, depending on the value that one takes for $\delta_K^{(RC)}$ and $\epsilon(R_K)$. To satisfy this constraint trivially, let us choose $|U_{13}| = |U_{23}|$. Then for $|U_{13}|^2 = |U_{23}|^2 = 0.001$, the ratio $N_e^F/N_\mu^F = B(F^+ \to e^+ + \cdots)/B(F^+ \to \mu^+ + \cdots) = 0.63$, down 12.5% from its conventional value of 0.72. Both the e^+ and μ^+ yields have decreased, but not too severely; $N_e^F/(N_e^F)_{\text{conv.}} = 0.64$ while $N_\mu^F/(N_\mu^F)_{\text{conv.}} = 0.75$. For the same $m(\nu_3)$, but the larger off-diagonal mixing coefficients $|U_{13}|^2 = |U_{23}|^2 = 0.01$, one finds similar results: $N_e^F/N_\mu^F = 0.64$, $N_e^F/(N_e^F)_{\text{conv.}} = 0.68$, and $N_\mu^F/(N_\mu^F)_{\text{conv.}} = 0.77$. Thus, the dominant effect is the differential reduction in N_e^F and N_μ^F due to the increase of $m(\nu_3)$ and the fact that N_μ^F has a significant contribution, from the direct decay $F^+ \to \mu^+ \nu_2$, whereas N_e^F does not. If the various unknown constants in Eqs. (4.1), (4.8), and (4.9) turn out to have values such that the single e and μ yields from F decay are large enough to be experimentally observable, then one can search for the change in N_e^F/N_μ^F which may serve as an indication that $m(\nu_3)$ is substantial. There would also be a small shift in the momentum spectra of the e^+ and μ^+ events which arise from the $F^+ \to \tau^+ \to (e^+, \mu^+) + \cdots$ cascade decay. The μ^+ peak from the direct DC decay $F^+ \to \mu^+ \nu_2$ would, of course, not shift. Because of the lepton mixing and growth of $m(\nu_3)$, there would appear a new peak in the e^+ spectrum located, in the rest frame of the F, at $|\vec{p}_e| = (m_F/2)(1 - \delta_3^F)$, corresponding to the first term in Eq. (4.8) with $M = F$. Similarly, there would appear a new peak in the μ^+ momentum spectrum positioned, in the F rest frame, at $|\vec{p}_\mu| = (m_F/2)\lambda^{1/2}(1, \delta_\mu^F, \delta_3^F)$, corresponding to the second term in the $M = F$ version of Eq. (4.9). However, numerical studies show that unless $m(\nu_3)$ is so large that the DC decay $F^+ \to \tau^+ \nu_3$ vanishes, these HSC peaks will have extremely small strengths relative to the smooth Lorentz-boosted three-body l_a^+ momentum distributions and, for $a = 2$, also relative to the μ^+ peak from the $F^+ \to \mu^+ \nu_2$ decay.

In the case $n = 3$, $M = M^+(c\bar{b})$ or $M^+(t\bar{b})$, the conventional value of N_e^M/N_μ^M would be closer to unity than it is for $M = F$, because the direct contribution to N_μ^M from $M^+ \to \mu^+ \nu_2$ would be considerably smaller than for the F. For example, if one estimates the mass of $B_c^+ \equiv M^+(c\bar{b})$ to be 6.5 GeV [and again uses $B(\tau^+ \to \bar{\nu}_\tau e^+ \nu_e) = B(\tau^+ \to \bar{\nu}_\tau \mu^+ \nu_\mu) = 0.175$], then $N_e^{B_c}/N_\mu^{B_c} = 0.98$. Moreover, in the general case of massive neutrinos, the effects of a substantial $m(\nu_3)$ would be proportionately smaller, since $m(\nu_3)_{\max}$ is a much smaller fraction of $m(B_c^+)$ or $m(T_b^+ \equiv M^+(t\bar{b}))$ than of m_F, and since both the decays $B_c^+ \to \tau^+ \nu_3$ and $T_b^+ \to \tau^+ \nu_3$ have

much more phase space available than does the decay $F^+ \to \tau^+ \nu_3$. Indeed, it is interesting to note that as $m(\nu_3)$ increases from 0 to its currently allowed maximum, the kinematic rate factors for the $\tau^+ \nu_3$ decay modes of these two heavier M's, $\rho(\delta_\tau^M, \delta_3^M)$, actually increase slightly, which is opposite to the behavior for $M=F$. For example, assuming the value given above for $m(B_c^+)$, one has $\rho(\delta_\tau^{B_c}, 0) = 0.064$, whereas with $m(\nu_3) = 100$ and 200 MeV, $\rho(\delta_\tau^{B_c}, \delta_3^{B_c}) = 0.065$ and 0.066, respectively.

Finally, in addition to the changes in the ratio N_e^M / N_μ^M and the single-e and-μ momentum spectra, one may observe some very striking events which, for $n=3$, would be predominantly of the form $M^+ \to (e^+ \text{ or } \mu^+) + [e^-\pi^+, e^-e^+]$ where the $e^-\pi^+$ pair in the square brackets would have a definite invariant mass $m(e^-\pi^+) \lesssim 250$ MeV and the e^+e^- pair (which would occur much less often) would have a variable invariant mass ranging up to the above value. These would arise from the cascade decays

$$M^+ \to \tau^+ \nu_3, \quad \tau^+ \to \begin{cases} \bar{\nu}_\tau e^+ \nu_e \\ \bar{\nu}_\tau \mu^+ \nu_\mu \end{cases}, \quad \begin{cases} \bar{\nu}_\tau e^+ \nu_e \to \bar{\nu}_\tau e^+ \nu_e \\ \bar{\nu}_\tau \mu^+ \nu_\mu \to e^- \nu_e e^+ \end{cases} \tag{4.10}$$

so that

$$m(e^-e^+) < m(e^-\pi^+) = m(\nu_3). \tag{4.11}$$

Let us examine the characteristics of these events in greater detail. First, unless $m(\nu_3) \gtrsim 200$ MeV, the ν_3 will have a sufficiently long lifetime τ_{ν_3} that it will escape from the detector before decaying. Specifically, if $2m_e < m(\nu_3) < m_\mu + m_e$, then the only available tree-level decay mode is $\nu_3 \to e^- \nu_e e^+$. The resultant lifetime is $\tau_{\nu_3} > \tau_\mu / |U_{31}|^2$, so that the ν_3 would not decay within the detection apparatus. For $m_e + m_\mu < m(\nu_3) < m_e + m_{\pi^-}$ the decay modes $\nu_3 \to e^- \nu_\mu \mu^+$ and $\nu_3 \to \mu^+ \nu_e e^+$ are available, but are strongly phase-space suppressed and do not change the statement made above about the escape of ν_3. The interesting range of the ν_3 mass is $m_e + m_{\pi^-} < m(\nu_3) < m(\nu_3)_{\max} \sim 250$ MeV, for which the decay channel $\nu_3 \to e^- \pi^+$ is open. The decay rates for the leptonic modes $\nu_3 \to l_a^- \nu_{1b} l^+$ with $(a,b) = (1,1)$, $(1,2)$, or $(2,1)$, are given by

$$\Gamma(\nu_3 \to l_a^- \nu_{1_b} l_b^+) = \sum_{j=1}^{2} \Gamma(\nu_3 \to l_a^- \nu_j l_b^+) \simeq \frac{G_0^2 m(\nu_3)^5}{192\pi^3} |U_{3a}|^2 \bar{\Gamma}\left(\frac{m_a}{m(\nu_3)}, \frac{m_b}{m(\nu_a)}, 0\right), \tag{4.12}$$

where we have approximated $\sum_{j=1}^{2} |U_{bj}|^2 \simeq 1$ for $b = 1, 2$. The function $\bar{\Gamma}(x,y,z)$ is the dimensionless phase-space function for three-body leptonic decay, which will be discussed further in paper II.[57] The rate for the semileptonic decay is[58]

$$\Gamma(\nu_3 \to e^-\pi^+) = \frac{G_0^2 m(\nu_3)^3 f_\pi^2}{16\pi} |V_{11}|^2 |U_{31}|^2 \lambda^{1/2}\left(1, \frac{m_e^2}{m(\nu_3)^2}, \frac{m_\pi^2}{m(\nu_3)^2}\right) \times \left[\left(1 - \frac{m_e^2}{m(\nu_3)^2}\right)^2 - \frac{m_\pi^2}{m(\nu_3)^2}\left(1 + \frac{m_e^2}{m(\nu_3)^2}\right)\right]. \tag{4.13}$$

Hence

$$\tau_{\nu_3}|_{m(\nu_3)=0.2 \text{ GeV}} = \frac{6.5 \times 10^{-9} \text{ sec}}{|U_{31}|^2 + 0.13 |U_{32}|^2}. \tag{4.14}$$

Thus, with $|U_{31}|^2 = |U_{32}|^2 = 0.01$, $\tau_{\nu_3} = 0.57 \times 10^{-6}$ sec, while for a hierarchical choice $|U_{31}|^2 = 0.001$ and $|U_{32}|^2 = 0.01$, $\tau_{\nu_3} = 2.8 \times 10^{-6}$ sec. Consequently, a slowly moving ν_3 might have a significant chance of decaying within the sensitive volume of an experimental detector. Next, we calculate the relevant branching ratios:

$$B(\nu_3 \to e^-\pi^+)_{m(\nu_3)=0.2 \text{ GeV}} = \frac{0.92}{[1 + 0.92 \times 10^{-3}(|U_{32}|^2/|U_{31}|^2)]}, \tag{4.15}$$

$$B(\nu_3 \to e^-\nu_e e^+)_{m(\nu_3)=0.2 \text{ GeV}} = \frac{0.0715}{[1 + 0.92 \times 10^{-3}(|U_{32}|^2/|U_{31}|^2)]}, \tag{4.16}$$

and

$$B(\nu_3 \to e^-\nu_\mu \mu^+)_{m(\nu_3)=0.2 \text{ GeV}} = \left|\frac{U_{31}}{U_{32}}\right|^2 B(\nu_3 \to \mu^-\nu_e e^+)_{m(\nu_3)=0.2 \text{ GeV}} = \frac{0.0092}{[1 + 0.92 \times 10^{-3}(|U_{32}|^2/|U_{31}|^2)]}. \tag{4.17}$$

Thus, unless $|U_{31}|^2/|U_{32}|^2 \ll 10^{-3}$, the dominant decay mode for this region of $m(\nu_3)$ is $\nu_3 \to e^-\pi^+$. The $\nu_3 \to e^-\nu_e e^+$ decay channel has a considerably smaller branching ratio, and the $e^*\mu^\mp$ leptonic modes are negligibly small. Note that if, indeed, $|U_{31}|^2/|U_{32}|^2 \ll 10^{-3}$, then τ_{ν_3} would be so long that the ν_3 would leave the apparatus before decaying, so that for this mass range one can conclude that the above magnitudes and order of branching ratios will apply in general to experimentally observable events. This order is quite fortunate, since in the

$\nu_3 \to e^-\pi^+$ decay mode the invariant mass $m(e^-\pi^+)$ will have the same value, $m(\nu_3)$, for all events, which (1) aids in the identification of these events and their separation from backgrounds, and (2) allows one to measure $m(\nu_3)$. In contrast, in the three leptonic modes the invariant mass $m(l_a^- l_b^+)$ does not have the same value in different $\nu_3 \to l_a^- \nu_{l_b} l_b^+$ decays, and so one loses both of the advantageous features mentioned above. [It is true that one could obtain information on $m(\nu_3)$ on a statistical basis for these leptonic decays.]

Next, we proceed to consider the case $n > 3$. Since the effects of a ν_3 with mass ranging up to its currently allowed maximum have already been analyzed, the present discussion will concentrate on the distinctive new features of the $n > 3$ case, namely, the possibility of one or more ν_i, $i \geq 4$, with masses $m(\nu_i) > m(\nu_3)_{\max}$, and, in addition, the possibility of an l_a, $a \geq 4$, which might occur in the decays of the $T_b^+ \equiv M^+(t\bar{b})$. We may thus divide our discussion and deal with the massive-neutrino effects first.

For the purpose of this analysis, it is helpful to plot the basic kinematic rate function for $M^+ \to l_a^+ \nu_i$ decay, $\rho(\delta_a^M, \delta_i^M)$, for the full range of both of its variables. This is done in Fig. 27, with units chosen such that $m_M \equiv 1$. As is clear from its definition, Eqs. (2.13) and (2.14), $\rho(x,y)$ is a symmetric function of its two variables. In the conventional theory, or the generalized theory in the case $\nu_i \in \{\nu_{i_L}\}$, the kinematic rate function reduces to $\rho(\delta_a^M, 0)$. Similarly, in the leptonic decays of heavy mesons yielding a light charged lepton and heavy neutrino with $m(\nu_i) \gg m_{l_a}$, ρ reduces to $\rho(0, \delta_i^M)$. The general function relevant to both of these cases is then $\rho(x,0) = x(1-x)^2$. This function is plotted for $x \equiv m_1^2 \equiv (m_a/m_M)^2$ as curve (a) in Fig. 27. It has a maximum at $x = \frac{1}{3}$, or $m_1 \simeq 0.577 m_M$, where it is equal to $\frac{4}{27}$. The decays $M^+ \to l_a^+ \nu_{l_a}$ in the conventional theory with $m(\nu_i) = 0$ for all i, and the decays $M^+ \to l_a^+ \nu_{i_L}$ in the general theory, can thus be classified according to where they lie on this universal curve, as determined by (m_a/m_M). All conventional M_{e2} decays, and, in addition, $M_{\mu 2}$ decays for $M = F$ or heavier mesons, lie too close to the origin to be marked clearly. The positions of the $K_{\mu 2}$, $\pi_{\mu 2}$, and $F_{\tau 2}$ decays (with $m_F = 2.03$ GeV in the last case) are indicated with circular dots on the horizontal axis

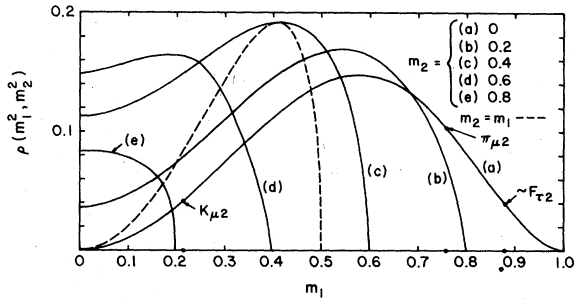

FIG. 27. Plot of the M_{l2} kinematic rate function $\rho(m_1^2, m_2^2)$, with the units of mass chosen such that $m_M \equiv 1$.

and curve (a) in Fig. 27. Because of the uncertainty in $m(B_c^+ \equiv M^+(c\bar{b}))$, we have not marked the position of the conventional $B_c^+ \to \tau^+ \nu_\tau$ or general $B_c^+ \to \tau^+ \nu_{i_L}$ decay in this graph. For $m(B_c^+) = 6.5$ GeV, it would lie at $m_1 = (m_\tau/m_{B_c}) \simeq 0.27$, with $\rho(\delta_\tau^{B_c}, 0) = 0.064$. As m_2 increases from 0, the position of the relative maximum in $\rho(m_1^2, m_2^2)$ for fixed m_2 moves from $m_1 = 1/\sqrt{3}$ toward 0. One can observe from Fig. 27 that for a large range of m_1, $\rho(m_1^2, m_2^2)$ increases as m_2 increases from 0 to positive values. Note how even for $m_2 = 0.8$ [curve (e)], as m_1 increases from 0, ρ grows slightly from its value at $m_1 = 0$ before eventually dropping sharply to 0. If one takes $m_1 = m(\nu_i)/m_\pi$ and $m_2 = m_\mu/m_\pi = 0.76$, one sees that this curve (e) is close to describing the dynamics of $\pi^+ \to \mu^+ \nu_i$ decay. In this context, one may recall the gradual maximum of $\bar{\rho}(\delta_i^\pi, \delta_\mu^\pi)$ or equivalently $\rho(\delta_i^\pi, \delta_\mu^\pi)$ at $m(\nu_i) = 3.4$ MeV (i.e., $m_1 = 0.024$) where $\bar{\rho}(\delta_i^\pi, \delta_\mu^\pi) \simeq 1.000\,04$. For mathematical purposes we have also included the curve $\rho(x, y = x) = 2x(1-4x)^{1/2}$ since, (1) for fixed $m_{\rm tot} = m_1 + m_2$, $\rho(m_1^2, m_2^2)$ has a relative maximum at the symmetric value $m_1 = m_2$, and hence (2) the absolute maximum of ρ occurs along the line $m_1 = m_2$, specifically at the value $m_1 = 1/\sqrt{6}$, where $\rho = 1/(3\sqrt{3})$.

In the case $n > 3$, the expressions for $\Gamma_r(M \to l_a^+ + \cdots)$ and $B(\tau^+ \to \bar{\nu}_\tau l_b^+ \nu_{l_b})$ are given by Eqs. (4.6) and (4.7) with the sums running from 1 to n, as allowed by phase space. For illustrative purposes, let us assume that there are $n-1$ neutrinos with masses that are sufficiently light that their kinematic effects are unimportant, and one heavy $\nu_i \equiv \nu_{[n]}$, with $i \neq 3$. Then, assuming that there is no l_a, $a \geq 4$, with $m_{l_a} < m_M$,

$$\Gamma_r(M^+ \to e^+ + \cdots) \simeq |U_{1i}|^2 \rho(0, \delta_i^M) + B(\tau^+ \to \bar{\nu}_\tau e^+ \nu_e)[(1 - |U_{3i}|^2)\rho(\delta_\tau^M, 0) + |U_{3i}|^2 \rho(\delta_\tau^M, \delta_i^M)] \tag{4.18}$$

and

$$\Gamma_r(M^+ \to \mu^+ + \cdots) \simeq |U_{22}|^2 \rho(\delta_\mu^M, 0) + |U_{2i}|^2 \rho(\delta_\mu^M, \delta_i^M) + B(\tau^+ \to \bar{\nu}_\tau \mu^+ \nu_\mu)[(1 - |U_{3i}|^2)\rho(\delta_\tau^M, 0) + |U_{3i}|^2 \rho(\delta_\tau^M, \delta_i^M)]. \tag{4.19}$$

There are clearly no changes in the DC direct or cascade terms as $m(\nu_i)$ changes. The HSC ν_i cascade contributions decrease and finally vanish as $m(\nu_i)$ grows beyond $m_M - m_\tau$, but these terms were already suppressed by the small coupling coefficient $|U_{3i}|^2$ and branching ratio $B(\tau^+ \to \bar{\nu}_\tau l_b^+ \nu_{l_b})$. The interesting point is that the kinematic rate functions for the $M^+ \to e^+\nu_i$ and $M^+ \to \mu^+\nu_i$ decay modes could reach values near to the absolute maximum, $1/3\sqrt{3}$, a feature which is not possible in the $n=3$ case. For example, choosing $M=F$ and taking $|U_{2i}|^2 = 0.01$ and $m(\nu_i) = 1$ GeV, one finds that in $\Gamma_\tau(F^+ \to \mu^+ + \cdots)$ the HSC term $|U_{2i}|^2 \rho(\delta_\mu^F, \delta_i^F) = 1.4 \times 10^{-3}$, which is a significant fraction of the LDC direct term $|U_{22}|^2 \rho(\delta_\mu^F, 0) \simeq \rho(\delta_\mu^F, 0) = 2.7 \times 10^{-3}$ and the LDC cascade term

$$B(\tau^+ \to \bar{\nu}_\tau \mu^+ \nu_\mu)(1 - |U_{3i}|^2)\rho(\delta_\tau^F, 0) \simeq B(\tau^+ \to \bar{\nu}_\tau \mu^+ \nu_\mu)\rho(\delta_\tau^F, 0) = 7.0 \times 10^{-3}.$$

A similar comment applies to the HSC contribution to $\Gamma_\tau(M^+ \to e^+ + \cdots)$. As regards the momentum spectra, the e^+ and μ^+ spectra from the LDC cascade, and the μ^+ peak from the LDC direct decay, are unaffected by $m(\nu_i)$. However, the peaks due to $M^+ \to l_a^+ \nu_i$, which are not necessarily negligibly small, will occur at progressively lower values of $|\vec{p}_a|$ for increasing $m(\nu_i)$ and may be distinguishable from the other spectra. As was discussed for light mesons in Sec. II F, the spectral test can be used as a probe of the number of generations. If one is able to detect the heavy ν_j peaks in the $l_a^+ = e^+$ or μ^+ momentum spectra from $M^+ \to l_a^+ \nu_j$ decays, then, given their number and the inferred values of the $m(\nu_j)$, one can set lower bounds on n in a manner similar to that explained in Sec. II F.

Concerning events in which the ν_i decays, for increasing $m(\nu_i)$, the rates for the leptonic modes $\nu_i \to l_a^- \nu_{l_a} l_b^+$ increase rapidly, since they are proportional to $m(\nu_i)^5$ for $m_a + m_b \ll m(\nu_i)$. The new leptonic decay channel $\nu_i \to \mu^- \nu_\mu \mu^+$ opens when $m(\nu_i)$ passes above $2m_\mu$, as does the semileptonic channel $\nu_i \to \mu^- \pi^+$ when $m(\nu_i) > m_\mu + m_\pi$. As $m(\nu_i)$ increases, since the semileptonic modes have rates which grow like $m(\nu_i)^3$ for meson masses small compared to $m(\nu_i)$, they will comprise a progressively smaller fraction of the rate compared to the totality of leptonic decay modes. The ν_i lifetime decreases rapidly for larger $m(\nu_i)$, so that these events in which the ν_i decays within the volume of the detector will become more predominant. For a given value of $m(\nu_i)$, it is straightforward to enumerate the main decay modes and calculate their branching ratios, as well as τ_{ν_i}. As noted, for sufficiently large $m(\nu_i)$, the leptonic decay modes would tend to predominate over any exclusive semileptonic modes such as the $e^-\pi^+$ channel which was dominant in the case of a heavy ν_3.

Finally, we consider the effects of a possible l_a, $a \geq 4$. Note that, given the present limit $m(l_a^-) \gtrsim 17$ GeV for $a \geq 4$ from experiments performed at PETRA,[59] such an $l_{a \geq 4}$ could not occur in F or B_c^+ decay. If there exists an $a \geq 4$ such that $m(l_a) < m(T_b^+)$, then the decay $T_b^+ \to l_a^+ \nu_{l_a}$ could occur, and, depending on the values of the $|U_{aj}|$ and $\delta_{l_a}^{T_b}$, $a \geq 4$, and $\delta_j^{T_b}$, one such decay $T_b^+ \to l_a^+ \nu_j$ might well be the dominant leptonic decay mode of the T_b^+. However, it seems premature at present to examine such possibilities further.

V. CONCLUSIONS

We have presented a general theory of weak leptonic and semileptonic decays which incorporates consistently the possibility of nonzero neutrino masses and associated lepton mixing. Since no experiment will ever show that all neutrino masses are strictly zero, and, indeed, present experiments do not rule out a mass of ~ 200 MeV for at least one neutrino, even assuming that there are only three generations, the necessity of such a generalized theory and corresponding generalized analysis of existing data on these decays is clear. We have given a precise statement of the meaning of current neutrino-mass limits. In this paper we have applied the general theory to the leptonic decays of charged pseudoscalar mesons. The analysis led to a new and very sensitive test for neutrino masses and mixing involving the measurement of the charged-lepton spectrum, which was shown to consist not just of a single line, but rather of a discrete set of lines. This test was applied to existing data on π_{l2} and K_{l2} data to derive correlated bounds on neutrino masses and mixing coefficients. We have proposed new, but not overly difficult, experiments to perform this test in π_{l2} and K_{l2} decays. The use of the test to probe the number of lepton generations was discussed, as well as an extension of it which includes a measurement of the charged-lepton polarization. We have also determined the constraints on lepton mixing arising from the ratio $B(M^+ \to e^+\nu_e)/B(M^+ \to \mu^+\nu_\mu)$, where $M = \pi$ or K, taking proper account of the experimental cuts which were used to define e^+"ν_e" and μ^+"ν_μ" events. Finally, we have given a general analysis of the leptonic decays of charged heavy pseudoscalar mesons.

Perhaps the most exciting aspect of this work is the prospect of new high-precision, high-statistics experiments which will apply our test to search for additional peaks due to heavy subdominantly cou-

pled neutrinos in the e or μ momentum or energy spectrum in π_{l2} and K_{l2} decays. Armed with a new understanding of the effects of massive neutrinos (viz., not just a slightly shifted main peak, but instead a multitude of peaks, with the main one not necessarily shifted at all), they will, it is hoped, search over regions of $|\vec{p}_e|$ and $|\vec{p}_\mu|$ never before studied as M_{l2} data. One awaits their findings with great interest.

Note added. The current status of experiments to apply the M_{l2} test proposed in Ref. 1 and discussed at length in this paper is as follows. First, at SIN a group has conducted a preliminary search for a second shoulder in the μ^+ momentum spectrum in $\pi_{\mu 2}$ decay, down to $|\vec{p}_\mu| \simeq 27$ MeV $\simeq 0.91\,|\vec{p}_\mu|_0$ and has reported the tentative upper limits $B(\pi^+ \to \mu^+ \nu_{\mathrm{HSC}\ i}) < 3\%$ for $4 < m(\nu_i) < 9$ MeV and $B(\pi^+ \to \mu^+ \nu_{\mathrm{HSC}\ i}) < 2\%$ for $6 < m(\nu_i) < 14$ MeV. See R. Abele *et al.*, SIN Newsletter, No. 13, p. 11 (1980). A more dedicated experiment is planned. Second, a University of Virginia proposal by R. Minehart, K. Ziock, and collaborators to use a Ge counter experiment to search for additional peaks in the $|\vec{p}_\mu|$ spectrum in $\pi_{\mu 2}$ decay has been submitted and approved at SIN. Third, a University of Tokyo-KEK-Tsukuba University proposal by T. Yamazaki and collaborators has been approved, as Experiment E89 at KEK, to search for an HSC peak in the $|\vec{p}_\mu|$ spectrum in $K_{\mu 2}$ decay. I thank R. Frosch, R. Minehart, K. Ziock, and T. Yamazaki for discussions concerning these developments.

ACKNOWLEDGMENTS

I would like to thank R. Frosch for providing tabulated data from the experiment of Ref. 8 and H. Siebert and A. Walenta for discussions of the data of Refs. 24 and 25. I am also grateful to H. Heckman for discussions concerning the Berkeley emulsion data of Ref. 27. Finally, I thank C. -N. Yang for a helpful conversation. This research was supported in part by NSF Contract No. PHY-79-06376.

[1] R. E. Shrock, Phys. Lett. 96B, 159 (1980); see also R. E. Shrock, p. S63, in Particle Data Group, Rev. Mod. Phys. 52, S1 (1980).

[2] Although we include this qualification about the possibility of massive but degenerate neutrinos, we consider such a possibility to be too artificial to be taken very seriously.

[3] More precisely, in the massive nondegenerate case the neutrino gauge-group eigenstates could coincide with the neutrino mass eigenstates only over a set of measure zero in the space of parameters determining the lepton mixing matrix U in Eq. (1.1). Without any symmetry principle to force such a singular occurrence, one would have to regard it as very unnatural.

[4] S. Weinberg, Phys. Rev. Lett. 19, 1264 (1967); A. Salam, in *Elementary Particle Theory: Relativistic Groups and Analyticity (Nobel Symposium No. 8)*, edited by N. Svartholm (Almqvist and Wiksell, Stockholm, 1968), p. 367; S. Glashow, Nucl. Phys. 22, 579 (1961). The versions of the theory with two- and three-quark doublets were discussed, respectively, by S. Glashow, J. Iliopoulos, and L. Maiani, Phys. Rev. D 22, 1285 (1970) and M. Kobayashi and T. Maskawa, Prog. Theor. Phys. 49, 652 (1973).

[5] B. W. Lee and R. E. Shrock, Phys. Rev. D 16, 1444 (1977).

[6] It is interesting that, according to present bounds on quark-mixing angles in the $n = 3$ version of the standard electroweak theory, the two orderings implied by the analogs of conventions (1) and (2) appear to coincide for quarks. Indeed, with the quark-mass eigenbasis defined naturally according to the analog of convention (2), these bounds on the quark mixing matrix V imply that it satisfies not just property (1) but also the stronger property $|V_{ai}| > |V_{bj}|$ *if* $|a-i| < |b-j|$. This has been called "hierarchical mixing"; it is an open question whether it is also true of leptons [with their mixing defined according to convention (2)]. See for the above bounds on quark mixing, R. E. Shrock and L.-L. Wang, Phys. Rev. Lett. 41, 1692 (1978); R. E. Shrock, invited talk at the Caltech Workshop on High Energy Physics, 1979 (unpublished); R. E. Shrock, S. B. Treiman, and L.-L. Wang, Phys. Rev. Lett. 42, 1589 (1979); and R. E. Shrock and M. B. Voloshin, Phys. Lett. 87B, 375 (1979). The finding that $|V_{ub}/V_{cb}|^2 \ll 1$ has recently received experimental support from studies of B-meson production at CESR; see K. Berkelman, in *High Energy Physics—1980*, proceedings of the XXth International Conference, Madison, Wisconsin, edited by L. Durand and L. G. Pondrom (AIP, New York, 1981); p. 1499; E. Thorndike, *ibid.*, p. 705.

[7] E.-E. Bergkvist, Nucl. Phys. B39, 317 (1972).

[8] M. Daum, G. H. Eaton, R. Frosch, H. Hirschmann, J. McCulloch, R. C. Minehart, and E. Steiner, Phys. Lett. 74B, 126 (1978); Phys. Rev. D 20, 2692 (1979); R. Frosch and R. C. Minehart, private communications.

[9] R. Cowsick and J. McClelland, Phys. Rev. Lett. 29, 669 (1972); Astrophys. J. 180, 7 (1973).

[10] B. W. Lee and S. Weinberg, Phys. Rev. Lett. 39, 165 (1977); S. Tremaine and J. Gunn, *ibid.* 42, 407 (1979).

[11] R. Cowsick, Phys. Rev. Lett. 39, 784 (1977); D. Dicus *et al.*, *ibid.* 39, 168 (1977); Phys. Rev. D 17, 1529 (1978); 19, 1522 (1979); Astrophys. J. 221, 237 (1978); J. Gunn *et al.*, *ibid.* 223, 1015 (1978); S. Falk and D. Schramm, Phys. Lett. 79B, 511 (1978). See also G. Steigman *et al.*, *ibid.* 66B, 202 (1977); J. Yang *et al.*, Astrophys. J. 227, 697 (1979); F. Stecker, Phys. Rev. Lett. 44, 1237 (1980).

[12] Z. Maki, M. Nakagawa, and S. Sakata, Prog. Theor. Phys. 28, 870 (1962); V. Gribov and B. Pontecorvo, Phys. Lett. 28B, 495 (1969); F. Reines, H. W. Sobel, and E. Pasierb, Phys. Rev. Lett. 45, 1307 (1980); see, however, R. P. Feynman and P. Vogel, Caltech report

(unpublished).

[13]W. Bacino *et al.*, Phys. Rev. Lett. 42, 749 (1979). It should be noted that this mass limit is self-consistent in the sense that the mass of the τ is determined from the threshold behavior of the cross section $\sigma(e^+e^- \to \tau^+\tau^-)$ and not, for example, from the end point of the μ or e in its leptonic decay, so that m_τ would not change if "$m(\nu_\tau)$" $\neq 0$.

[14]Particle Data Group, Rev. Mod. Phys. 52, S1 (1980).

[15]J. Simpson, in *Neutrino '79*, proceedings of the International Conference on Neutrinos, Weak Interactions, and Cosmology, Bergen, Norway, 1979, edited by A. Haatuft and C. Jarlskog (Univ. of Bergen, Bergen, 1980), Vol. 2, p. 208. Other less stringent upper limits on "$m(\nu_e)$", again from experiments on tritium β decay, include "$m(\nu_e)$" < 86 eV (90% C.L.), from B. Röde and H. Daniel, Lett. Nuovo Cimento 5, 139 (1972) and "$m(\nu_e)$" < 100 eV (90% C.L.) from W. Piel, Nucl. Phys. A203, 369 (1972).

[16]E. Tretyakov *et al.*, in *Proceedings of the International Neutrino Conference, Aachen, 1976*, edited by H. Faissner, H. Reithler, and P. Zerwas (Vieweg, Braunschweig, West Germany, 1977), p. 663; E. Tretyakov *et al.*, Izv. Akad. Nauk. SSSR Ser. Fiz. 40, 2026 (1976) [Bull. Acad. Sci. USSR, Phys. Ser. 40, 1 (1976)].

[17]V. Lyubimov, E. Novikov, V. Nozik, E. Tretyakov, and V. Kosik, Phys. Lett. 94B, 266 (1980). Since the experimental situation regarding the question of whether "$m(\nu_e)$" $\neq 0$ is quite unsettled at the present time, we shall make the conservative choice of continuing to use the upper limit of 60 eV (90% C.L.) obtained by Bergkvist (Ref. 7) and accepted by the Particle Data Group (Ref. 14).

[18]Specifically, m_μ is determined, via comparison of $(g-2)_\mu$ with $(g-2)_e$, in terms of m_e, which in turn is derived from atomic physics. The masses of m_{π^+} and m_{K^+} are determined most accurately from measurements of the spectra of pionic and kaonic atoms, respectively. These facts also underlie the self-consistency of the M_{l2} test proposed in Ref. 1.

[19]For earlier experiments which obtained limits on "$m(\nu_\mu)$", see Ref. 14 and Sec. II C.

[20]C. Blocker, Univ. of California at Berkeley Ph.D. thesis, LBL Report No. 10801 (unpublished); J. Dorfan, private communication. This limit assumes the value $m_\tau = 1.782^{+0.002}_{-0.007}$ GeV obtained by W. Bacino *et al.*, Phys. Rev. Lett. 41, 13 (1978).

[21]The test to search for discrete spectral lines due to the decays $M^\pm \to l_a^\pm(\overline{\nu})_l$ can also be applied to heavier pseudoscalar mesons such as the F. This will be discussed in Sec. IV.

[22]More precisely, the lines are monochromatic in the limit of no e or μ energy loss in the target or by soft bremsstrahlung, and perfect spectrometer resolution. Obviously, as the $m(\nu_i) \to 0$, the incoherent line spectrum smoothly approaches the single (coherent) $m(\nu_i) = 0$ line, and $\sum_i |U_{ai}|^2 \rho(\delta_a^M, \delta_i^M) \to \rho(\delta_a^M, 0)$, where the property $U^\dagger U = 1$ has been used. This occurs when $m(\nu_i)^2 \ll m_M^2, m_a^2$. It is easily shown that, given the values of $m_{K,\pi}$, $m_{\mu,e}$, the momentum or energy resolution of possible M_{l2} experiments, and the spatial resolution of neutrino detectors, these trivial kinematic considerations render the spectrum effectively coherent long before any quantum-mechanical effects associated with the propagation of neutrinos become important, i.e., before this propagation is characterized by oscillation wavelengths which are large enough to be detectable in a practical experiment. Thus, as is implicit in the text, these quantum-mechanical effects are not relevant to our present analysis.

[23]E. Di Capua, R. Garland, L. Pondrom, and A. Strelzoff, Phys. Rev. B133, 1333 (1964). See also D. Bryman and C. Picciotto, Phys. Rev. D 11, 1337 (1975) which updates the original experimental result of Di Capua *et al.* by using the currently accepted value of the π^+ lifetime.

[24]K. Heard, J. Heintze, G. Heinzelmann, P. Igo-Kemenes, W. Kalbreier, E. Mittag, H. Rieseberg, B. Schurlein, H. Siebert, V. Soergel, K. Streit, A. Wagner, and A. Walenta, Phys. Lett. 55B, 327 (1975); J. Heintze *et al.*, *ibid.* 60B, 302 (1976); G. Heinzelmann, H. Siebert, and A. Walenta, private communications. Although we have used the events with $220 < |\vec{p}_{\mu,e}| < 230$ MeV for our bounds, we record the warning that "below 230 MeV the spectrum shape is affected by an imprecise momentum cut in the early stages of the analysis."

[25]J. Heintze *et al.*, Nucl. Phys. B149, 365 (1979). The $|\vec{p}_e|$ spectrum given in (Fig. 9 of) this reference, extending down to 215 MeV, was operationally defined as the spectrum of e^+'s (which satisfied the trigger and velocity cut imposed by the Čerenkov counter) without coincident photons. We are thus considering it, apart from the contributions of certain backgrounds, as a spectrum for K_{e2} decay. However, it was actually used for the purpose of studying the structure-dependent terms in $K^+ \to e^+\nu_e\gamma$ decay. The justification for this entailed the tacit assumption that the K_{e2} spectrum consisted only of a single peak. Since this assumption is not guaranteed to be valid, it is necessary to reinterpret one of the results obtained in the $K^+ \to e^+\nu_e\gamma$ experiment. This will be done in a later article. An additional upper bound on $B(K^+ \to \mu^+\nu_{\mathrm{HSC}\ i})$ and hence R_{2i} can be extracted from an experiment that searched for the decay $K^+ \to \mu^+\nu_\mu\nu\overline{\nu}$ by C. Y. Pang *et al.*, Phys. Rev. D 8, 1989 (1973). Reanalyzing the results of this experiment, we obtain the limit $R_{2i} < 2.0\times10^{-6}/[D(T_\mu^{(i)})\rho(\delta_\mu^K, \delta_i^K)]$ for $100 > T_\mu^{(i)} > 60$ MeV, i.e., $230 \lesssim m(\nu_i) \lesssim 300$ MeV, where $D(T_\mu)$ is the experimental detection efficiency, given in this reference (which varies rapidly over the above interval of T_μ), and $\overline{\rho}(\delta_\mu^K, \delta_i^K)$ is shown in Fig. 4 of this paper. The most stringent bound is reached for $m(\nu_i) \simeq 280$ MeV and is $R_{2i} < 0.4\times10^{-6}$. We thank T. Yamazaki for discussions about this experiment.

[26]As one example of such a situation, consider a model in which the right-handed components of (Dirac) neutrinos are nonsinglets under some factor group in the total electroweak gauge group. Then one would have mixing matrices for both the left- and right-handed neutrinos, $U^{(L)}$ and $U^{(R)}$. The standard experimental evidence concerning the Lorentz structure of charged weak currents then implies that for DC ν_i, i.e., those for which $|U_{ai}^{(L)}|^2 \simeq |U_{ai}^{(R)}|^2 \not\simeq 1$ and for $1 \leq a \leq 3$,

$$\left(\frac{g_R^2}{m_{W_R}^2}\right)^2 \left|U_{ai}^{(R)}\right|^2 \lesssim 10^{-2}\left(\frac{g_L^2}{m_{W_L}^2}\right)^2 \left|U_{ai}^{(L)}\right|^2 .$$

However, this does *not* imply that for the HSC modes

$$\left(\frac{g_R^2}{m_{W_R}^2}\right)^2 \left|U^{(R)}_{a,\mathrm{HSC}\ i}\right|^2 \ll \left(\frac{g_L^2}{m_{W_L}^2}\right)^2 \left|U^{(L)}_{a,\mathrm{HSC}\ i}\right|^2$$

as long as both are small compared to the DC $V-A$ effective coupling given above. Thus in general some HSC ν_i lines in $M^+ \to l_a \nu_{l_a}$ decay might be dominantly due to $V-A$ $l_a \nu_i$ vertices, while others, for which $|U^{(R)}_{a,\mathrm{HSC}\ i}|^2 \gg |U^{(L)}_{a,\mathrm{HSC}\ i}|^2$ could be mainly due to $V+A$ $l_a \nu_i$ vertices. Another example is provided by the following admittedly artificial but nevertheless possible situation: in an $SU(2)_L \times U(1)$ theory with multiple Higgs doublets, the regular left-handed W-boson-exchange graph, with effective strength (including also the quark-mixing-matrix coefficient) $(g^2/m_W{}^2)^2 |U_{ai}|^2 |V_{bj}|^2$, might be severely suppressed by a very small coupling coefficient $|U_{ai}|^2$. In contrast, a charged-Higgs-boson graph might have an anomalously large effective strength, much greater than the usual $\sim$ (Higgs-boson coupling matrix) $(g^2/m_{\mathrm{Higgs}}{}^2)^2 (m_{\mathrm{lepton}} m_{\mathrm{quark}}/m_W{}^2)^2$. In such a case the effective Lorentz structure of the interactions responsible for some HSC ν_i modes could contain a non-negligible S,P part. We do not mean to imply that either of these examples is natural or likely, but rather only use them to illustrate the range of general phenomenological possibilities.

[27]See C. F. Powell, P. H. Fowler, and D. H. Perkins, *The Study of Elementary Particles by the Photographic Method* (Pergamon, New York, 1959); H. Yagoda, *Radioactive Measurements with Nuclear Emulsions* (Wiley, New York, 1949); *ibid.* W. H. Barkas, *Nuclear Research Emulsions* (Academic, New York, 1963); Vol. 1; *ibid.* (Academic, New York, 1973), Vol. 2, and references to the literature therein. For range-energy relations, see, e.g., Table 2.3.1 in W. H. Barkas, *ibid.*, Vol. 2. Some of the work by the Berkeley group is reported in W. H. Barkas, W. Birnbaum, and F. M. Smith, Phys. Rev. 101, 778 (1954); W. Birnbaum, University of California Radiation Laboratory Reports Nos. UCRL-2503 and UCRL-2522 (unpublished); Ph.D. thesis, 1954 (unpublished). In this thesis (p. 54) Birnbaum reports having observed an anomalous muon track with $R_\mu = 268$ μm but concludes that it could be due to π decay in flight. Another short muon track observed by F. M. Smith was reported in W. H. Barkas, Am. J. Phys. 20, 5 (1952) but was explicable as due to the same source. See also Refs. 34 and 35.

[28]L. Hyman, J. Loken, E. Pewitt, M. Derrick, J. Fields, J. McKenzie, I. Wang, J. Fetkovich, and G. Keyes, Phys. Lett. 25B, 376 (1967); L. Hyman and M. Derrick, private communications.

[29]E. Shrum and K. Ziock, Phys. Lett. 37B, 114 (1971); K. Ziock, private communication.

[30]P. Booth *et al.*, Phys. Lett. 26B, 39 (1967).

[31]Kaon experiments which only sought to determine $B(K^+ \to \mu^+ \nu_\mu)$ but did not report momentum spectra cannot be used for our analysis. These include, for example, I. Chiang *et al.*, Phys. Rev. D 6, 1254 (1972).

[32]Earlier experiments which did publish $|\vec{p}_e|$ spectra as part of their measurements of $B(K^+ \to e^+ \nu_e)/B(K^+ \to \mu^+ \nu_\mu)$ include D. Botterill *et al.*, Phys. Rev. Lett. 19, 982 (1967); D. R. Bowen *et al.*, Phys. Rev. 154, 1314 (1967); R. Macek *et al.*, Phys. Rev. Lett. 22, 32 (1969); and A. Clark *et al.*, *ibid.* 29, 1274 (1972). Compared with the CERN-Heidelberg experiment of Refs. 24 and 25, these experiments had similar momentum cuts but smaller statistics.

[33]This value for the energy cut will be needed in Sec. III; it is in agreement with an estimate, in lieu of records, by L. Pondrom (private communication).

[34]W. F. Fry, Phys. Rev. 91, 130 (1953) and references therein.

[35]C. Castagnoli and M. Muchnik, Phys. Rev. 112, 1779 (1958). In their data these authors found 26 events which clearly satisfied the selection criteria and 6 which they labeled as dubious. They used all 32 events for the integral range distribution of Fig. 14. Accordingly, we have included the 6 dubious events in our differential spectrum, Fig. 15, but have represented them with dotted lines to distinguish them from the more reliable 26 events in this experiment and the 8 events from Ref. 34, which are represented with solid lines.

[36]For calculations of the spectral distributions for $\pi^+ \to \mu^+ (\overline{\nu})_\mu \gamma$, see H. Primakoff, Phys. Rev. 84, 1255 (1951); Nakano *et al.*, Prog. Theor. Phys. 6, 1028 (1951); T. Eguchi, Phys. Rev. 85, 943 (1952); G. Fialho and J. Tiomno, Anais. Acad. Brasil. Cienc. 24, 245 (1952); B. Joffe and A. Rudik, Dokl. Akad. Nauk SSSR 82, 359 (1952); V. Vaks and B. Joffe, Nuovo Cimento 10, 342 (1958); S. Kamefuchi and S. Oneda, Nucl. Phys. 6, 114 (1958); and K. Huang and F. Low, Phys. Rev. 109, 1400 (1958). Given the standard $V-A$ charged-current couplings, these spectral distributions can be computed reasonably reliably since the structure-dependent terms (of which the axial-vector parts cannot be calculated in a model-independent manner) yield contributions which are small compared with those of the inner bremsstrahlung terms. Parenthetically, one might note that this is not true of $M^+ \to e^+ (\overline{\nu})_e \gamma$ decays; see, e.g., S. B. Treiman and H. W. Wyld, Phys. Rev. 101, 1552 (1956); D. Neville, *ibid.* 124, 2037 (1961); S. Brown and S. Bludman, *ibid.* 136, B1160 (1964); P. De Baenst and J. Pestiau, Nuovo Cimento 53A, 137 (1968); and the review in A. Stetz *et al.*, Nucl. Phys. B138, 285 (1978).

[37]Photons with energies corresponding to the muon momenta and ranges under consideration would have mean free paths and collision lengths for interaction via Compton scattering and pair production sufficiently large that they would usually not have been detected in the emulsion experiments of Refs. 34 and 35. It was for this reason that the selection criteria for the supposed $\pi^+ \to \mu^+ (\overline{\nu})_\mu \gamma$ events did not require the photon to be detected.

[38]We use the Bjorken-Drell Dirac-matrix conventions.

[39]Such "usual" charged-Higgs-boson couplings would also involve factors of $m_W{}^{-1}$ and hence be negligible; only anomalously large Higgs-boson couplings are of interest here.

[40]In the $V-A$ case one could also predict the relative strength of the HSC ν_i line in each of these other decays, but for general (V,A) or (S,P,V,A) couplings this would not be possible. It should be noted that we are, of course, assuming that the requisite experimental corrections have been made for $l_a = e$ or μ energy loss by bremsstrahlung and scattering in the target. For sufficiently slow l_a's these would be impor-

tant.

[41]For an analysis of the restrictions on right-handed currents in a left-right-symmetric gauge model where it was tacitly assumed that $m(\nu_i)=0$ for all i, so that $U^{(L)}=U^{(R)}=1$, see M. A. B. Bég *et al.*, Phys. Rev. Lett. 38, 1252 (1977); 39, 54(E) (1977).

[42]A. Alikhanov *et al.*, Zh. Eksp. Teor. Fiz. 38, 1918 (1960) [Sov. Phys.—JETP 11, 1380 (1960)].

[43]G. Backenstoss *et al.*, Phys. Rev. Lett. 6, 415 (1961).

[44]H. Bardon, P. Franzini, and J. Lee, Phys. Rev. Lett. 7, 23 (1961).

[45]H. Siebert, private communication.

[46]E. Kolb and T. Goldman, Phys. Rev. Lett. 43, 897 (1979). These authors only presented bounds resulting from the R_K constraint.

[47]H. L. Anderson *et al.*, Phys. Rev. 119, 2050 (1960).

[48]T. Kinoshita, Phys. Rev. Lett. 2, 477 (1959); S. Berman, *ibid.* 1, 468 (1958). See also T. Kinoshita and A. Sirlin, Phys. Rev. 113, 1652 (1959). The value quoted from the Kinoshita correction to $R_\pi^{(0)}$ assumes that one integrates over electrons of all energies, i.e., it really applies to the ratio $[\Gamma(\pi^+\to e^+\nu_e)+\Gamma(\pi^+\to e^+\nu_e\gamma)]/[\Gamma(\pi^+\to\mu^+\nu_\mu)+\Gamma(\pi^+\to\mu^+\nu_\mu\gamma)]$ (where the second term in the denominator is negligible). This corresponds to the experimental situation in Ref. 23, after certain experimental corrections were made for energy cuts. Later, a number of authors investigated strong-interaction or structure-dependent (SD) effects on the radiative corrections, which had not been included by Berman or Kinoshita; see, e.g., W. Marciano and A. Sirlin, Phys. Rev. Lett. 36, 1425 (1976) and references therein. These estimates suggest that the SD term makes a contribution which is negligible compared with the present experimental uncertainty in $\overline{R}_\pi^{(\mathrm{exp})}$. Accordingly, we have used the original Kinoshita result for our work. The situation is less satisfactory for R_K. In this case, estimates suggest that the SD correction to $R_K^{(0)}$ might be considerably larger than that to $R_\pi^{(0)}$, and, in particular, larger in magnitude than the Kinoshita correction $(R_K^{(0;\mathrm{RC})}-R_K^{(0)})/R_K^{(0)}=(\alpha/\pi)[-0.303+\ln(m_e/m_\mu)]=-3.64\%$, thereby rendering the sign of the total correction uncertain. It is for this reason that we have defined $\overline{R}_K^{(\mathrm{exp})}$ as in Eq. (3.5). For our bounds we use the $\delta_K^{(\mathrm{RC})}=0$ value of $\Delta\overline{R}_K^{(\mathrm{exp})}$ but caution that the actual value could be larger. [It should be noted that since we rely primarily on the data of Ref. 24, we have followed their definition of $R_K^{(\mathrm{exp})}$, which has the inner-bremsstrahlung correction extracted. This definition differs from the various ones used in Macek *et al.*, Bowen *et al.*, and Botterill *et al.*, Ref. 32. However, since only the ratio $\overline{R}_K^{(\mathrm{exp})}$ is significant in the comparison of theory and experiment, these differences in the definition of $R_K^{(\mathrm{exp})}$ (accompanied, of course, by correspondingly different definitions of $R_K^{(0;\mathrm{RC})}$) are irrelevant.]

[49]As usually defined, this statement applies to the couplings in the Lagrangian. There will, of course, be one- and higher-loop corrections to the lowest-order results calculated in a theory incorporating the e-μ universality relation (3.36). The Kinoshita correction to $R_M=B(M^+\to e^+\nu_e)/B(M^+\to\mu^+\nu_\mu)$ provides an example of this (see Ref. 48).

[50]There is no mystery behind this result; it is an obvious consequence of the fact that an M_{12} amplitude containing the (S,P) couplings of Eq. (3.39) can be written as P_M^α contracted with the corresponding (V,A) leptonic current, and hence is exactly proportional to the corresponding (V,A) amplitude.

[51]R. E. Shrock and L.-L. Wang, Phys. Rev. Lett. 41, 1692 (1978). The former standard Cabibbo fit was due to M. Roos, as quoted by K. Kleinknecht, in *Proceedings of the XVII International Conference on High Energy Physics, London, 1974,* edited by J. R. Smith (Rutherford Laboratory, England, 1975), p. III-23; and M. Roos, Nucl. Phys. B77, 420 (1974).

[52]D. Andrews *et al.*, Phys. Rev. Lett. 45, 219 (1980); G. Finocchiaro *et al.*, *ibid.* 45, 222 (1980); K. Berkelman and E. Thorndike, in *High Energy Physics—1980,* proceedings of the XXth International Conference, Madison, Wisconsin, edited by L. Durand and L. G. Pondrom (AIP, New York, 1981).

[53]See, e.g., V. Novikov *et al.*, Phys. Rev. Lett. 38, 627 (1977); 38, 791(E) (1977); R. Cahn and S. D. Ellis, Phys. Rev. D 16, 1484 (1977); J. F. Donoghue and K. Johnson, *ibid.* 21, 1975 (1980).

[54]C. H. Albright and R. E. Shrock, Phys. Lett. 84B, 123 (1979); C. H. Albright, R. E. Shrock, and J. Smith, Phys. Rev. D 20, 2177 (1979). In these papers the value of m_F used for the estimate of $\Gamma(F^+\to\tau^+\nu_\tau)$ was $m_F=2.0395\pm0.001$ GeV from a preliminary SLAC-LBL report by D. Luke, in *Particles and Fields—1977,* proceedings of the Meeting of the Division of Particles and Fields of the APS, Argonne, Illinois, edited by P. Schreiner, G. H. Thomas, and A. B. Wicklund (AIP, New York, 1978). Since this result has been published only in preliminary form, we now prefer to use the DASP value (see Ref. 55).

[55]R. Brandelik *et al.* (DASP Collaboration), Phys. Lett. 70B, 132 (1977); 80B, 412 (1979).

[56]J. Prentice and L. Voyvodic, in *Proceedings of the 1979 International Symposium on Lepton and Photon Interactions at High Energies, Fermilab,* edited by T. B. W. Kirk and H. D. I. Abarbanel (Fermilab, Batavia, Illinois, 1980), pp. 563, 569; R. Ammar *et al.*, Phys. Lett. 94B, 118 (1980); G. Trilling, in *High Energy Physics—1980* (Ref. 6). Prentice quoted the values $m_F=2.068\pm0.055$ GeV and $\tau_F=3.6\times10^{-13}$ sec for one well-identified F^- event and $\langle T_F\rangle\sim9\times10^{-13}$ sec for a weighted sum of several F events, some with ambiguous interpretations. Ammar *et al.* report $m_F=2.017\pm0.025$ GeV and $\tau_F=1.5\times10^{-13}$ sec for their single F^+ event.

[57]See also Eqs. (4.39)–(4.45) in B. W. Lee and R. E. Shrock, Phys. Rev. D 17, 2410 (1978).

[58]With obvious changes, this formula is similar to one given for $E^+\to E^0\pi^+$ decay by J. D. Bjorken and C. H. Llewellyn Smith, Phys. Rev. D 7, 887 (1973).

[59]B. Wiik, in *High Energy Physics—1980* (Ref. 6).